



Università degli Studi di Napoli Federico II

*Dottorato di Ricerca in Fisica Fondamentale ed Applicata
XVIII ciclo*

Valeria Pettorino

**Dark Energy
in generalized theories of gravity**

Il Coordinatore:
Prof. Arturo Tagliacozzo

Novembre 2005

Acknowledgments

This work has been supervised by

Prof. Carlo Baccigalupi

Prof. Gianpiero Mangano

Prof. Gennaro Miele

I sincerely thank Gianpiero Mangano and Rino Miele, for their helpful support and useful discussions as well as for giving me the freedom to follow the research direction I considered most interesting, making their group a little *darker*.

I have not enough words to thank Carlo Baccigalupi, for his ability to join the rigor of his work to a deep and involving enthusiasm, constantly encouraging me to trust my skills and widen my knowledge.

I would also like to express my gratitude to Francesca Perrotta for pointing out some precious mistakes I have done along the way.

Part of this work was done in Heidelberg; I would like to thank Christof Wetterich, Michael Doran and the whole cosmology group at the Institut of Theoretical Physics for kindly hosting me and for introducing me to the appeal of ‘Weyl Reskalierung’. I particularly and warmly thank Mona Frommert for sharing amusing cosmological efforts.

I also mention my creative writing group because writing can be as fun as reading.

Finally, I deeply thank all the readers who will enjoy reading my PhD-thesis more carefully than these acknowledgments.

*Can you remember that Ph-D thesis
on Extended Quintessence?*

(La Repubblica, 28th March 2059)

No, I can't.

(La Repubblica, 29th March 2059)

Contents

Introduction	i
1 Linear perturbation theory	1
1.1 Homogeneous and isotropic background	1
1.2 Linear perturbations	11
1.2.1 Choosing the gauge	14
1.2.2 Metric perturbations	15
1.2.3 Stress energy tensor perturbations	18
1.2.4 Einstein equations	21
1.3 Cosmic Microwave Background anisotropies	22
1.3.1 Characterization of the radiation field	23
1.3.2 Evolution of the CMB	27
2 Cosmological Concordance Model	35
2.1 Evidences for Cosmic Acceleration	35
2.1.1 Cosmic Microwave Background	35
2.1.2 Large Scale Structure	41
2.1.3 Type Ia supernovae	49
3 Quintessence scalar field	59
3.1 Dark energy as a minimally coupled scalar field	59
3.1.1 Perturbations	63
3.2 Tracking solutions	65
3.2.1 Exponential potential	68
3.2.2 Ratra-Peebles potential	68
3.2.3 SUGRA	70
3.3 Effects on cosmological perturbations	70
3.3.1 CMB	70
3.3.2 LSS	74
4 Generalized Cosmologies	77
4.1 Scalar-tensor theories	77
4.1.1 Action and rescaling	78

4.1.2	Background	81
4.1.3	Linear Perturbations	84
4.2	Experimental constraints	88
4.2.1	Solar system	88
4.2.2	Binary pulsars	90
4.2.3	Cosmological observations	90
4.2.4	Big Bang Nucleosynthesis	91
5	A general approach to Extended Quintessence cosmologies	95
5.1	Dark Energy as a modification of gravity	95
5.2	R-boost	96
5.3	Scaling solutions in scalar-tensor cosmologies	98
5.3.1	Case $m = n$	99
5.3.2	Case $m \neq n$	100
5.3.3	Summary and consistency criteria	102
5.4	Attractors	103
5.4.1	Attractor behavior for $m \neq n$	103
5.4.2	Attractor behavior for $m = n$	104
5.5	Exponential coupling	107
5.5.1	R-boost for an exponential coupling	109
5.5.2	Radiation dominated era (RDE)	110
5.5.3	Matter dominated era (MDE)	114
5.5.4	Stability	114
5.6	Weyl scaled exponential extended quintessence	116
5.7	Effects on cosmological perturbations	121
5.7.1	Observational constraints from BBN	123
	Conclusion	127

Introduction

Cosmology has recently gone through an outstanding revolution which has raised an enthusiastic interest in the embarrassing case of the 96% Dark Universe we live in. The concordance among a wide variety of independent experimental efforts, including observations from both Earth and satellites, carried on by distinct groups of research and concerning different phenomena (Cosmic Microwave Background (CMB) anisotropies [15], Large Scale Structures [125], type Ia Supernovae [79, 80, 131], data from the Hubble Space Telescope [72]) is astonishing. All clues impressively point in the same direction, defining the so called Cosmological Concordance Model: the Universe is nearly spatially flat, with an expansion rate of about 70 km/s/Mpc, and with structures grown out of a primordial linear spectrum of nearly Gaussian and scale invariant energy density perturbations. Several evidences, though, confirm that the amount of Dark Matter is not sufficient to have a flat Universe: only about 5% of the critical energy density is made of baryons, while about 25% is thought to be composed by non luminous particles interacting at most weakly with ordinary matter (Cold Dark Matter, CDM). Moreover, neither radiation nor matter can provide the observed acceleration which characterizes the expansion. The remaining 70% is some sort of vacuum component, the Dark Energy, with negative pressure acting as a repulsive gravitational force and responsible for a late time cosmic acceleration era.

The first tentative of giving an explanation to Dark Energy was to recover a Cosmological Constant: the latter consists in a homogeneous contribution to the energy density which doesn't vary with time and whose issue goes back to Einstein, who first introduced it in 1917 in order to find a static description of the Universe. The Cosmological Constant (usually indicated with Λ) is indeed the simplest model for a fluid with negative pressure, characterized by an equation of state $\omega_\Lambda \equiv p_\Lambda/\rho_\Lambda = -1$ and is still, nowadays, in perfect agreement with all experimental observations; Λ represents the main ingredient of the so called Λ CDM model, which has assumed the role of a standard cosmological model [37, 105].

Nevertheless, the amount of papers which has been devoted to Dark Energy and to its alternative interpretations is impressive. The reason can be clearly found in the fact that the Cosmological Constant is affected by intrinsic theoretical problems which will hardly ever be solved within a Cos-

mological Constant framework.

In particular, there are two main reasons which make the Λ CDM model very disappointing.

First of all, there is no understanding of why the value of the cosmological constant is so small with respect to any particle physics scale, leading to a fine tuning of 123 orders of magnitude with respect to the Planck scale. Indeed, if Λ is interpreted as vacuum energy, the expected contribution to vacuum (supposing that ordinary quantum field theory is valid up to the Planck scale) is $\rho_{\Lambda}^{Pl} \sim (10^{19} GeV)^4$ while the observed value amounts at maximum at $\rho_{\Lambda}^{(obs)} \sim 10^{-47} GeV^4 = 10^{-123} M_P^4$. Hence we need to adjust the energy densities of matter and of Λ in the early epoch very carefully so that $\rho_{\Lambda} \geq \rho_m$ at present.

A second issue regards the so called ‘coincidence problem’: there is no reason why the Cosmological Constant should be of the same order of matter density right now, while it has been completely negligible until a few redshifts ago and it will be completely dominant soon in the future. This framework clearly marks the present time as a special moment in the whole cosmological history, which is at least suspicious and at most definitely unsatisfactory.

Hence, one of the main goals for present cosmology consists in looking for more physical alternatives which free from the unpleasant temptation to rely on anthropic considerations as a solution to the fine-tuning and the coincidence problem.

The most popular alternative to a Cosmological Constant tries to employ in the present Universe the same physical mechanisms used for inflation in the early Universe: Dark Energy is then thought to be a time varying contribution related to the evolution of a classical minimally coupled scalar field ϕ named Quintessence which rolls down a suitably chosen potential $V(\phi)$.

Most of Quintessence models, however, still suffer the same worrying problems of fine tuning of the initial conditions which affect Λ , especially when trying to reproduce the cosmological conditions observed today, both in the value of the Dark Energy equation of state ω_{DE} and in the amount of the Dark Energy density component.

A hint in view of a possible solution to this issue has come from a subclass of Quintessence models in which, depending on the potential assumed for the evolution of the field, the equation of motion admits tracking solutions: starting from some more or less extended range of initial values for the field and for its first derivative, quintessence trajectory always converges to the same attractor path [90, 134], thus avoiding the fine tuning of the initial conditions.

Recently, however, the problem of initial fine tuning has become particularly serious even for those minimal coupling models admitting a tracking behavior: this is due to the fact that the observational bounds on the Dark Energy equation of state are increasingly converging towards a value of ω_{DE}

very close to -1 [125]. As ω_{DE} gets closer to -1 , the potential has to be flattened, resembling more and more to a Cosmological Constant, thus shrinking the range of allowed initial conditions for the scalar field [18]. Furthermore, the best fit of the latest Sn Ia data [80] also allows values $\omega_{DE} < -1$, which are certainly excluded in the context of minimally coupled quintessence models.

Again, the lack of a clear prediction for the Dark Energy scalar field from any fundamental theory has encouraged the search for new challenging ideas which might describe the present Universe: a competing model is then provided when Dark Energy closely mimics a Λ -like contribution at present, though allowing for a very different dynamics of the field in the past. In particular, it becomes essential to investigate how the Dark Energy scalar field interacts with other entities in the Universe, namely with matter fields [4] or Gravity [96]. Within the latter context, in particular, it was recently pointed out that Extended Quintessence (EQ) (i.e. Quintessence in which the scalar field that provides an accelerated expansion behaves as a Brans-Dicke like field, non minimally coupled to the Ricci scalar) might save the attractor features of minimally coupled models and still agree with present cosmological observations. This behavior is provided by the enhanced dynamics of the field at early times which goes under the name of R-boost [96, 8]. Furthermore, as noticed in [19] [99] [107] [136], such an Extended Quintessence component can cross the cosmological constant value and get to $\omega_{DE} < -1$.

In light of these considerations, it is worth pointing our attention to Extended Quintessence and extensions of General Relativity like scalar-tensor theories [74], tempted by the possibility of attributing the Dark Energy dynamics to a modification of Gravity. Despite the interest in this subject most of past works have limited their investigations to the case of non minimal coupling or induced gravity theories, in which the coupling to gravity depends quadratically on the scalar field which provides the Dark Energy contribution. There is however no strong motivation to prefer such a coupling rather than other expressions. The need of a general understanding of attractor properties in scalar-tensor theories is therefore the aim of our work. At this purpose, we will first present a complete theoretical investigation which will allow us to classify all the scalar-tensor theories able to provide attractors; then we will modify the existing Boltzmann codes which allow to follow the evolution of perturbations, in order to identify the impact of scalar-tensor theories on observations.

The work of thesis will be organized as follows.

In Chapter I, after a description of the main features of a homogeneous and isotropic Universe, we illustrate linear perturbation theory, from Einstein perturbed equations to the formulation of CMB anisotropies.

In Chapter II we review the most recent observations responsible of the

strong evidence for the Dark Universe, from CMB to type Ia Supernovae to matter estimates coming from various experiments.

Chapter III is devoted to minimal coupling Quintessence models and in particular to the subclass of tracker models; we remark the possibility of the latter to provide attractor solutions and emphasize the problems which have been recently argued against this issue.

In Chapter IV we introduce generalized theories of gravity, both with regard to the background and to cosmological perturbations; here we also illustrate the Weyl scaling formalism which allows to interpret a scalar-tensor model as a coupled quintessence model in which the scalar field is minimally coupled to gravity but universally coupled to matter fields. Moreover, we recall the constraints put by experiments on scalar-tensor theories, both in the solar system and within a cosmological context.

In Chapter V we describe our work within Extended Quintessence theories. First, we provide a general theoretical investigation of EQ models through a classification of all possible scalar-tensor models which admit attractor solutions [113]. The latter are chosen to have the form of scaling solutions, in which the quintessence energy density scales as a power law of the cosmological scale factor, generalizing to Extended Quintessence what had been done in [90] in the context of minimally coupled quintessence models. As a further step, we investigate the particular case in which the coupling to gravity depends exponentially on the Dark Energy scalar field, inspired by the fact that a similar behavior can be found in dilatonic theories, where an exponential multiplies all Lagrangian terms. We therefore apply the previous general discussion to this case and consistently find the existence of attractor solutions. Moreover, we illustrate how such a model can be transformed when Weyl scaling is applied, showing the equivalence of our exponential Extended Quintessence with a Coupled Quintessence model in which the scalar field is universally coupled to all matter fields. Finally, we investigate the effects of such a coupling both on the background and on cosmological perturbations; in particular, besides presenting bounds on this specific model coming from Big Bang Nucleosynthesis, we illustrate the impact on CMB and LSS, whose prediction has been performed via an implementation of DEfast, a numerical code which is itself a modification of CMBfast [46, 155].

Finally, we draw our Conclusions.

Chapter 1

Linear perturbation theory

1.1 Homogeneous and isotropic background

General Relativity is a powerful theoretical mean which allows us to relate the geometry of the space-time to the energy content of the Universe, through Einstein equations:

$$G_{\mu\nu} = 8\pi GT_{\mu\nu} \quad (1.1)$$

Here the geometry is part of the covariant symmetric tensor $G_{\mu\nu} \equiv R_{\mu\nu} - 1/2Rg_{\mu\nu}$, related to the metric tensor $g_{\mu\nu}$ and to its first and second derivatives through the Riemann tensor $R_{\mu\nu}$ and the Ricci scalar R ; the energy content is instead included in the stress energy tensor $T_{\mu\nu}$ and contains contributions from all species in the Universe.

Eq.(1.1) can be greatly simplified once we observe that on large scales, greater than the ones typical of the largest known structures (i.e. superclusters with $d \sim 100 \text{ Mpc}^1$), the Universe appears to be very isotropic and homogeneous in its spatial dimensions. Hints in this sense come from both Cosmic Microwave Background (CMB) measurements and from the observation of galaxy distribution by the deepest galaxy catalogs (2dF and SDSS). In particular the former tell us that deviations from homogeneity and isotropy were just of a few parts per million at the time of photon decoupling. The cosmological principle assumes that these two symmetries hold at sufficiently large scales ($d \gg 100 \text{ Mpc}$). On smaller scales departure from homogeneity is progressively more non-linear and the Universe looks very inhomogeneous and anisotropic, the Solar System being at 8.5 kpc from the center of the Milky Way, within the Virgo cluster (a few Mpc), itself part of a supercluster (100 Mpc) within our visible Universe today (10^3 Mpc). Since, however, inhomogeneities are supposed to grow due to the gravitational infall, one may expect that in the early Universe only small deviations from homogeneity

¹ $1 \text{ Mpc} = 3.1 \times 10^{24} \text{ cm} = 3.26 \times 10^6 \text{ light years}$.

and isotropy are present; consequently, density fluctuations can be treated as linear perturbations to the homogeneous model².

The geometry of space, necessary to explicitly solve Einstein equations, is specified by the space-time distance ds between two points

$$ds^2 \equiv g_{\mu\nu}(x)dx^\mu dx^\nu \quad (1.2)$$

where the most general metric, in the case of a homogeneous and isotropic Universe, is the Friedmann-Robertson-Walker (FRW) metric

$$ds^2 = -dt^2 + a^2(t)d\mathbf{x}^2 = -dt^2 + a^2(t) \left[\frac{dr^2}{1 - kr^2} + r^2(d\theta^2 + \sin^2\theta d\phi^2) \right] \quad (1.3)$$

The k parameter determines the spatial curvature of the Universe and assumes only three different discrete values: $k = -1$ corresponds to a three dimensional sphere (closed geometry), $k = 0$ to a 3D plane Universe (flat geometry) and $k = +1$ to a three dimensional hyperboloid (open geometry). The expansion of the Universe is contained in the scale factor $a(t)$, related to the physical size of the Universe and chosen to be dimensionless by taking $c = 1$. With regard to the time variable, two choices can be convenient: the cosmic time, indicated with t , is the proper time of a particle at rest; the conformal time, indicated with η , is defined as

$$d\eta \equiv a(t)^{-1}dt \quad (1.4)$$

in terms of which, for a flat Universe, the invariant interval (1.3) can be rewritten as

$$ds^2 = a^2(\eta)\eta_{\mu\nu}dx^\mu dx^\nu \quad , \quad (1.5)$$

so that the metric

$$g_{\mu\nu}(\eta, \mathbf{x}) = a^2(\eta)\eta_{\mu\nu} = g_{\mu\nu}(\eta) \quad (1.6)$$

$$g^{\mu\nu}(\eta, \mathbf{x}) = a^{-2}(\eta)\eta^{\mu\nu} \quad (1.7)$$

differs from Minkowski metric (defined as $\eta_{\mu\nu} = \eta^{\mu\nu} \equiv \text{diag}(-1, 1, 1, 1)$) by a factor $a^2(t)$ and only depends on the time coordinate η .

An immediate consequence of the expansion of the Universe is that the physical wavelength and momentum of photons travelling in space are redshifted. Even though in terms of the coordinates $x \equiv (\eta, \mathbf{x})$, photons seem to propagate in the same way as in Minkowski space-time (according to superpositions of plane waves of the form $e^{i(\mathbf{k}\mathbf{x} - |\mathbf{k}|\eta)}$ with wavelength $\lambda_x = 2\pi/|\mathbf{k}|$) the spatial coordinates \mathbf{x} are not physical coordinates: \mathbf{x} in (1.3) represent in fact the fixed spatial coordinates comoving on the

²For recent reviews see [64, 75, 116, 119].

sphere/plane/hyperboloid while the infinitesimal physical distance $d\mathbf{l}$ between two points of fixed spatial coordinates $d\mathbf{x}$ increases with time

$$d\mathbf{l} = a(t)d\mathbf{x} \quad (1.8)$$

The same holds for the time η and for the photon momentum \mathbf{k} and wavelength λ_x whose physical counterparts are the cosmic time t and the following expressions respectively:

$$\lambda = a(\eta)\lambda_x \quad , \quad \mathbf{p}(t) = \frac{\mathbf{k}}{a(t)} \quad (1.9)$$

with an energy scaling as

$$E = \hbar\omega(t) = \frac{|\mathbf{k}|}{a(t)} \quad (1.10)$$

In other words, if a photon has been emitted at time t_{em} with wavelength λ_{em} (whose value at the moment of the emission is fixed by the source) we receive today a photon of longer wavelength λ_{obs} , stretched in proportion to the scale factor by which the Universe expands, as shown in (1.9). The redshift z is defined as

$$z \equiv \frac{\lambda_{obs} - \lambda_{em}}{\lambda_{em}} = \frac{a_{obs}}{a(t_{em})} - 1 \quad (1.11)$$

Moving to the right hand side of eq.(1.1), it is a common choice to describe the matter content of the Universe in terms of a perfect fluid whose stress energy tensor is given by

$$T_{\mu\nu} = pg_{\mu\nu} + (\rho + p)u_\mu u_\nu \quad (1.12)$$

where $\rho(t)$ and $p(t)$ are the energy density and isotropic pressure of the fluid at time t as measured by an observer comoving with the fluid and u_μ is the 4-velocity for the isotropic fluid in co-moving coordinates, whose background value can be obtained from $u_\mu u^\mu = -1$, independently on the cosmological component we are considering:

$$u_\mu \equiv (a, 0, 0, 0) \quad (1.13)$$

$$u^\mu \equiv (a^{-1}, 0, 0, 0) \quad (1.14)$$

so that:

$$T_\nu^\mu(t) = \text{diag}(-\rho(t), p(t), p(t), p(t)) \quad (1.15)$$

Using the metric defined in (1.3) and substituting (1.15) in the (0,0) and (i, i) components of Einstein equations, we obtain the Friedmann and the

acceleration equations, which relate the energy content to the rate of the expansion and thus to the dynamics of the scale factor $a(t)$:

$$H^2(t) \equiv \left(\frac{\dot{a}}{a}\right)^2 = \frac{8\pi G}{3}\rho - \frac{k}{a^2} \quad (1.16)$$

$$\frac{\ddot{a}}{a} = -\frac{4\pi G}{3}(\rho + 3p) \quad (1.17)$$

Here we have defined the Hubble parameter $H(t)$ whose measurement from the Hubble Space Telescope Key Project [72] is one of the most reliable results:

$$H_0 = 72 \pm 3 \text{ (statistical)} \pm 7 \text{ (systematic)} \quad , \quad (1.18)$$

a value which is in very good agreement with estimations of CMB and large-scales structure observations [88]. In eq.(1.16, 1.17) the dot means derivative with respect to the cosmic time³ t , ρ is the total energy density in the Universe, k is the parameter introduced in (1.3) to describe the spatial curvature of the Universe and G is the Gravitational constant⁴. In the approximation in which a single cosmological constituent dominates over the other contributions, we can rewrite the acceleration equation (1.17) as

$$\frac{\ddot{a}}{a} = -\frac{4\pi G}{3}\rho_i(1 + 3\omega_i) \quad (1.19)$$

where we have introduced the equation of state ω_i , defined as

$$\omega_i \equiv \frac{p_i}{\rho_i} \quad (1.20)$$

where the subscript i indicates that the corresponding quantities are those of the i component (i.e. matter, radiation, vacuum etc.). Note from eq.(1.17) that in order to have an accelerated expansion ($\ddot{a} > 0$), one needs some form of energy with negative pressure and whose equation of state is $\omega_i < -1/3$ different from dust or radiation which can only decelerate the expansion. A third useful equation is

$$\dot{\rho}_i = -3H(\rho_i + p_i) = -3H(1 + \omega_i)\rho_i \quad (1.21)$$

which can be derived either combining equations (1.16) and (1.17) or requiring energy conservation, due to the covariance of Einstein equations that guarantee that $T^{\mu\nu}_{;\mu} = 0$ since $G^{\mu\nu}_{;\mu} = 0$.

³Note that in terms of the conformal time η , eq. (1.16) gets a factor $a^2(t)$ multiplying the right hand side term if the Hubble parameter on the left hand side is redefined as $\mathcal{H} \equiv \frac{a'}{a}$.

⁴In natural units $c = 1$ and the Planck mass is $M_{Pl} = \frac{1}{\sqrt{G}} \sim 1.2 \times 10^{19}$ GeV.

The energy content of the Universe is conventionally expressed in terms of the critical density, defined as

$$\begin{aligned}\rho_c &= \frac{3H_0^2}{8\pi G} = 1.05 \times 10^{-5} h^2 \text{ GeV cm}^{-3} & (1.22) \\ &= 1.88 h^2 10^{-29} \text{ g cm}^{-3} \\ &= 11.26 h^2 \text{ protons m}^{-3} \\ &= 2.78 h^{-1} \times 10^{11} \frac{M_{sol}}{(h^{-1} \text{ Mpc})^3}\end{aligned}$$

which corresponds to the value of the total energy density of all the constituents of the Universe when the geometry is flat ($k = 0$). In (1.22) the h parameter is defined as

$$H \equiv 100 h \text{ km s}^{-1} \text{ Mpc}^{-1} \quad (1.23)$$

In particular, if $h = 0.7$ we have $\rho_c \approx 5 \times 10^{-6} \text{ GeV cm}^{-3}$. In terms of ρ_c we can define the energy contribution of each component i in the Universe as

$$\Omega_i(t) \equiv \frac{\rho_i(t)}{\rho_c(t)} = \frac{8\pi G \rho_i}{3H_0^2} \quad (1.24)$$

and rewrite Friedmann equation (1.16) as

$$\Omega_{tot} = 1 - \frac{k}{a^2 H^2} \quad , \quad (1.25)$$

where Ω_{tot} includes contributions from all the existing forms of energy. Note that flat Universes ($k = 0$) correspond to $\Omega_{tot} = 1$, open Universes ($k = -1$) correspond to $\Omega_{tot} < 1$ and closed Universes ($k = +1$) correspond to $\Omega_{tot} > 1$, no matter what components are summed up in the value of Ω_{tot} .

But what's exactly in the Universe? As we have announced in the Introduction and we will discuss later on in the next chapter in greater detail, a wide variety of different experiments have recently pointed out an astonishing composition of the Universe, whose constituents we will briefly review here, as part of the so called "cosmological concordance model":

Radiation Radiation includes both photons and neutrinos and at early times it constituted the dominant contribution to the energy of the Universe up to matter-radiation equivalence which occurred at $z_{eq} \sim 3200$ ($a_{eq} \sim 10^{-4}$). Photons continued to be more numerous than matter particles even for some time after the equivalence while today both photons and neutrinos are only present in small amounts. In particular, photons mainly constitute the relic background of the Big Bang and their contribution, first observed as a very isotropic radiation characterized by a black body spectrum of temperature $T = 2.725 \pm 0.002 \text{ K}$, is now determined to high precision by CMB experiments.

Today's photon energy is negligible: $\Omega_\gamma = (2.471 \pm 0.004) \times 10^{-5} h^{-2}$. With regard to neutrinos, their amount can be simply calculated [119] without the need of any cosmological data, apart from constraints on the mass:

$$\Omega_{\nu,tot} < 0.16 \quad \text{if } m_{\nu_e} < 2.6 \text{ eV} \quad (1.26)$$

Stronger bounds come from the analysis of WMAP+2dF [153] which allow to derive the limit

$$\Omega_\nu < 0.0067 h^{-2} \quad (95\% \text{CL}) \quad (1.27)$$

The contribution of radiation as a whole is [82]: $\Omega_r h^2 = 4.17 \times 10^{-5}$. Both relativistic photons and (massless) neutrinos are characterized by an equation of state $\omega_\gamma = \omega_\nu = 1/3$.

Baryonic matter As we will see, observations of the CMB and of the primordial element abundances incredibly show that only 5% of the total energy content is made of baryonic matter and $\Omega_b = 0.228 h^{-2}$. CMB data are in striking good agreement with estimations found independently through quasar absorption lines, supporting the evidence that there is a missing matter component in the Universe. Baryons are non-relativistic and their equation of state is $\omega_b = 0$.

Dark Matter Observations of rotational curves of galaxies, together with surveys of large scale structures, reveal that, besides luminous matter, there is a 25% contribution of non luminous matter (whose baryonic dark part is very small). This extra component, which does not emit any detectable radiation, has been called ‘‘Dark Matter’’ (DM). Possible candidates are weakly interactive particles (WIMPs) not yet detected⁵. In the concordance model, Dark Matter is mainly cold (CDM) with equation of state $\omega_{DM} = 0.123 h^{-2}$.

Dark Energy CMB provides a strong evidence that the Universe is spatially flat, with $\Omega_{tot} = 1.02 \pm 0.02$ [88]. However, since matter, in both its luminous and dark contributions, accounts only for a 30% of the total energy amount, there needs to be another 70% of some different unknown energy, which has been called Dark Energy (DE) with $\rho_\Lambda = 10^{-30} \text{g/cm}^3 \sim 10^{-47} \text{GeV}^4$. As we will see, observations on Supernovae support this evidence, and suggest that DE might also be responsible for the acceleration of the Universe expansion: this is due to the fact that, as we have seen from eq.(1.19), acceleration can be provided only by a component with $\omega_i < -1/3$, which is not the case of any of the components described up to now. We will refer to

⁵We just mention that DAMA claimed to relate an observed annual modulation to Dark Matter [51].

dark energy with various symbols, such as Ω_Λ (which is usually used to identify the cosmological constant) or Ω_{DE} .

In the case in which Dark Energy is provided by a constant contribution Λ , Einstein equations (1.1) acquire an extra term and become [36, 37]:

$$G_{\mu\nu} = 8\pi G T_{\mu\nu} + \Lambda g_{\mu\nu} \quad (1.28)$$

which is the same expression we would get with no cosmological constant but with an energy-momentum contribution for the vacuum defined as

$$T_{\mu\nu}^{(vac)} \equiv \rho_{vac} g_{\mu\nu} = \frac{\Lambda}{8\pi G} g_{\mu\nu} \quad (1.29)$$

equivalent to a perfect fluid with

$$\rho_\Lambda = -p_\Lambda \equiv \frac{\Lambda}{8\pi G} \quad (1.30)$$

and equation of state $w_\Lambda \equiv p_\Lambda/\rho_\Lambda = -1$. The acceleration equation (1.17) and the Friedmann equation (1.16) change too:

$$H^2 \equiv \left(\frac{\dot{a}}{a}\right)^2 = \frac{8\pi G}{3}\rho - \frac{k}{a^2} + \frac{\Lambda}{3} \quad (1.31)$$

$$\frac{\ddot{a}}{a} = -\frac{4\pi G}{3}\rho(1+3\omega) + \frac{\Lambda}{3} \quad (1.32)$$

whose extra terms reveal the repulsive nature of Λ to gravity. Nevertheless, one could still use the standard equations (1.16) and (1.17) provided one includes an energy term given by (1.30).

In the standard cosmological picture most of the life of the Universe can be described if either radiation or matter dominate on the total energy content. If the Universe is dominated by a single perfect fluid characterized by a constant equation of state then eq.(1.21) can be integrated giving

$$\rho \sim \rho_i \propto a^{-3(1+\omega)} \quad (1.33)$$

Substituting in eq.(1.16) and supposing that the curvature term is negligible and the Universe is nearly flat, we obtain the scale parameter time dependence which, provided $\omega_i \neq -1$, is given by:

$$a(t) \propto t^{\frac{2}{3}(1+\omega)} \quad (1.34)$$

Before illustrating in more detail what happens whether radiation, matter or vacuum dominate the energy contribution, we will recall a few more notions which will be useful in the following. First, the presence of a cosmological particle horizon, defining the maximal distance radiation can have travelled since the beginning of time. The particle horizon is defined as

$$l_h = a(t)x_h = a(t) \int_0^t c d\eta = a(t) \int_0^t \frac{dt'}{a(t')} \quad (1.35)$$

where we have made $c = 1$ explicit for clarity and we have used (1.4) and (1.8). The sphere centered in the observer position and of radius equal to the cosmological particle horizon is causally connected to us, while the part of the Universe outside this sphere is causally disconnected from us. Note that this differs from the event horizon

$$l_{he} = a(t) \int_t^\infty \frac{dt'}{a(t')} \quad (1.36)$$

which represents the maximum distance that signals we send can reach.

Furthermore, note that the Hubble parameter defined in (1.16) can be rewritten as a function of the redshift in terms of the cosmological content of the Universe:

$$H^2(z) = H_0^2 \left(\Omega_{r0}(1+z)^4 + \Omega_{m0}(1+z)^3 + \Omega_{\Lambda 0} + \Omega_{x0} e^{\left[3 \int_0^z (1+\omega_x(z')) \frac{dz'}{1+z'} \right]} \right) \quad (1.37)$$

where we have put $k = 0$ for simplicity and we have included the contributions of matter, radiation, a cosmological constant Ω_Λ and of other possible unknown fluids of energy Ω_x , characterized by an equation of state ω_x .

Finally, besides the Hubble parameter, whose definition involves the first derivative of the scale factor, there are other two parameters often used in cosmology and related to the second and third derivatives of the scale factor: the first one is the deceleration parameter q_0 defined as

$$q_0 \equiv - \left[\frac{(\ddot{a}/a)}{(\dot{a}/a)^2} \right]_{t_0} = \frac{4\pi G}{3H_0^2} \sum_i \rho_i(t_0) [1 + 3\omega_i(t_0)] \quad (1.38)$$

$$= \Omega_{r0} + \frac{\Omega_{m0}}{2} - \Omega_{\Lambda 0} + \frac{1}{2} \sum_x (1 + 3\omega_x) \Omega_{x0} \quad (1.39)$$

where, assuming a flat Universe, we have used the acceleration equation (1.19) in (1.38) as well as eq.(1.16) and the definition (1.24) in (1.39). The dot means derivative with respect to the cosmic time. The second parameter is called ‘‘jerk’’ (recently introduced by [142, 80] for SNeIa measurements) and is related to the third derivative of the scale factor:

$$j(t) = \frac{(\ddot{\ddot{a}}/a)}{(\dot{a}/a)^3} = 3\Omega_r + \Omega_m + \Omega_\Lambda + \frac{1}{2} \sum_x (1 + 3\omega_x)(2 + 3\omega_x) \Omega_x \quad (1.40)$$

where again we have expressed the parameter in terms of the cosmological content of the Universe. A Taylor expansion of the scale parameter then becomes:

$$a(t) = a_0 \left\{ 1 + H_0(t-t_0) - \frac{1}{2} q_0 H_0^2 (t-t_0)^2 + \frac{1}{3!} j_0 H_0^3 (t-t_0)^3 + o[(t-t_0)^4] \right\} \quad (1.41)$$

We will now briefly review what happens in the case of matter and radiation dominations, as well as in a third case interesting for our purposes, in which a cosmological constant dominates over the other components.

Radiation Dominated Era (RDE)

During the first stages of its life the Universe was made of a very hot and dense plasma, dominated by relativistic particles whose equation of state is $\omega_r = 1/3$. In this case, from eq.(1.33), we get

$$\rho_r \propto a^{-4} \quad (1.42)$$

a result of clear interpretation since not only is the energy density scaling with the expanding volume but, in addition, each particle's energy is decreasing as $E \propto \nu \propto a^{-1}$. From eq.(1.34) it follows that

$$a(t) \propto t^{1/2} \quad ; \quad H = \frac{1}{2t} \quad (1.43)$$

so that the energy density scales as

$$\rho_r \propto t^{-2} \quad . \quad (1.44)$$

For $t \rightarrow 0$ the scale factor $a \rightarrow 0$ and the energy density $\rho_r \rightarrow \infty$, identifying the cosmological singularity called Big Bang. From eq.(1.43) and (1.38) it is easy to see that $\ddot{a} < 0$ and $q_0 > 0$ during RDE with a consequent deceleration of the Universe expansion. Moreover, both the particle horizon and the lifetime of a radiation dominated Universe have finite values.

Matter Dominated Era (MDE)

Non-relativistic particles in the Universe are characterized by an equation of state $\omega_m = 0$ and therefore, from eq.(1.33), they scale as:

$$\rho_m \propto a^{-3} \quad (1.45)$$

as expected, since matter simply scales with the expanding volume. Consequently, at some point in the Universe history, matter density came to dominate over radiation, which scales faster (1.42). In particular, RDE ended when:

$$\frac{\rho_m}{\rho_r} = \frac{\rho_{m0}}{\rho_{r0}} \frac{a^4}{a^3} = \frac{\rho_{m0}}{\rho_{r0}} (1 + z_{eq})^{-1} = 1 \quad (1.46)$$

and thus the redshift at the equivalence between matter and radiation was $z_{eq} \sim 3000$.

Substituting the value of the equation of state for matter particles in eq.(1.34), we get

$$a \propto t^{2/3} \quad (1.47)$$

so that the Hubble parameter is related to the cosmic time according to

$$H \equiv \frac{\dot{a}}{a} = \frac{2}{3t} \quad (1.48)$$

Hence, if the Universe were always matter dominated, an estimate of its present age would be given by $t_0 \sim \frac{2}{3}H_0^{-1} \approx 10^{10}$ yrs. This value, smaller than the lives of other objects in the Universe, has represented a problem for a long time and it has been solved only with the recent discovery of a Dark Energy dominated epoch.

Combining (1.45) and (1.47) one can immediately see that during MDE the background energy density scales again as

$$\rho_m \propto t^{-2} \quad (1.49)$$

and therefore has the same time dependence as during RDE (1.44).

Also note that, during MDE, $\ddot{a} < 0$ and $q_0 > 0$; the integral in (1.35) converges and hence the particle horizon distance is finite and equal to

$$l_h^{MDE} = 3t = 2H^{-1} \quad (1.50)$$

where t is the time at which we receive the radiation. For $t = t_0$, the latter expression gives a measure of the visible part of the Universe today

$$l_{h_0} \approx 3\frac{2}{3}H_0^{-1} \approx 3 \times 10^{23} \text{ km} \approx 10^4 \text{ Mpc} \quad (1.51)$$

Vacuum Dominated Era

The total amount of matter and radiation today sums up, as we have announced, to only about 30%; hence, in order to satisfy eq.(1.25) with a flat geometry ($k \sim 0$), a new non ordinary component must be present in the Universe, capable of accelerating the expansion thanks to its negative pressure. At this purpose, it is interesting to see what happens if the Universe is dominated by a component whose energy density is constant (the case of a cosmological constant or vacuum energy). In this case, the equation of state $\omega_\Lambda = -1$, and therefore equation (1.33) is not valid anymore; we can however still integrate (1.16) obtaining

$$a(t) \propto e^{H_\Lambda t} \quad (1.52)$$

where H_Λ is given by

$$H_\Lambda = \sqrt{\frac{8\pi G}{3}\rho_\Lambda} \quad (1.53)$$

We have now $\ddot{a} > 0$ (1.17), which tells us that a cosmological constant is indeed able of accelerating the Universe expansion. A scale factor evolving as in (1.52) in a flat space describes a De Sitter space-time which has the characteristic property of having no singularity since the scale factor a converges to a finite value for $t \rightarrow 0$.

Furthermore, the integral in (1.35) diverges, implying that the entire Universe is causally connected [119].

Equation (1.17) allows us to estimate the value of the redshift at which the transition from a MDE, decelerating expansion during which large scale structures form, to a new regime of accelerating expansion occurs. Neglecting radiation and for $k = 0$ we have that $\ddot{a} = 0$ when

$$\frac{\rho_m}{2\rho_\Lambda} = \frac{\Omega_{m_0}}{2\Omega_{\Lambda_0}}(1 + z_{acc})^3 = 1 \quad , \quad (1.54)$$

which corresponds to a redshift $z_{acc} \sim 0.7$ if we assume a constant value $\Omega_\Lambda = 0.7$.

1.2 Linear perturbations

As we have already anticipated at the beginning of the previous chapter, the observed Universe is not exactly homogeneous and isotropic: the CMB manifests anisotropies on the scale of one part over 10^5 and at smaller scales we are surrounded by a variety of galaxies and all sort of large scale structures (LSS). However, departures from the FRW background can be treated as cosmological perturbations whose main purpose is to relate the physics of the early Universe to CMB anisotropies and LSS, examining the properties of primordial density fluctuations necessary to provide the initial conditions for the formation of the observed structures. The idea is that the latter might have formed as a result of the growth of density fluctuations whose amplitudes were very small in the early Universe. Here we will review the case in which such perturbations are treated linearly [61, 83, 87, 56, 17].

In order to study the evolution of perturbations we need to perturb Einstein equations (1.1), both in the metric and in its stress energy tensor parts.

A convenient way to proceed is to expand the metric and stress energy tensor perturbations in the Fourier space; since we consider only first order perturbations, we neglect the coupling between different modes \mathbf{k} and \mathbf{k}' so that Fourier modes decouple from each other. Before proceeding in defining perturbations for our relevant quantities, let's briefly overview how to classify them: fluctuations can be decomposed in a general way into different "types" (scalar, vector and tensor modes) which, at first order, will behave without mixing.

This classification has a starting point in the consideration that when we deal with scalars, vectors and tensors we can decompose the latter in different type of components. In particular, any three dimensional vector $\mathbf{v}(\mathbf{x})$ can always be decomposed into a longitudinal part \mathbf{v}^{\parallel} (parallel to the corresponding wave vector in the Fourier domain) and a transverse part \mathbf{v}^{\perp} (perpendicular to the wave vector):

$$v_i = v^{\parallel}_i + v^{\perp}_i \quad (1.55)$$

with

$$\nabla \times \mathbf{v}^{\parallel} = \nabla \cdot \mathbf{v}^{\perp} = 0 \quad (1.56)$$

where ∇ is the covariant derivative, the divergence being $\nabla \cdot \mathbf{v} = \eta^{ij} \nabla_i v_j$ and the curl being similarly defined. The longitudinal part \mathbf{v}^{\parallel} can be obtained by deriving once a chosen scalar field v :

$$\mathbf{v}^{\parallel} = \nabla_i v \quad (1.57)$$

Consequently, expression (1.55) corresponds to decompose vector \mathbf{v} into a part \mathbf{v}^{\parallel} that can be expressed in terms of a scalar (scalar type component of vector \mathbf{v}) and a part \mathbf{v}^{\perp} that cannot be obtained from a scalar (vector type component of vector \mathbf{v}).

With regard to tensors, any symmetric tensor S_{ij} can be decomposed into three parts:

$$S_{ij} = S^{\parallel}_{ij} + S^{\perp}_{ij} + S^T_{ij} \quad (1.58)$$

where

$$S^{\parallel}_{ij} = \left(\nabla_i \nabla_j - \frac{1}{3} \eta_{ij} \nabla^2 \right) s \quad (1.59)$$

is the scalar type component of tensor S , obtained by deriving twice a given scalar field s ,

$$S^{\perp}_{ij} = \frac{1}{2} (\nabla_i S_j + \nabla_j S_i) \quad (1.60)$$

is the vector type component of tensor S obtained by deriving once a given vector S_i and, finally, S^T_{ij} is the tensor type component of tensor S satisfying the condition

$$\eta^{jk} \nabla_k S^T_{ij} = 0 \quad (1.61)$$

When perturbing a FRW spacetime, it can be demonstrated that scalar, vector and symmetric second-rank tensor equations, if covariant under coordinate transformations in the 3D space, separate into three groups of equations, each group containing only components of one type. These decompositions allow us to distinguish among scalar, vector and tensor perturbations.

Scalar perturbations

Scalar modes include all scalar type components of the perturbation. A scalar quantity $f(x)$ can be expanded in the Fourier space in terms of spherical harmonics $Y_{\mathbf{k}}^{(0)}$:

$$f(\eta, \mathbf{x}) = \int \frac{d^3 k}{(2\pi)^3} \tilde{f}(\mathbf{k}) Y_{\mathbf{k}}^{(0)}(\mathbf{x}) \quad (1.62)$$

where $Y_{\mathbf{k}}^{(0)}(\mathbf{x})$ form a complete set of eigenfunctions of the 3-dimensional Laplacian operator:

$$\nabla^2 Y_{\mathbf{k}}^{(0)} = -k^2 Y_{\mathbf{k}}^{(0)} \quad (1.63)$$

where $\nabla^2 = \eta^{ij}\nabla_i\nabla_j$. In particular, in a flat FRW space-time the eigenfunctions are given by plane waves $Y_{\mathbf{k}}(\mathbf{x}) = e^{i\mathbf{k}\cdot\mathbf{x}}$ and since Fourier modes do not mix we can compare integrands of functions like (1.62) directly. Scalar perturbations will involve both the set $Y_{\mathbf{k}}^{(0)}$ and its first and second derivatives obtained as in (1.57) and (1.59), describing scalar-type components of vectors and tensors:

$$Y_i^{(0)} = -\frac{1}{k}\nabla_i Y_{\mathbf{k}}^{(0)} \quad (1.64)$$

$$Y_{ij}^{(0)} = \left[\frac{1}{k^2}\nabla_i\nabla_j + \frac{1}{3}\delta_{ij} \right] Y_{\mathbf{k}}^{(0)} \quad (1.65)$$

Vector perturbations

Vector modes include all vector type components of the perturbation. Proceeding analogously to the scalar case, vector modes can be expanded in the Fourier space in terms of vector type eigenfunctions of the Laplacian

$$\nabla^2 Y_i^{(\pm 1)} = -k^2 Y_i^{(\pm 1)} \quad (1.66)$$

where $Y_i^{(\pm 1)}$ are transverse vectors satisfying the divergenceless condition

$$\nabla^i Y_i^{(\pm 1)} = 0 \quad (1.67)$$

where we have omitted the subscript \mathbf{k} for simplicity. In a flat FRW space-time the eigenfunctions can be conveniently represented as

$$Y_i^{(\pm 1)} = -\frac{i}{\sqrt{2}} (\hat{e}_1 \pm i\hat{e}_2) e^{i\mathbf{k}\cdot\mathbf{x}} \quad (1.68)$$

Vector perturbations will include both $Y_i^{(\pm 1)}$ and their first derivatives, obtained as in (1.60) and representing the vector-type component of tensors:

$$Y_{ij}^{(\pm 1)} = -\frac{1}{k} \left(\nabla_i Y_j^{(\pm 1)} + \nabla_j Y_i^{(\pm 1)} \right) \quad (1.69)$$

Tensor perturbations

Tensor modes include all tensor type components of the perturbation, consisting in the part of the perturbation that cannot be obtained by derivation from scalars or vectors. Tensor perturbations can be expanded in the Fourier space in terms of tensor type eigenfunctions of the Laplace operator

$$\nabla^2 Y_{ij}^{(\pm 2)} = -k^2 Y_{ij}^{(\pm 2)} \quad (1.70)$$

where $Y_{ij}^{(\pm 2)}$ are symmetric tensors satisfying the transverse and traceless conditions

$$\nabla^i Y_{ij}^{(\pm 2)} = 0 \quad (1.71)$$

$$Y^i_i^{(\pm 2)} = 0 \quad (1.72)$$

In a flat FRW space-time a suitable representation of the eigenfunctions is given by

$$Y_{ij}^{(\pm 2)} = -\sqrt{\frac{3}{8}}(\hat{e}_1 \pm i\hat{e}_2)_i \times (\hat{e}_1 \pm i\hat{e}_2)_j e^{i\mathbf{k}\cdot\mathbf{x}} \quad (1.73)$$

To conclude this section, we note that scalar, vector and tensor modes evolve independently in linear perturbation theory. Only scalar modes produce density perturbations while vector and tensor modes, though affecting the microwave background, are unimportant for structure formation. Before proceeding in defining perturbations to the FRW metric and to the stress energy tensor, we will first introduce another aspect which is important to understand the meaning of perturbations, that is the gauge problem.

1.2.1 Choosing the gauge

General Relativity allows us to perform general coordinate transformations without losing the meaning of our theory, which changes covariantly. However, we are not interested in all possible coordinate transformations but only in those which leave the FRW background and the equations we have seen in the previous section unchanged [56, 87]. This is what is called a ‘‘gauge’’ transformation which consists in an infinitesimal coordinate transformation:

$$x^\mu \rightarrow \tilde{x}^\mu = x^\mu + \epsilon(\eta, \mathbf{x}) \quad (1.74)$$

Under the gauge transformation (1.74), a chosen tensor $T_\nu^\mu(x)$ changes according to the Lie derivative $\tilde{T}(x) = T(x) - L_\epsilon \bar{T}$, where we have indicated with $\bar{T}(x)$ the background, with $T(x)$ the perturbed tensor and with $\tilde{T}(x)$ the perturbed tensor after the gauge transformation. The Lie derivative acts on the tensor in the following way:

$$\tilde{T}_\nu^\mu(x) = T_\nu^\mu(x) - \bar{T}_{\nu,\alpha}^\mu(\eta)\epsilon^\alpha + \bar{T}_\nu^\alpha(\eta)\epsilon_{,\alpha}^\mu - \bar{T}_\alpha^\mu(\eta)\epsilon_{,\nu}^\alpha \quad (1.75)$$

In particular, a scalar θ transforms as

$$\tilde{\theta}(x) = \theta(x) + L_\epsilon \phi(x) = \frac{\partial \theta}{\partial x^\lambda} \epsilon^\lambda(x) \quad (1.76)$$

The four vector $\epsilon(\eta, \mathbf{x})$ which specifies the coordinate transformation (1.74) can be decomposed into scalar and vector parts and can be set to [87]:

$$\tilde{\eta} = \eta + T(\eta)Y(\mathbf{x}) \quad (1.77)$$

$$\tilde{x}^i = x^i + L(\eta)Y^i(\mathbf{x}) + L^{(1)}(\eta)Y^{(1)i}(\mathbf{x}) \quad (1.78)$$

where we have added the apex ‘⁽¹⁾’ to distinguish vector type components from scalar ones. Note that there exist no tensor type gauge transformations.

All the perturbation variables depend on the gauge, making it more difficult to understand their physical meaning. One possibility to solve this ambiguity is to rewrite the evolution equations for perturbations in terms of gauge invariant quantities and evaluating the results only in terms of the physical degrees of liberty, which do not depend on the choice of coordinates⁶. However, when dealing with specific problems, it is often convenient to fix a particular gauge. For example, when studying formation of large structures like galaxies or clusters of galaxies, linear perturbations are very appropriate to investigate the evolution of density perturbations, generally characterized by small amplitudes on scales larger than the cosmic horizon size. This analysis allows one to fix the initial conditions for a subsequent phase, in which fluctuations grow to a non linear regime on scales well below the horizon size when a more complete treatment is required. As a consequence, it can be very useful, or even necessary, to express the results of the analysis of the early stage in a specific gauge well suited for the later Newtonian treatment.

In order to specify a gauge, we will need to impose two relations among the gauge-dependent variables which will be introduced in the perturbation, in order to fix both time and space coordinates of the perturbed space-time. The simplest way to specify the time slicing is to choose $T(\eta)$ in (1.77) so that one of the gauge-dependent variables by which we will parametrize the perturbed metric and/or stress energy tensor, vanishes. In particular, we have to set to zero a gauge-dependent variable whose change under the gauge transformation (1.74) is expressed only in terms of $T(\eta)$; for each time slicing the standard way to eliminate the spatial coordinate gauge freedom is to fix $L(\eta)$ so that a gauge-dependent quantity whose gauge transformation involves only $L(\eta)$, vanishes.

1.2.2 Metric perturbations

The FRW metric can be perturbed by adding a perturbation metric tensor $h_{\mu\nu}$ to the background metric tensor defined in (1.6) and that will here redefine as $\tilde{g}_{\mu\nu}$:

$$\tilde{g}_{\mu\nu}(\eta, \mathbf{x}) = \bar{g}_{\mu\nu}(\eta) + a^2 h_{\mu\nu}(\eta, \mathbf{x}) = a^2(\eta) [\eta_{\mu\nu} + h_{\mu\nu}(\eta, \mathbf{x})] \quad (1.79)$$

where η is the conformal time, $\eta_{\mu\nu}$ is the Minkowski metric tensor for a flat geometry and the perturbation metric tensor satisfies, in the linear regime, the condition

$$h_{\mu\nu} \ll 1 \quad (1.80)$$

⁶Note that there exist no gauge in which the evolution equations of perturbations become simpler than the gauge-invariant equations.

The most general way to parametrize the metric perturbation is

$$\delta g_{\mu\nu}(x) = \begin{pmatrix} -2a^2(\eta)A(x) & -a^2(\eta)B_i(x) \\ -a^2(\eta)B_i(x) & 2a^2(\eta)H_{ij}(x) \end{pmatrix} \quad (1.81)$$

where A is a scalar, B_i is a 3-vector and H_{ij} is a symmetric transverse traceless tensor. Hence the space-time distance ds whose background formulation is given by (1.3) assumes the following perturbed expression:

$$ds^2 = a^2(\eta) [-(1 + 2A)d\eta^2 - 2B_i d\eta dx^i + (\delta_{ij} + 2H_{ij})dx^i dx^j] \quad (1.82)$$

Note the the inverse perturbed metric tensor is obtained via the relation: $\delta g^{\mu\nu}(x) = -\bar{g}^{\mu\lambda}\bar{g}^{k\nu}\delta g_{\lambda k}$ where $\bar{g}^{\mu\nu}$ is the background metric. The perturbation metric parameters (A, B_i, H_{ij}) can then be decomposed into scalar, vector and tensor modes, according to the perturbation classification we have illustrated in the previous paragraph: in particular, B_i splits as in eq.(1.55) and H_{ij} as in eq.(1.58). The three types of perturbations will then evolve independently and while scalar modes will correspond to density perturbations, tensor modes will correspond to gravitational waves. Also we can expand all the parameters in Fourier modes in terms of the spherical harmonics (1.63), (1.66) and (1.70) according to their type. Eventually we have:

$$A = A(\mathbf{k}, \eta)Y^{(0)} \quad (1.83)$$

$$B_i = B(\mathbf{k}, \eta)Y_i^{(0)} + B^{(1)}(\mathbf{k}, \eta)Y_i^{(1)} \quad (1.84)$$

$$H_{ij} = H_L Y^{(0)}\eta_{ij} + H_T Y_{ij}^{(0)} + H^{(1)}Y_{ij}^{(1)} + H^{(2)}Y_{ij}^{(2)} \quad (1.85)$$

where the decomposition (1.84) includes a scalar-like and a vector-like component and in (1.85) the tensor $H_{ij} = H_L\eta_{ij} + S_{ij}$ has been decomposed into a scalar part $H_L\eta_{ij}$ and a tensor S_{ij} , in order to assign 10 degrees of freedom to the symmetric tensor $h_{\mu\nu}$ ⁷. In eq.(1.85) we have omitted for simplicity the dependence on (η, \mathbf{k}) of the perturbation parameters $H_L, H_T, H^{(1)}$ and $H^{(2)}$. Grouping different types of perturbations, we finally have the following perturbations for the metric:

- scalar type metric perturbations:

$$h_{00}^{(0)} = 2AY^{(0)} = h_{00} \quad (1.86)$$

$$h_{0i}^{(0)} = -BY_i^{(0)} \quad (1.87)$$

$$h_{ij}^{(0)} = 2H_L Y^{(0)}\eta_{ij} + 2H_T Y_{ij}^{(0)} \quad (1.88)$$

where $Y_i^{(0)}$ is a scalar type vector given by (1.64) and $Y_{ij}^{(0)}$ is a scalar type tensor given by (1.65).

⁷The symmetric tensor S_{ij} has then been decomposed into scalar, vector and tensor like components as in (1.58).

- vector type metric perturbations:

$$h_{0i}^{(1)} = -B^{(1)}Y_i^{(1)} \quad (1.89)$$

$$h_{ij}^{(1)} = 2H^{(1)}Y_{ij}^{(1)} \quad (1.90)$$

where $Y_i^{(1)}$ is a vector type vector and $Y_{ij}^{(1)}$ is a vector type tensor given by (1.69).

- tensor type metric perturbations:

$$h_{ij}^{(2)} = 2H^{(2)}Y_{ij}^{(2)} \quad (1.91)$$

where $Y_{ij}^{(2)}$ is a tensor type tensor.

Up to now we have considered all ten degrees of freedom of the symmetric perturbation tensor $h_{\mu\nu}$. Nevertheless, only six of these are physical since we can always transform the four space-time coordinates (η, x_i) without changing any physical quantity. In particular, according to (1.75), the gauge transformation for the metric is given by:

$$\tilde{g}_{\mu\nu}(x) = g_{\mu\nu}(x) - \bar{g}_{\alpha\nu}\epsilon_{,\mu}^\alpha - \bar{g}_{\mu\alpha}\epsilon_{,\nu}^\alpha - \epsilon^\alpha\bar{g}_{\mu\nu,\alpha} \quad (1.92)$$

where ϵ is again specified by (1.77, 1.78). In particular, the metric perturbation variables change under a gauge transformation according to:

$$\tilde{A}(\eta) = A(\eta) - \frac{a'}{a}T(\eta) - T'(\eta) \quad (1.93)$$

$$\tilde{B}(\eta) = B(\eta) + L' + kT(\eta) \quad (1.94)$$

$$\tilde{H}_L(\eta) = H_L(\eta) - \frac{a'}{a}T - \frac{k}{3}L(\eta) \quad (1.95)$$

$$\tilde{H}_T(\eta) = H_T(\eta) + kL(\eta) \quad (1.96)$$

$$\tilde{B}^{(1)} = B^{(1)} + L'^{(1)} \quad (1.97)$$

$$\tilde{H}^{(1)} = H^{(1)} + kL^{(1)} \quad (1.98)$$

$$\tilde{H}^{(2)} = H^{(2)} \quad (1.99)$$

A possible choice for the gauge is the Newtonian gauge, also called longitudinal gauge, which corresponds to fix:

$$B = 0 \text{ and } H_T = 0 \quad (1.100)$$

in scalar perturbations (1.87), (1.88) and

$$H^{(1)} = 0 \quad (1.101)$$

in vector perturbations (1.90). The remaining parameters can be rewritten in terms of gauge-invariant variables while tensor-type components are already

gauge invariant. In the Newtonian gauge, one then obtains the following scalar, vector and tensor types components:

$$h_{00}^{(0)} = 2\Psi Y \quad (1.102)$$

$$h_{ij}^{(0)} = 2\Phi Y \delta_{ij} \quad , \quad (1.103)$$

$$h_{0i}^{(1)} = -V Y_i^{(1)} \quad , \quad (1.104)$$

$$h_{ij}^{(2)} = 2H Y_{ij}^{(2)} \quad (1.105)$$

where Ψ and Φ are gauge invariant combinations of A and H_L respectively and are usually referred to as Bardeen potentials [87]:

$$\Phi \equiv H_L + \frac{H_T}{3} + \frac{\mathcal{H}}{k} \left(B - \frac{H'_T}{k} \right) \quad (1.106)$$

$$\Psi \equiv A + \frac{\mathcal{H}}{k} \left(B - \frac{H'_T}{k} \right) + \frac{1}{k} \left(B' - \frac{H''_T}{k} \right) \quad (1.107)$$

Another popular gauge is the synchronous one, used in codes like CMBFAST [46] when integrating perturbation equations; this gauge corresponds to fix $A = B = 0$.

1.2.3 Stress energy tensor perturbations

The perturbed stress energy tensor can be written as

$$T_\mu^\nu = \bar{T}_\mu^\nu + \delta T_\mu^\nu \quad (1.108)$$

where \bar{T}_μ^ν is the background stress energy tensor, that we will consider equal to the case of a perfect fluid given by eq.(1.12); δT_μ^ν is the perturbation, whose decomposition in modes we are now going to make explicit. Note that we will write mixed components of the perturbed tensor in order to simplify the factor $a^2(t)$.

The perturbation can be parametrized and expanded in spherical harmonics similarly to what has been done for the metric. For scalar perturbations we then have

$$\rho \equiv \bar{\rho}(\eta) \left[1 + \delta_{\mathbf{k}}(\eta, \mathbf{k}) Y^{(0)} \right] \quad (1.109)$$

$$p\delta_j^i \equiv \bar{p}(\eta) \left[1 + \pi_L(\eta, \mathbf{k}) Y^{(0)} \right] \delta_j^i \quad (1.110)$$

$$\pi_j^i \equiv \bar{p} \pi_T(\eta, \mathbf{k}) Y_j^{i(0)} \quad (1.111)$$

$$u^i \equiv \frac{1}{a} v(\eta, \mathbf{k}) Y^{i(0)} \quad (1.112)$$

which define four parameters: the density perturbation δ_k , the isotropic and anisotropic stress perturbations π_L and π_T respectively and the velocity perturbation v for the single k mode. The stress-energy tensor scalar

perturbations can then be written as:

$$\delta T_0^{0(0)} = -\bar{\rho} \delta Y^{(0)} \quad (1.113)$$

$$\delta T_i^{0(0)} = (\bar{\rho} + \bar{p})(v - B)Y_i^{(0)} \quad (1.114)$$

$$\delta T_0^{i(0)} = -(\bar{\rho} + \bar{p})vY^{i(0)} \quad (1.115)$$

$$\delta T_i^{j(0)} = \bar{p}[\pi_L \delta_i^j Y^{(0)} + \pi_T Y_i^{j(0)}] \quad (1.116)$$

where $Y_i^{(0)}$ is a scalar type vector given by (1.64) and $Y_{ij}^{(0)}$ is a scalar type tensor given by (1.65). Comparing to eq.(1.12), equations (1.113, 1.114, 1.115, 1.116) correspond to setting the 4-velocity u_μ defined in (1.13, 1.14) as:

$$u_0 = a(1 + A) \quad u_i = a(v - B)Y_i \quad (1.117)$$

$$u^0 = a^{-1}(1 - A) \quad u^i = a^{-1}vY^i \quad (1.118)$$

Similarly, vector-type components are:

$$\delta T_i^{0(1)} = (\rho + p)(v^{(1)} - B^{(1)})Y_i^{(1)} \quad (1.119)$$

$$\delta T_i^{j(1)} = p\pi_T^{(1)}Y_i^{j(1)} \quad (1.120)$$

where $Y_i^{(1)}$ is a vector type vector and $Y_{ij}^{(1)}$ is a vector type tensor given by (1.69) and tensor type components are:

$$\delta T_i^{j(2)} = p\pi_T^{(2)}Y_i^{j(2)} \quad (1.121)$$

where $Y_{ij}^{(2)}$ is a tensor type tensor.

We omit to write how the parameters change under a gauge transformation (this can be found for example in [87]) and only notice that the Newtonian gauge corresponds to the choice $B = 0$. Gauge invariants can be constructed combining energy-momentum perturbations with metric pertur-

bations, thus obtaining, for example [61]:

$$V \equiv v - \frac{1}{k}H'_T \quad (1.122)$$

$$\Delta_g \equiv \delta + 3(1 + \omega) \left(H_L + \frac{1}{3}H_T \right) \quad (1.123)$$

$$\Delta_s \equiv \delta + 3(1 + \omega)\mathcal{H}\frac{\sigma_g}{k} = \Delta_g - 3(1 + \omega)\Phi \quad (1.124)$$

$$\Delta_c \equiv \delta + 3(1 + \omega)\mathcal{H}\frac{1}{k}(v - B) \quad (1.125)$$

$$\sigma_g \equiv \frac{1}{k}H'_T - B \quad (1.126)$$

$$\Gamma \equiv \pi_L - \frac{c_s^2}{\omega}\delta \quad (1.127)$$

$$\Pi^{(0)} \equiv \pi_T \quad (1.128)$$

$$V_s^{(1)} \equiv v^{(1)} - \frac{1}{k}H'^{(1)} \quad (1.129)$$

$$V^{(1)} \equiv v^{(1)} - B^{(1)} \quad (1.130)$$

$$\sigma^{(1)} \equiv \frac{1}{k}H'^{(1)} - B^{(1)} = \mathcal{V}^{(1)} - \mathcal{V}_s^{(1)} \quad (1.131)$$

$$\Pi^{(1)} \equiv \pi_T^{(1)} \quad (1.132)$$

$$\Pi^{(2)} \equiv \pi_T^{(2)} \quad (1.133)$$

where V is the gauge invariant velocity, Δ_g , Δ_s and Δ_c are different possible gauge invariant combinations corresponding to the density perturbation, σ_g is the shear, Γ can be interpreted as the amplitude of the entropy perturbation and we have defined the the adiabatic speed of sound of the fluid is defined [87] as $c_s^2 \equiv \bar{p}'/\bar{\rho}'$. As for vector perturbations, $V_s^{(1)}$ and $V^{(1)}$ represent the amplitude of the shear and of the vorticity respectively. Note that the anisotropic stresses π_T , $\pi_T^{(1)}$ and $\pi_T^{(2)}$ are already gauge invariant. In the Newtonian/longitudinal gauge $v_{\text{long}} = V$ and another often used combination for the density perturbation⁸ is

$$\Delta \equiv \delta^{\text{long}} + 3(1 + \omega)\frac{a'}{a}\frac{V}{k} \quad (1.134)$$

Furthermore, it can be shown [87] that if the anisotropic stress $\pi_T = 0$, then the metric variables have the property that $\Phi = -\Psi$ and Ψ can be interpreted as the usual gravitational potential satisfying an equation of the type $\Delta^2\Psi \sim \rho$.

⁸This expression only holds if no coupling between different components is considered otherwise see (5.27 b) [87].

1.2.4 Einstein equations

We can now write first order perturbations of Einstein equations

$$\delta G^\mu{}_\nu = 8\pi G \delta T^\mu{}_\nu \quad (1.135)$$

explicitly for scalar, vector and tensor type perturbations; in order to do this we will follow [61, 56].

Scalar Einstein equations The scalar part of Einstein equations (1.135), perturbed at first order, if expressed in terms of gauge invariant variables, read as:

$$k^2 \Phi = 4\pi G a^2 \bar{\rho} \Delta \quad (00) \quad (1.136)$$

$$k \left(\frac{a'}{a} \Psi - \Phi' \right) = 4\pi G a^2 \bar{\rho} (1 + \omega) V \quad (0i) \quad (1.137)$$

$$k^2 (\Psi + \Phi) = -8\pi G a^2 \bar{p} \Pi^{(0)} \quad (ij) \quad (1.138)$$

The conservation of the stress energy tensor $T_{0;\nu}^\mu = 0$ and $T_{i;\nu}^\mu = 0$ lead respectively to the evolution of the perturbed energy density δ and momentum density v or, in terms of gauge invariant variables:

$$\Delta'_g = -3(c_s^2 - \omega) \frac{a'}{a} \Delta_g - (1 + \omega) k V - 3 \frac{a'}{a} \omega \Gamma \quad (1.139)$$

$$V' = -\frac{a'}{a} (1 - 3c_s^2) V + k (\Psi - 3c_s^2 \Phi) + \frac{c_s^2 k}{1 + \omega} \Delta_g + \frac{\omega k}{1 + \omega} \left(\Gamma - \frac{2}{3} \Pi^{(0)} \right) \quad (1.140)$$

Vector Einstein equations As for vector perturbations, Einstein equations become:

$$-\frac{k^2}{2} \sigma_g^{(1)} = 8\pi G a^2 \bar{\rho} (1 + \omega) V^{(1)} \quad (0i) \quad (1.141)$$

$$k \left(\sigma'_g{}^{(1)} + 2 \frac{a'}{a} \sigma_g^{(1)} \right) = 8\pi G a^2 \bar{p} \Pi^{(1)} \quad (ij) \quad (1.142)$$

and the conservation of the stress energy tensor leads to

$$V^{(1)'} + (1 - 3c_s^2) \frac{a'}{a} V^{(1)} = -\frac{k}{2} \frac{\omega}{1 + \omega} \Pi^{(1)} \quad (1.143)$$

Tensor Einstein equations The tensor part of Einstein perturbed equations (1.135) consists in a single gauge invariant equation:

$$H^{(2)''} + 2 \frac{a'}{a} H^{(2)'} + k^2 H^{(2)} = 8\pi G a^2 \bar{p} \Pi^{(2)} \quad (1.144)$$

Solutions for perfect fluids

Simple applications and solutions of Einstein equations can be found in [61] where, in particular, the cases in which the energy is that of a perfect fluid with vanishing anisotropic stress $\Pi^{(0)} = 0$ and entropy $\Gamma = 0$ are discussed, either when the content of the system is pure dust ($\omega = 0$, $c_s = 0$) or when it consists of pure radiation ($\omega = 1/3$, $c_s = 1/\sqrt{3}$). Here we will just recall the results for the latter case:

$$V = \frac{A}{2\sqrt{3}x} \quad (1.145)$$

$$\Delta_g = -2A - \frac{A}{3\sqrt{3}}x^2 \quad (1.146)$$

$$\Psi = \frac{A}{3} \quad (1.147)$$

on super-horizon scales, where $x \equiv c_s k \eta = \frac{k\eta}{\sqrt{3}} \ll 1$ and

$$V = \frac{\sqrt{3}A}{2} \sin x \quad (1.148)$$

$$\Delta_g = 2A \cos x \quad (1.149)$$

$$\Psi = -A \frac{\cos x}{x^2} \quad (1.150)$$

on sub-horizon scales when $x \gg 1$. As we can see, in a radiation dominated Universe perturbation variables oscillate with constant amplitude within the sound horizon⁹. As we will see in more detail in the next section, CMB photons are emitted during RDE: therefore, we can already expect to find some oscillation pattern in their anisotropies, depending on the k mode and consequently on the scale with respect to the sound horizon.

1.3 Cosmic Microwave Background anisotropies

Soon after the Big Bang, the Universe consisted of a photon-baryon plasma of mainly electrons, protons, photons and a small amount of helium and heavier elements containing neutrons. Electrons were coupled to photons through Thomson scattering and to baryons through electromagnetic interactions. While gravity attempted to compress the fluid in potential wells created by density perturbations due to primordial quantum fluctuations (related for example to some inflaton scalar field), radiation pressure provided by photons opposed to the compression of the fluid, resulting in oscillations at all scales, with modes behaving independently. The resulting sound waves

⁹The sound horizon is the maximum distance a sound wave can have travelled since the Big Bang.

left their imprint on the temperature of the photons, hotter or cooler in regions where the acoustic wave caused compression or rarefaction respectively. As the Universe expanded, photons wavelength stretched, decreasing their energy; then, when the Universe was about 300.000 years old, electrons decoupled from photons and joined baryons to form neutral atoms in a process called “recombination”. From that moment on sound waves stopped oscillating and the Universe became transparent to photons, which free streamed until they were detected as Cosmic Microwave Background (CMB) in 1965 for the first time.

The CMB spectrum first appeared very uniform, behaving as a very good black body with a nearly uniform temperature $T = 2.725 \pm 0.002$ K across the sky. However, in 1992 the COBE satellite detected for the first time anisotropies in the CMB, giving the way to a series of subsequent experiments. Nowadays, the general treatment of the CMB consists in describing the photon distribution in terms of small perturbations around the mean values of the CMB observables. Since fluctuations are small and if the sources of the anisotropies are also linear fluctuations, linear perturbation theory can be applied. As we will see CMB anisotropies include both primary and secondary anisotropies, depending on the time of their production (at or after last scattering respectively).

In the next paragraphs we will recall the formalism of CMB anisotropies following the total angular momentum method exposed in [83, 154] (see also [60]). We will then see in the next chapter how the CMB analysis can be used to estimate the energy content of the Universe and other important cosmological parameters.

1.3.1 Characterization of the radiation field

Electromagnetic radiation travelling in a fixed z direction is characterized by the electric field

$$\mathbf{E} = \epsilon e^{i(\omega t + kz)} \quad (1.151)$$

where $\vec{\epsilon}$ is the polarization vector

$$\epsilon = \begin{pmatrix} a_x e^{i\phi_x} \\ a_y e^{i\phi_y} \end{pmatrix} \quad (1.152)$$

and different choices of a_x , a_y , ϕ_x and ϕ_y give different polarization states¹⁰. The corresponding intensity tensor is then constructed as the average, over a time long compared to the characteristic frequency of the radiation, of

$$I_{ij} = E_i^* E_j = \begin{pmatrix} a_x^2 & a_x a_y e^{i(\phi_x - \phi_y)} \\ a_x a_y e^{i(\phi_y - \phi_x)} & a_y^2 \end{pmatrix} \quad (1.153)$$

¹⁰ $\phi_x = \phi_y$ for linear polarization; $a_x = a_y$ and $\phi_x = \phi_y + \pi/2$ for circularly polarized light.

which is a function of the direction $\hat{\mathbf{n}}$ of the CMB radiation in the sky and of two perpendicular directions $\hat{\mathbf{e}}_1$ and $\hat{\mathbf{e}}_2$.

Radiation is then characterized by both temperature and polarisation, which can both be described by the temperature fluctuation tensor \mathbf{T} : the latter can be decomposed in terms of the unit matrix $\mathbf{1}$ and of the three σ matrices in the $\hat{\mathbf{e}}_1 \times \hat{\mathbf{e}}_2$ subspace:

$$\mathbf{T} = \Theta \mathbf{1} + Q\sigma_3 + U\sigma_1 + V\sigma_2 \equiv \begin{pmatrix} T_{11} & T_{12} \\ T_{21} & T_{22} \end{pmatrix} \quad (1.154)$$

where the Pauli matrices are equal to

$$\sigma_1 = \begin{pmatrix} 0 & 1 \\ 1 & 0 \end{pmatrix} ; \quad \sigma_2 = \begin{pmatrix} 0 & i \\ -i & 0 \end{pmatrix} ; \quad \sigma_3 = \begin{pmatrix} 1 & 0 \\ 0 & -1 \end{pmatrix} \quad (1.155)$$

and the four numbers Θ, Q, U, V are the Stokes parameters for temperature fluctuations, described as follows. Θ is the total temperature fluctuation summed over polarisation states, given by:

$$\Theta = \frac{\text{Tr}(\mathbf{T} \cdot \mathbf{1})}{2} = \frac{T_{11} + T_{22}}{2} = \frac{\delta T}{T} \quad (1.156)$$

Furthermore

$$Q = \frac{\text{Tr}(\mathbf{T} \cdot \sigma_3)}{2} = \frac{(T_{11} - T_{22})}{2} \quad (1.157)$$

represents the difference in temperature fluctuation linearly polarised along the $\hat{\mathbf{e}}_1$ and the $\hat{\mathbf{e}}_2$ directions;

$$U = \frac{1}{2} \text{Tr}(\mathbf{T} \cdot \sigma_1) \quad (1.158)$$

is the difference in temperature fluctuations linearly polarized along $(\hat{\mathbf{e}}_1 \pm \hat{\mathbf{e}}_2)/\sqrt{2}$ axes, hence rotated by $\pi/4$ with respect to $\hat{\mathbf{e}}_1$ and $\hat{\mathbf{e}}_2$ and

$$V = \frac{\text{Tr}(\mathbf{T} \cdot \sigma_2)}{2} \quad (1.159)$$

represents circular polarization.

Under a clockwise rotation of the axes of an angle ψ in the $(\hat{\mathbf{e}}_1, \hat{\mathbf{e}}_2)$ plane, Q and U go one into another, V remains distinct and the Pauli matrices transform as

$$\sigma'_3 \pm \sigma'_1 = e^{\mp 2i\psi} (\sigma_3 \pm \sigma_1) \quad (1.160)$$

leading to the unpleasant consequence that the Stokes parameters depend on an arbitrary choice of the coordinates. In order to encompass this ambiguity, another convenient representation of the T matrix is often used:

$$T = \Theta I + V\sigma_2 + (Q + iU)M_+ + (Q - iU)M_- \quad (1.161)$$

where

$$M_{\pm} = \frac{1}{2}(\sigma_3 \mp \sigma_1) \quad , \quad (1.162)$$

and $Q \pm iU$ transform into themselves under rotation. In the following we will ignore V and reexpress the \mathbf{T} matrix as a vector specified by only three numbers

$$\mathbf{T}(\eta, \hat{\mathbf{n}}, \mathbf{x}) = (\Theta, Q + iU, Q - iU) \quad , \quad (1.163)$$

where we have explicated the perturbation dependence on the conformal time η , on the observed direction in the sky $\hat{\mathbf{n}}$ and on the position \mathbf{x} of the observer. Θ , Q and U all depend on these three variables as well.

The total temperature fluctuation $\Theta(\eta, \hat{\mathbf{n}}, \mathbf{x})$ is a spin-0 scalar field and can therefore be expanded as in eq.(1.62) in the Fourier space:

$$\Theta(\eta, \hat{\mathbf{n}}, \mathbf{x}) = \int \frac{d^3k}{(2\pi)^3} \Theta(\eta, \hat{\mathbf{n}}, \mathbf{k}) Y^{(0)}(\mathbf{x}) \quad (1.164)$$

where the $Y^{(0)}$ functions have been defined in (1.63). Following [83] we then expand the angular dependence contained in the choice of the radiation direction $\hat{\mathbf{n}}$, while fixing \mathbf{k} ; for each fixed \mathbf{k} we define a reference frame in which the \mathbf{k} direction is chosen as the polar axis $\hat{\mathbf{k}} \equiv \hat{\mathbf{e}}_3$; proceeding with this criteria and in the case of a flat cosmology, we obtain the following expansion:

$$\Theta(\eta, \hat{\mathbf{n}}, \mathbf{x}) = \int \frac{d^3k}{(2\pi)^3} \left[\sum_{lm} \Theta_{lm}(\eta, \mathbf{k}) Y_{lm}(\hat{\mathbf{n}}) \right] Y^{(0)}(\mathbf{x}) \quad (1.165)$$

$$= \int \frac{d^3k}{(2\pi)^3} \sum_l \sum_{m=-2}^{+2} \Theta_{lm}(\eta, \vec{k}) G_{lm}(\hat{\mathbf{n}}, \mathbf{x}) \quad (1.166)$$

where we have defined¹¹

$$G_{lm}(\hat{\mathbf{n}}, \mathbf{x}) = (-i)^l \sqrt{\frac{4\pi}{2l+1}} Y_{lm}(\hat{\mathbf{n}}) Y^{(0)} = \quad (1.167)$$

$$= \sum_{\tilde{l}} (-i)^{\tilde{l}} \sqrt{4\pi(2\tilde{l}+1)} j_{\tilde{l}m}^{(\tilde{l})}(kr) Y_{\tilde{l}}^m(\hat{\mathbf{n}}) \quad , \quad (1.168)$$

where $j_{lm}^{(\tilde{l})}(kr)$ are the spherical Bessel functions. In (1.166) each value of $m = 0, \pm 1, \pm 2$ is stimulated by scalar, vector and tensor metric perturbations respectively which behave independently due to the orthogonality of spherical harmonics.

¹¹For example, for $m = 0$, $Y_{l0} = \sqrt{\frac{2l+1}{4\pi}} P_l(\hat{\mathbf{n}})$ where $P_l(\hat{\mathbf{n}})$ are the Legendre polynomials; hence $\Theta(\eta, \mathbf{x}, \hat{\mathbf{n}})_{m=0} = \int \frac{d^3k}{(2\pi)^3} \sum_l (-i)^l \Theta_{l0}(\eta, \mathbf{k}) P_l(\hat{\mathbf{n}}) \exp(i\mathbf{k}\mathbf{x})$.

If we define as a_{lm} the Fourier coefficients of the temperature decomposition in spherical harmonics so that

$$\Theta(\eta, \hat{\mathbf{n}}, \mathbf{x}) \equiv \sum_{l=0}^{\infty} \sum_{m=-l}^{+l} a_{T,lm} Y_{lm}(\hat{\mathbf{n}}) \quad (1.169)$$

then the angular power spectrum of temperature anisotropies can be defined as

$$C_l^{\Theta\Theta} \equiv \langle |a_{T,lm}|^2 \rangle = \frac{1}{2l+1} \sum_{m=-l}^{+l} |a_{T,lm}|^2 \quad (1.170)$$

Large multipole moments $l = \frac{\pi}{\theta}$ correspond to small angular scales with $l \sim 100$ representing one degree scale separation.

We can proceed analogously for $(Q \pm iU)$:

$$Q \pm iU = \int \frac{d^3k}{(2\pi)^3} \sum_l \sum_m (E_{lm} \pm iB_{lm})_{\pm 2} G_{lm}(\hat{\mathbf{n}}, \mathbf{x}) \quad (1.171)$$

where

$$\pm 2 G_{lm}(\hat{\mathbf{n}}, \mathbf{x}) = (-i)^l \sqrt{\frac{4\pi}{2l+1}} \pm 2 Y_{lm}(\hat{\mathbf{n}}) Y^{(0)} \quad (1.172)$$

where we have used spin-2 spherical harmonics since $(Q \pm iU)$ transform as vectors under rotation. In particular

$$\pm 2 G_{2m} = \sum_l (-i)^l \sqrt{4\pi(2l+1)} [\epsilon_{lm}(kr) \pm \beta_{lm}(kr)]_{\pm 2} Y_{lm}(\hat{\mathbf{n}}) \quad (1.173)$$

where ϵ_{lm} and β_{lm} are combinations of the Bessel functions [83]; in (1.171) E_{lm} is the electric type component of the expansion in normal modes of the polarisation while B_{lm} is called the magnetic type component. Together with Θ they are invariant under a rotation of $\hat{\mathbf{n}}$ while, under a parity transformation, when $\hat{\mathbf{n}} \rightarrow -\hat{\mathbf{n}}$, they behave as a vector and a pseudo-vector respectively in analogy to the electric and magnetic fields:

$$\hat{\mathbf{n}}' = -\hat{\mathbf{n}} \quad (1.174)$$

$$E'(\hat{\mathbf{n}}') = E(\hat{\mathbf{n}}) \quad (1.175)$$

$$B'(\hat{\mathbf{n}}') = -B(\hat{\mathbf{n}}) \quad (1.176)$$

If the polarisation is parallel or perpendicular to the plane wave direction, it is called an E-mode polarization while if it is crossed at 45 degree angles, it is called a B-mode polarization. Both can be decomposed in terms of multipole moments:

$$E(\eta, \hat{\mathbf{n}}, \vec{x}) = \sum_{l=0}^{\infty} \sum_{m=-l}^{+l} a_{E,lm} Y_{lm}(\hat{\mathbf{n}}) \quad (1.177)$$

$$B(\eta, \hat{\mathbf{n}}, \vec{x}) = \sum_{l=0}^{\infty} \sum_{m=-l}^{+l} a_{B,lm} Y_{lm}(\hat{\mathbf{n}}) \quad (1.178)$$

and we can define analogously to (1.170) the following angular power spectra:

$$C_l^{EE} \equiv \langle |a_{E,lm}|^2 \rangle = \frac{1}{2l+1} \sum_{m=-l}^{+l} |a_{E,lm}|^2 \quad (1.179)$$

$$C_l^{BB} \equiv \langle |a_{B,lm}|^2 \rangle = \frac{1}{2l+1} \sum_{m=-l}^{+l} |a_{B,lm}|^2 \quad (1.180)$$

Note that (1.167) and (1.172) separate the intrinsic angular dependence of the fluctuation due to the choice of the $\hat{\mathbf{n}}$ direction of observation (which corresponds to Y_{lm} or $\pm 2Y_{lm}$) and the space angular dependence due to the expansion in the \mathbf{k} mode (corresponding to $Y_l^{(0)}$).

While CMB temperature anisotropies are an effect of density perturbations, we will see in the following that one of the main sources of polarisation is the motion of the baryon-photon fluid, which causes a Doppler shift. Since density and velocity are correlated in the early universe, we expect a similar correlation between the temperature and polarisation power spectra measured today:

$$C_l^{\Theta E} \equiv \langle a_{\Theta,lm}^* a_{E,lm} \rangle = \frac{1}{2l+1} \sum_{m=-l}^{+l} a_{\Theta,lm}^* a_{E,lm} \quad (1.181)$$

which is called cross-correlation and is always larger than the polarisation autocorrelation described in (1.170, 1.179, 1.180). Due to no parity violation, the cross correlation between B and Θ or B and E vanish since they have different parities.

1.3.2 Evolution of the CMB

The evolution of vector (1.163) is described by the Boltzmann equation which takes into account all the relevant interactions of the CMB photons along the line of sight. In particular, temperature and polarisation can change because of the photons interaction both with the gravitational metric tensor $g_{\mu\nu}$ and with free charged particles, via Thomson scattering:

$$\frac{d}{d\eta} \mathbf{T}(\eta, \mathbf{x}, \hat{\mathbf{n}}) = \vec{C}[\mathbf{T}] + \vec{G}[\mathbf{T}, h_{\mu\nu}] \quad (1.182)$$

$$\frac{\partial \mathbf{T}}{\partial \eta} + \frac{\partial \mathbf{T}}{\partial x^i} \dot{x}^i + \frac{\partial \mathbf{T}}{\partial n^i} \dot{n}^i = \frac{\partial \mathbf{T}}{\partial \eta} + n^i \nabla_i \mathbf{T} = \vec{C}[\mathbf{T}] + \vec{G}[\mathbf{T}, h_{\mu\nu}] \quad (1.183)$$

where $\vec{C}[\mathbf{T}]$ is the collisional source term, $\vec{G}[\mathbf{T}, h_{\mu\nu}]$ is the gravitational source term. In (1.183) we have used $\dot{n} = 0$ to rewrite the l.h.s. (since in flat cosmologies photons propagate in straight lines) and $\dot{x}^i = n^i$ since the

position of the observer is $\mathbf{x} = r\hat{\mathbf{n}}$ when viewed from the photon position. We have already seen how to write the l.h.s. of the Boltzmann equation, in which \mathbf{T} can be written in terms of the decompositions (1.165) and (1.171) which relate Θ , $Q \pm iU$ to Θ_{lm} , E_{lm} and B_{lm} ; note that we can consider only the integrand of the two decompositions and treat each single mode independently since we are in linear perturbation theory. The left hand side can also be developed further, the gradient term corresponding in the Fourier space to:

$$\hat{\mathbf{n}} \cdot \vec{\nabla} \rightarrow i\hat{\mathbf{n}} \cdot \mathbf{k} = i\sqrt{\frac{4\pi}{3}}kY_{10}^{(0)} \quad (1.184)$$

Hence, the term $n^i \nabla_i \mathbf{T}$ in (1.183) contains, as we have seen in (1.165, 1.172), scalar and tensor harmonics $Y_{lm}^{(s)}$. The product of angular momenta $Y_{10}^{(0)} Y_{lm}^{(s)}$ can be performed using the Clebsch-Gordan coefficients which couple the amplitudes of states with l and $l \pm 1$ terms

$$\begin{aligned} \sqrt{\frac{4\pi}{3}}Y_{10}^{(0)}(Y_{lm}^{(s)}) &= \frac{\kappa_{lm}^{(s)}}{\sqrt{(2l+1)(2l-1)}} - \frac{ms}{l(l+1)}Y_{lm}^{(s)} + \\ &+ \frac{\kappa_{l+1,m}^{(s)}}{\sqrt{(2l+1)(2l+3)}}Y_{l+1,m}^{(s)} \end{aligned} \quad (1.185)$$

where the coupling coefficient is

$$\kappa_{lm}^{(s)} = \sqrt{\frac{(l^2 - m^2)(l^2 - s^2)}{l^2}}. \quad (1.186)$$

We will now proceed in making the two sources on the r.h.s. of equation (1.182, 1.183) explicit.

Thomson scattering The first effect we consider is the scattering of CMB photons on electrons encountered on the way, when moving under the effect of electromagnetic fields. A convenient reference system in which this collision is investigated is the one in which the scattered electron is at rest and a photon arrives along direction $\hat{\mathbf{n}}$ and leaves along $\hat{\mathbf{n}}' \equiv \hat{\mathbf{z}}$. Let the scattering plane be individuated by these two directions and β be the scattering angle between $\hat{\mathbf{n}}$ and $\hat{\mathbf{n}}'$. Then the differential cross section is given by

$$\frac{d\sigma}{d\Omega} = \frac{3\sigma_T}{8\pi} |\hat{\epsilon}' \cdot \hat{\epsilon}|^2 \quad (1.187)$$

where $\hat{\epsilon}'$ and $\hat{\epsilon}$ are the polarisation vectors of the incoming and of the scattered radiation respectively and σ_T is the total Thomson scattering cross section. If we identify with \parallel and \perp the directions parallel and perpendicular to the scattering plane, then ϵ_{\perp} has a probability $3\sigma_T/8\pi$ to be in the same direction after the scattering, while ϵ_{\parallel} has a probability $(3\sigma_T/8\pi)\cos^2\beta$

to be in the scattering plane after collision: hence radiation polarised perpendicularly to the scattering plane is isotropically intense, while the one polarised on the scattering plane depends on $\cos^2 \beta$. As a consequence, unpolarised light coming from one direction acquires linear polarisation after scattering since the component of incoming radiation polarized in the scattering plane is suppressed; however, if unpolarized light comes from all directions isotropically, the effect is cancelled and the scattered radiation is not polarised. Therefore, we need some anisotropy in the incoming radiation in order to have polarization. As we will see, a dipole of anisotropy is not sufficient and what is needed is a quadrupole anisotropy in the incoming radiation.

In the scattering \mathbf{T} transforms as

$$\Theta_{\parallel} = \frac{3\sigma_T}{16\pi} \cos^2 \beta \Theta_{\parallel}' \quad (1.188)$$

$$\Theta_{\perp} = \frac{3\sigma_T}{16\pi} \Theta_{\perp}' \quad (1.189)$$

$$U = \frac{3\sigma_T}{16\pi} \cos \beta U' \quad (1.190)$$

which, together with the fact that $\Theta = \Theta_{\parallel} + \Theta_{\perp}$ and $Q = \Theta_{\parallel} - \Theta_{\perp}$, gives the scattering matrix of the \mathbf{T} vector, calculated in the scattering frame in which ($\hat{n}' \equiv \hat{z}$):

$$\mathbf{T} = (\Theta, Q + iU, Q - iU) = \mathbf{S}\mathbf{T}' \quad (1.191)$$

$$= \frac{3\sigma_T}{8\pi} \begin{pmatrix} \cos^2 \beta + 1 & -\frac{1}{2}\sin^2 \beta & -\frac{1}{2}\sin^2 \beta \\ -\frac{1}{2}\sin^2 \beta & \frac{1}{2}(\cos \beta + 1)^2 & \frac{1}{2}(\cos \beta - 1)^2 \\ -\frac{1}{2}\sin^2 \beta & \frac{1}{2}(\cos \beta - 1)^2 & \frac{1}{2}(\cos \beta + 1)^2 \end{pmatrix} \mathbf{T}' \quad (1.192)$$

For any given incoming radiation in a (r', θ', Φ') frame, we first move to the scattering reference frame (where the scattered electron is at rest) in which we can apply the \mathbf{S} matrix to vector \mathbf{T}' as in (1.191) and then we perform a second rotation of the reference frame, moving back from the scattering frame to a (r, θ, Φ) in which the scattered wavevector $\hat{\mathbf{k}} \equiv \hat{\mathbf{e}}_3$ so that:

$$\mathbf{T} = \mathbf{R}_1 \mathbf{S}(\beta) \mathbf{R}_2 \mathbf{T}' \quad (1.193)$$

In this k -frame all trigonometric functions that appear in the scattering matrix can be rewritten in terms of spherical harmonics, involving only the quadrupole ($l = 2$) terms in the temperature anisotropies. After integration over all the incoming angles, one can obtain the collisional term for Thomson scattering:

$$\vec{C}[\mathbf{T}] = -\dot{\tau} \left[\mathbf{T}(\Omega) - \left(\left(\int \frac{d\Omega'}{4\pi} \Theta' + \hat{\mathbf{n}} \cdot \mathbf{v}_B \right), 0, 0 \right) \right] + \dot{\tau} \int \frac{d\Omega'}{4\pi} \mathbf{T}(\Omega') \quad (1.194)$$

The differential optical depth τ represents the probability that a given photon scatters once and is defined such as $\tau' = n_e a \sigma_T$, where the free electron density n_e is multiplied to the total Thomson scattering cross section σ_T and the expansion factor a takes into account that the derivative is done with respect to the conformal time η . The terms in square brackets in (1.194) indicate that Thomson scattering subtracts part of the incoming radiation and redistributes it in the last directional term, which is the anisotropic term of Thomson scattering and can be written as:

$$\dot{\tau} \int \frac{d\Omega'}{4\pi} \mathbf{T}(\Omega') = \int \frac{d\Omega'}{10} \sum_{m=-2}^{m=2} \mathbf{P}^{(m)}(\Omega, \Omega') \mathbf{T}'(\Omega') \quad (1.195)$$

where the angular dependence is included in the spherical harmonic terms contained in $\mathbf{P}^{(m)}$:

$$\mathbf{P}^{(m)} = \begin{pmatrix} Y_{2m'}^{(0)} Y_{2m}^{(0)} & -\sqrt{\frac{3}{2}} Y_{2m'}^{(2)} Y_{2m}^{(0)} & -\sqrt{\frac{3}{2}} Y_{2m'}^{(-2)} Y_{2m}^{(0)} \\ -\sqrt{6} Y_{2m'}^{(0)} Y_{2m}^{(2)} & 3 Y_{2m'}^{(2)} Y_{2m}^{(2)} & 3 Y_{2m'}^{(-2)} Y_{2m}^{(2)} \\ -\sqrt{6} Y_{2m'}^{(0)} Y_{2m}^{(-2)} & 3 Y_{2m'}^{(2)} Y_{2m}^{(-2)} & 3 Y_{2m'}^{(-2)} Y_{2m}^{(-2)} \end{pmatrix} \quad (1.196)$$

As we can see, the collisional term (1.194), which can be considered for a fixed single Fourier mode \mathbf{k} , consists of three terms. The first one refers to radiation scattered out of a given angle hence decreasing the contribution to \mathbf{T} of a factor proportional to τ' ; the second one is the Doppler shift correction due to the fact that in general the electrons will have their peculiar velocities \mathbf{v}_B with respect to baryons; the third one includes the contribution just investigated of incoming radiation, integrated in $d\Omega$ since radiation is coming from every direction. Note that the scattering contribution to polarisation is important mainly only at recombination: before that time ($z \geq 10^3$) the Universe was very opaque and the mean free path of the photons was $\zeta_* \sim 0$ hence the large number of scattering events cancelled any polarised component; after recombination there were no charged particles, the Universe became transparent and the CMB photons kept the polarised anisotropies acquired at the surface of last scattering. As a consequence, polarisation anisotropy in the CMB can probe directly the physical conditions at the epoch of recombination. Also, any difference in temperature rapidly goes away because of the scattering that exponentially reduces the level of anisotropy in the radiation. However, we have seen that light gets polarised via Thomson scattering only if the incident radiation has a quadrupole anisotropy in the temperature (for example an excess in photons coming from both top and bottom with respect to the sides) at recombination while if the incident radiation is isotropic or presents a dipole (for example a temperature higher from the top and lower from the bottom with the average intensity incident from the sides) by symmetry there can be no net polarisa-

tion¹². Note also that B type polarisation cannot be generated by Thomson scattering and that CMB photons may have scattered again on free electrons during a second subsequent ionized phase of the Universe when the hydrogen was ionized by the first stars¹³; this process, which may alter the pattern of CMB anisotropies, is called reionization and its signature might be seen in the polarisation spectra of the CMB.

Gravitational redshift The second effect in Boltzmann equation is due to the effect of gravitational interactions with the perturbed metric tensor and has effect only on the temperature perturbation Θ of the CMB radiation and not on the polarization. Without going in details, we just recall that it can be demonstrated that the gravitational term can be written in the \mathbf{T} representation as follows:

$$\vec{G}[h_{\mu\nu}] = \left(\frac{1}{2}n^i n^j \dot{h}_{ij} + n^i \dot{h}_{0i} + \frac{1}{2}n^i \nabla_i h_{00}, 0, 0 \right) . \quad (1.197)$$

Boltzmann equation We have now all the ingredients to write the explicit form of the Boltzmann equation describing the evolution of CMB perturbations. This can be done separately for scalar, vector and tensor modes.

Substituting expressions (1.166), (1.171), (1.184) (1.185) in the l.h.s. of the Boltzmann equation and considering the sources as derived in (1.194) and (1.197) we obtain the equations for Θ_{lm} ($s=0$), E_{lm} and B_{lm} ($s \pm 2$):

$$\Theta'_{lm} = k \left[\frac{\kappa_{lm}^{(0)}}{(2l-1)} \Theta_{l-1,m} - \frac{\kappa_{l+1,m}^{(0)}}{(2l+3)} \Theta_{l+1,m} \right] - \tau' \Theta_{lm} + S_{lm} \quad (l \geq m) \quad (1.198)$$

The term in the square brackets is the free streaming effect we have evaluated in (1.184, 1.185). Thomson scattering effect is mainly included in the second term, which implies that, with no sources, temperature anisotropies are exponentially suppressed with τ ; the other scattering terms (Doppler effect and directional terms) are contained in the source term S_{lm} which includes also the gravitational redshift effect. Substituting the explicit values of the metric perturbation sources we get:

$$S_{00} = \tau' \Theta_{00} - \Phi' , \quad S_{10} = \tau' v_{B0} + k\Psi , \quad S_{20} = \tau' P^{(0)} \quad (1.199)$$

$$S_{11} = \tau' v_{B1} + V' , \quad S_{21} = \tau' P^{(1)} \quad (1.200)$$

$$S_{22} = \tau' P^{(2)} - H' \quad (1.201)$$

where

$$P^{(m)} = \frac{1}{10} [\Theta_{2m} - \sqrt{6} E_{2m}] \quad (1.202)$$

¹²For further details see [154].

¹³In any case, formation of structure will eventually reionize the Universe at some redshift otherwise radiation from distant quasars would be heavily absorbed in the ultra-violet.

Note that, in this formalism, terms in the source S_{lm} with $m = 0, \pm 1, \pm 2$ are stimulated by scalar (Φ, Ψ), vector (V) and tensor (H) metric perturbations respectively while the Doppler effect enters only in the dipole terms ($l = 1$). As for polarization we have:

$$E'_{lm} = k \left[\frac{\kappa_{lm}^{(2)}}{(2l-1)} E_{l-1,m} - \frac{2m}{l(l+1)} B_{lm} - \frac{\kappa_{l+1,m}^{(2)}}{(2l+3)} E_{l+1,m} \right] + \quad (1.203)$$

$$- \tau' [E_{lm} + \sqrt{6} P^{(m)} \delta_{l,2}]$$

$$B'_{lm} = k \left[\frac{\kappa_{lm}^{(2)}}{(2l-1)} B_{l-1,m} - \frac{2m}{l(l+1)} E_{lm} - \frac{\kappa_{l+1,m}^{(2)}}{(2l+3)} B_{l+1,m} \right] + \quad (1.204)$$

$$- \tau' B_{lm}$$

Note that the polarisation source $P^{(m)}$ appears only in the E -mode quadrupole.

Integral solutions

The easiest way to solve Boltzmann equations is to integrate them along the photon line of sight in the sky; the temperature for a single mode can be found formally integrating eq.(1.198):

$$\frac{\Theta_{lm}(\eta_0, k)}{2l+1} = \int_0^{\eta_0} d\eta e^{-\tau(\eta)} \sum_{\bar{l}} S_{\bar{l}m}(\eta) j_{l\bar{l}}^{(\bar{l})}(k(\eta_0 - \eta)) \quad (1.205)$$

where

$$\tau(\eta) = \int_{\eta}^{\eta_0} \tau'(\tilde{\eta}) d\tilde{\eta} \quad (1.206)$$

is the optical depth between time η and the present time η_0 and $j_l(x)$ are the spherical Bessel functions, containing the angular behavior of the temperature anisotropy source S_{lm} . The product $g \equiv \tau' e^{-\tau}$ is also called the visibility function and represents the probability of a photon to last scatter between $d\eta$ and η : hence it is nearly zero everywhere but at the recombination epoch, where it has a sharp peak. Solution (1.205) can be integrated

by parts and rewritten in the Newtonian gauge as [83]:

$$\begin{aligned} \frac{\Theta_{l0}(\eta_0, k)}{2l+1} &= \int_0^{\eta_0} d\eta \left[(g(\Theta_{00} + \Psi) + e^{-\tau}(\Psi' - \Phi')) j_{l0}^{(0)} + \right. \\ &\quad \left. + g v_{B0} j_{l0}^{(1)} + g P^{(0)} j_{l0}^{(2)} \right] \end{aligned} \quad (1.207)$$

$$\begin{aligned} \frac{\Theta_{l1}(\eta_0, k)}{2l+1} &= \int_0^{\eta_0} d\eta \left[g(v_{B1} - V) j_{l1}^{(1)} + \right. \\ &\quad \left. + \left(g P^{(1)} + e^{-\tau} \frac{kV}{\sqrt{3}} \right) j_{l1}^{(2)} \right] \end{aligned} \quad (1.208)$$

$$\frac{\Theta_{l2}(\eta_0, k)}{2l+1} = \int_0^{\eta_0} d\eta \left[(g P^{(2)} - e^{-\tau} H') j_{l2}^{(2)} \right] \quad (1.209)$$

In this formulation, the scalar mode ($m = 0$) for the CMB temperature in the direction $\hat{\mathbf{n}}$ gets a first contribution from the isotropic temperature monopole at the last scattering surface Θ_{00} , which is the intrinsic temperature of the CMB and is the same in all directions up to 1 part in 10^3 ; this term is corrected by the metric fluctuation via the gravitational potential Ψ , through the Sachs Wolfe effect which accounts for the gravitational redshift of photons climbing out of the potential wells. The Sachs Wolfe effect includes an ordinary (SW) and an integrated (ISW) contribution: the former influences the source S_{lm} in (1.198) with a term proportional to $g\Psi$ which has therefore only effect around recombination, when the visibility function g is different from zero; at last scattering photons have to climb out the potential wells where the baryons are and since they escape in different directions and from different potential wells they are more or less redshifted. The SW effect is dominant at scales well outside the horizon, at low multiples, when k is very small and the gravitational potential is bigger due to the Poisson equation $\Phi \propto \delta\rho/k^2$. The ISW contribution is due to the presence of the term $\int_0^{\eta_0} d\eta (e^{-\tau}[\Psi' - \Phi'])$ in the scalar solution (1.207), due to the redshift or blueshift of photons as the latter pass through time varying gravitational potential wells along the path the photon travels from last scattering to the present; the ISW consists in an early (EISW) and a late (LISW) effect.

The EISW is due to the effect at last scattering of the change of potential wells which occurs when the Universe goes from a RDE to a MDE: radiation, which is still present in a non negligible amount after RDE, tends to flatten the potential well so that Φ decays within the sound horizon; this effect acts even at scales slightly bigger than the sound horizon at last scattering; photons are redshifted (blueshifted) if they come from an underdense (overdense) region until radiation actually becomes negligible in the Universe.

The LISW is due to the change in Φ and Ψ which occurs when a Λ or DE term dominates stretching the potential again. As it happens for the

EISW, the LISW is dumped at small scales since photons will be redshifted and blueshifted several times, having the same probability to pass through several wells and hills; at large scales and small multipoles, up to the sound horizon, the effect is much bigger since they pass at most through one hill or well.

Another contribution in (1.207) is given by the Doppler term, proportional to the velocity of the photon-baryon fluid at last scattering, which only enters in the dipole anisotropy term ($\tilde{l} = 1$); finally, the quadrupole term includes the effect of the anisotropic nature of Thomson scattering. Eq.(1.208, 1.209) represent the vector and tensor mode solutions respectively.

With regard to polarisation, formal integral solutions of equations (1.203, 1.204) are given by

$$\frac{E_l^{(m)}(\eta_0, k)}{2l+1} = -\sqrt{6} \int_0^{\eta_0} d\eta \tau' e^{-\tau} P^{(m)}(\eta) \epsilon_l^{(m)}(k(\eta_0 - \eta)) \quad (1.210)$$

$$\frac{B_l^{(m)}(\eta_0, k)}{2l+1} = -\sqrt{6} \int_0^{\eta_0} d\eta \tau' e^{-\tau} P^{(m)}(\eta) \beta_l^{(m)}(k(\eta_0 - \eta)) \quad (1.211)$$

where the angular behavior of the polarisation anisotropy source $P^{(m)}$ is contained in $\epsilon_l^{(m)}$ and $\beta_l^{(m)}$, defined in (1.173). Since $\beta_{l0} = 0$, the B polarisation has no scalar mode ($m = 0$). B-modes are produced only by gravitational waves (tensor modes which also generate E-modes), hence polarisation could be used to detect the presence of gravitational waves in the early universe¹⁴.

In order to actually calculate the coefficients $C_l^{\Theta\Theta}$, $C_l^{\Theta E}$, C_l^{EE} , the following expression can be used:

$$(2l+1)^2 C_l^{X\tilde{X}} = \frac{2}{\pi} \int k^2 dk \sum_{m=-2}^2 X_{lm}^*(\eta_0, k) \tilde{X}_{lm}(\eta_0, k) \quad (1.212)$$

where X and \tilde{X} stand for Θ , E or B ¹⁵. These quantities, representing angular power spectra for temperature and polarization as shown in (1.170, 1.180, 1.179), are nowadays an inestimable and largely used tool to estimate the content and characteristics of the Universe; furthermore, their value at different angular scales is a reference point, whenever one wishes to test and make a comparison among different models, as we will see in detail in the next Chapter.

¹⁴Limits on the gravitational wave contribution to the temperature anisotropy imply B-modes less than a few tenths of a μK .

¹⁵Recall that cross correlation to B vanishes due to parity invariance.

Chapter 2

Cosmological Concordance Model

2.1 Evidences for Cosmic Acceleration

In the last few years, several new theoretical models and experiments have managed to make an astonishing revolution in our way to look at the Universe. At present, the favored cosmological model consists in a nearly spatially flat Universe containing, as we have seen, mainly unknown ingredients like Dark Matter and Dark Energy. Furthermore, another quite surprising discovery consists in the fact that at $z \sim 1.7$ the Universe started accelerating its expansion.

Before proceeding in investigating Dark Energy in detail, we will briefly review the main experimental evidences that have contributed to give the astonishingly new picture of the Universe we have just described. The main tests come from Cosmic Microwave Background (CMB) (which provides evidences for flatness, acceleration and Dark Matter), galaxies and clusters of galaxies (for the matter amount in the Universe), type Ia Supernovae (SNe) (for the accelerated expansion), data from the Hubble Space Telescope (HST) (for the determination of the Hubble parameter) and Big Bang Nucleosynthesis (BBN). All these experiments nicely complement each other and all currently indicate that not only dark energy exists but is the dominant form of energy density in the Universe today.

2.1.1 Cosmic Microwave Background

The most stringent constraints come from the observation of CMB anisotropies whose power spectrum, usually plotted as $l(l+1)C_l$ vs l (fig.2.1, top), shows a series of oscillatory features at angular scales smaller than one degree ($l \geq 200$). These features, known as acoustic peaks, represent the oscillations

of the photon-baryon fluid in potential wells up to the time of decoupling (primary anisotropies). At recombination, when protons and electrons join to form neutral atoms, all modes frozen at extrema of their oscillations become peaks in the CMB power spectrum, at angular scales below the horizon size at the last-scattering surface: for example, the first peak corresponds to the mode for which the fluid had just time to compress once before recombination, the second represents the mode at which the fluid had time to compress once and then rarefy. Other effects (secondary anisotropies) can then influence the photons pattern along the way, up to their detection: CMB can scatter on ionized matter due either to reionization or to the presence of hot gas in central regions of galaxy clusters (Sunyaev Zeldovich (SZ) effect); also, we have seen that gravitational interactions can cause redshift (SW effect) and lensing effects.

COBE first detection, in 1992, of CMB temperature fluctuations across the sky [47], only allowed to observe the dipole induced by our motion with respect to the CMB. Starting from 2000, however, the Boomerang [20, 21, 22, 23, 24] and Maxima [97, 98] experiments first, WMAP [150, 151, 153] later, measured the position and amplitude of the peaks, providing the most accurate results to date of the temperature power spectrum up to $l \sim 900$ while the EE-spectrum was first measured by DASI [52, 53] in 2002. At present, several ground based experiments are running (VSA [143], CBI [39], ACBAR [1]) and there is great expectation for the next one to come, the PLANCK satellite [114], scheduled for launch in 2007.

The characteristics of the CMB spectra have very relevant implications in the determination of cosmological parameters. The position of the first peak, in particular, depends on the sound horizon at the time of decoupling; the latter is equal to $r_s = 147$ Mpc as seen today¹, corresponding, in a flat Universe, to an angle of about 1° ; this is exactly the scale at which the first peak in the CMB is located, demonstrating that the Universe spatial geometry is indeed Euclidean.

While the first acoustic peak points out that the Universe is flat, the presence of a second peak, observed to be substantially lower than the first peak, is evidence of a good interpretation of sound waves from gravitational potential perturbations in the early universe; furthermore, since odd and even peaks are respectively associated with how much the plasma compresses or rarefies inside gravitational potential wells, odd peaks are enhanced with respect to even peaks if the amount of baryons in the universe increases. Also, since at recombination CMB photons random walk a bit through the baryons

¹Note that the value of the sound horizon usually refers to the value (147 Mpc) it has ‘as seen today’ after the expansion, and not to its physical value at the time of interest, i.e. decoupling. Hence, given the physical value of the horizon at a_* , the reported value is usually obtained multiplying by a_0/a_* .

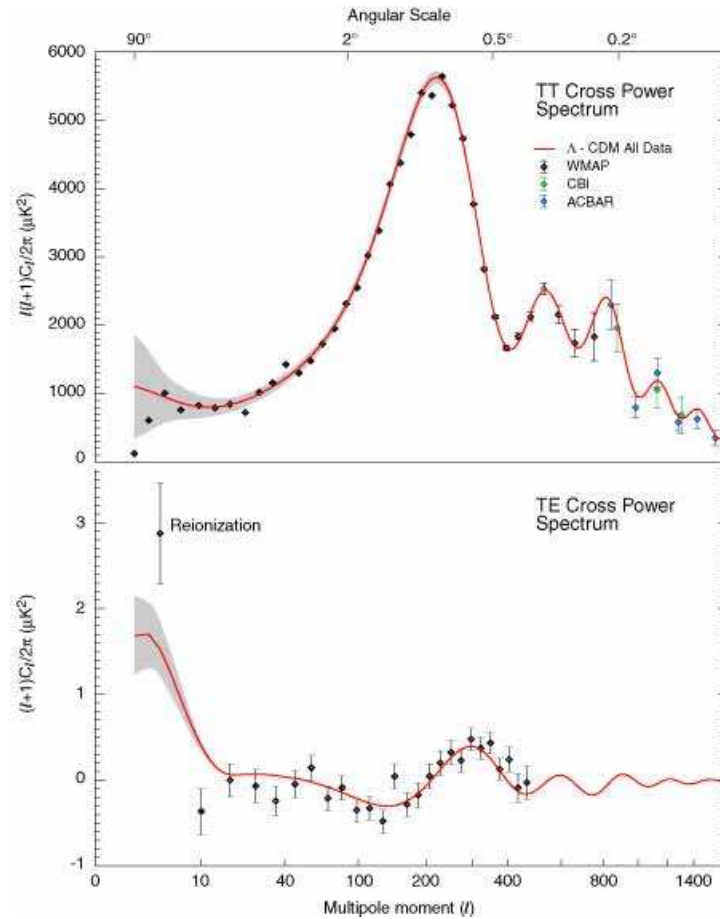


Figure 2.1: The WMAP angular power spectrum. Top: the WMAP temperature (TT) results are consistent with the ACBAR and CBI measurements. The grey band represents the cosmic variance expected for that model. The quadrupole has a surprisingly low amplitude. Bottom: The temperature-polarization (TE) cross-power spectrum. The figure is from [15].

before free streaming, hot and cold photons mix and the acoustic peaks are exponentially damped on scales smaller than the distance photons random walk at last scattering: raising the number of baryons decreases the mean free path and hence shortens this distance, thus lowering the damping to smaller scales or larger angular momenta; this effect can also be understood by noticing that the more are the baryons, the slower is the sound velocity $c_s^2 = p'/\rho' = p'_\gamma/(\rho'_\gamma + \rho'_b) < p'_\gamma/\rho'_\gamma$; as a consequence, if less baryons are present, the sound horizon is smaller; angular scales which enters the horizon at last scattering are therefore smaller too, shifting CMB peaks to higher multipoles.

The third peak, as well as the higher order acoustic peaks, is sensitive to the energy density of Dark Matter² and together with the first peak indicates the need for Dark Energy; there is however no evidence yet for dynamics of the Dark Energy component, the data being consistent with a pure Cosmological Constant.

Note also that since the fit to estimate the parameters is done in a multi-parameter space, it is often necessary to assume priors on the range of some parameters (e.g. assume that the Hubble constant is in the range $0.5 < h < 1$), and there may be some dependence of the estimated values on the assumed priors³. Also, the spectra are ultimately limited by “cosmic variance”, shown in fig.(2.1), due to the fact that there are only $2l + 1$ samples over which one can perform the statistical mean in (1.170, 1.179, 1.180) with a consequent inevitable error of

$$\Delta C_l = \sqrt{\frac{2}{2l + 1}} C_l \quad (2.1)$$

which is especially relevant at very low multipoles. A definite test of the interpretation of the temperature peaks is polarisation, discussed in section (1.2.4), whose importance has soon become an extremely appealing field of study, being the most direct probe of the Universe at the epoch of recombination and a possible way to the detection of gravitational waves and reionization (fig.2.2). As shown in fig.(2.1, bottom), polarisation and temperature are partially correlated; also, the amplitude of the polarisation spectrum is smaller than the temperature spectrum by at least a factor of ten (see fig.2.3). With regard to the spectrum shape, since the quadrupole temperature anisotropies that generate polarisation are themselves formed from the acoustic motion of the baryon-photon fluid, the polarisation spectrum presents peaks too, though out of phase with the temperature peaks.

²Note that Dark Matter influences CMB differently than baryons, since the latter have been coupled to photons and suffer of a Doppler shift.

³For example, if the Hubble parameter had the very low value $h = 0.3$, WMAP alone allows closed Universes with $\Omega_{tot} = 1.3$

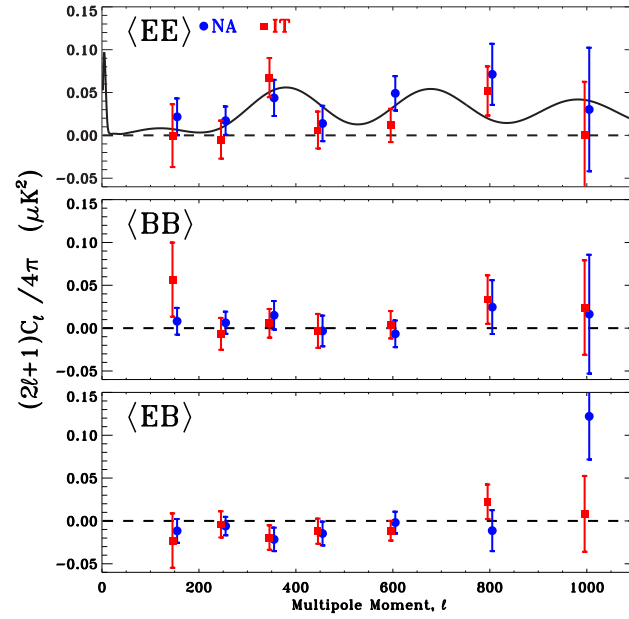


Figure 2.2: Angular power spectrum for EE, BB and EB polarizations. The plot has been found from Boomerang data relative to the Antarctic flight which took place in January 2003. NA (North America) and IT (Italy) refer to two different methods of analysis. The solid line in the $\langle EE \rangle$ plot is the best fit Λ_{CDM} model to the WMAP TT results. The figure is from [24].

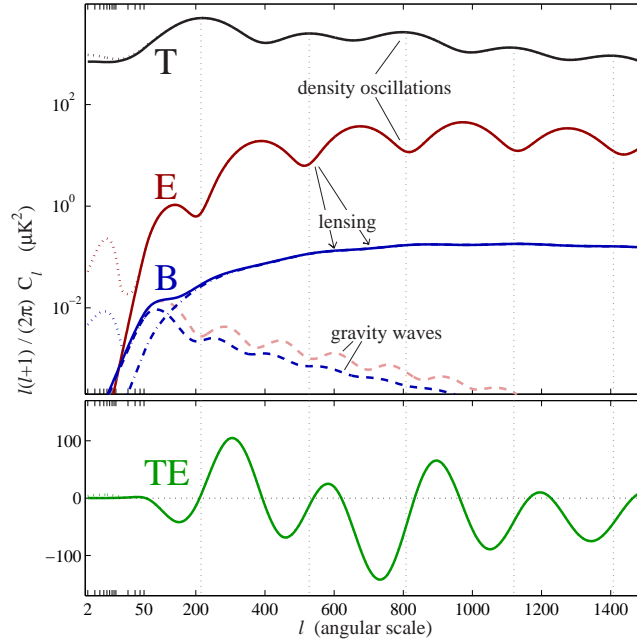


Figure 2.3: Predicted power spectra for: Temperature (T), E-mode polarisation (E), B-mode polarisation (B), and Temperature-E-mode cross correlation (TE). The modification of each spectrum resulting from reionization observed by WMAP is shown by the dotted lines. Gravitational waves at a level allowed by current data introduce contributions to the E-mode and B-mode spectra shown by the dashed lines. The dot-dash line shows the contribution to the B-mode signal resulting from lensed E-modes. The figure is from [35].

Parameter	WMAP data
Matter density	$\Omega_m h^2 = 0.14 \pm 0.02$
Baryon density	$\Omega_b h^2 = 0.024 \pm 0.001$
Hubble parameter	$h = 0.72 \pm 0.05$
Amplitude	$A = 0.9 \pm 0.1$
Optical depth	$\tau = 0.166^{+0.076}_{-0.071}$
Spectral index	$n = 0.99 \pm 0.04$

Table 2.1.1: Cosmological parameters using WMAP data. The errors are at 1σ as reported in [153].

We conclude this paragraph remarking that several numerical codes allow to calculate CMB primary anisotropies and polarization as well as density perturbations: among them we recall the ones we have used, namely the CMBfast fortran code published by U.Seljak and M.Zaldarriaga [155, 46] and the CMBeasy C++ code published by M.Doran [45, 57, 59]. Power spectra of the temperature and polarisation maps can then be used to constrain cosmological parameters and models. In tab.(2.1.1) and tab.(2.1.2) we show a summary of the most important parameters and derived parameters estimated by WMAP alone, with errors at 1σ as reported in [153].

2.1.2 Large Scale Structure

Another fundamental source of information for cosmology consists in matter density fluctuations generated from quantum mechanical fluctuations originated when the Universe was a fraction of a second old. In particular, Large Scale Structures (LSS) formed from small gravitational instabilities consistent with CMB, thus implying that the gravitational potential $\Psi \sim 10^{-5}$. Note that even though both matter inhomogeneities and CMB anisotropies originated from the same source, they appear very different today: indeed, while matter inhomogeneities grew to form large scale structures through gravitational instability, pressure prevents photons from realizing the same process. Galaxies then form after a factor of about 1000 in expansion since recombination.

The major information on LSS comes from the density perturbation δ defined in (1.109). Linear perturbation theory tells us that the density perturbation in the baryon-radiation fluid grows only logarithmically during Radiation Dominated Era (RDE): at that time the gravitational potential

Derived Parameter	WMAP data
Matter density	$\Omega_m = 0.29 \pm 0.07$
Baryon density	$\Omega_b = 0.047 \pm 0.006$
Amplitude of galaxy fluctuations	$\sigma_8 = 0.9 \pm 0.1$
Age of the Universe	$t_0(\text{Gyr}) = 13.4 \pm 0.3$
Redshift at matter-radiation equality	$z_{eq} = 3454_{-392}^{+385}$
Redshift at decoupling	$z_{dec} = 1088_{-2}^{+1}$
Redshift at reionization	$z_r = 17 \pm 5$
Dark Energy equation of state	$\omega_{DE} < -0.78(95\%CL)$

Table 2.1.2: Derived cosmological parameters using WMAP data. All errors but the last one are at 1σ as reported in [153].

is constant on super-horizon scales and oscillates and decays on sub-horizon scales; in Matter Dominated Era (MDE) δ starts increasing linearly with the scale parameter ($\delta \propto a$) with a factor of proportionality which depends on the value of the gravitational potential Φ at the equivalence; the gravitational potential is instead $\Psi \sim \text{const}$ at all scales [17, 61].

The matter power spectrum is then obtained as the mean quadratic value of the fluctuation for the k mode:

$$P_k \equiv \langle |\delta_k(\eta)|^2 \rangle \quad (2.2)$$

where the average is done over the volume in k -space or, equivalently, as the Fourier transform of the two-point correlation function:

$$\langle \delta(\mathbf{x})\delta(\mathbf{x} + \mathbf{r}) \rangle = \int d^3\mathbf{k} P(k) e^{i\mathbf{k}\cdot\mathbf{r}} \quad (2.3)$$

The evolution of density perturbation is regulated by Einstein equations; ignoring the radiation terms and for scales smaller than the horizon, the CDM density contrast grows according to the following equation:

$$\delta_m'' + \mathcal{H}\delta_m' - \frac{3}{2}\Omega_m\mathcal{H}_0^2\frac{\delta_m}{a} = 0 \quad (2.4)$$

This is a second order differential equation with homogeneous coefficients whose solution can be written separating the space and time dependence:

$$\delta_m(\eta, \mathbf{x}) = \delta_+(\mathbf{x})D_+(\eta) + \delta_-(\mathbf{x})D_-(\eta) \quad (2.5)$$

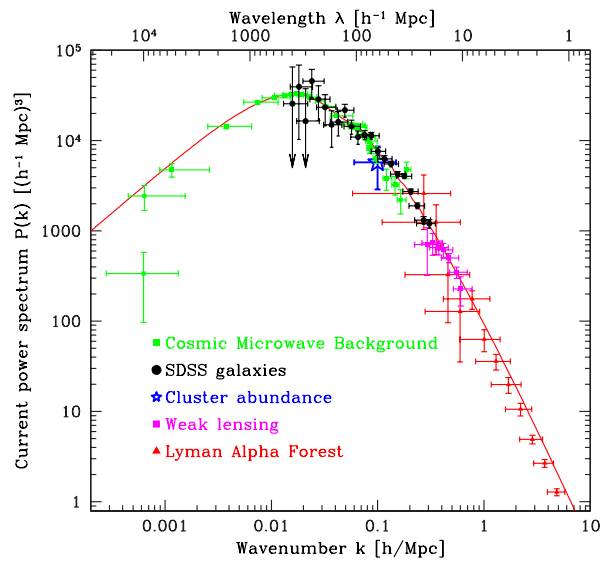


Figure 2.4: Matter density power spectrum $P(k)$ as a function of k as constrained by CMB, SDSS, cluster abundancies, gravitational lensing and the Lyman- α forest [126].

where, given $\Omega_m > 0$, D_+ and D_- grow and decay in time respectively.

Note that a necessary requirement for any consistent theory of structure formation is that the density perturbation, whose amplitude was $\delta \sim 10^{-5}$ at the last scattering surface ($z = 1100$), needs to expand up to $\delta \sim 10^2$ at redshifts of $z \ll 1$ in order to allow the formation of galaxies.

The primordial spectrum of density perturbations (fig.2.4), is observed to be equal to

$$P_{k_0} = \langle \delta_k(0)^2 \rangle = Ak^{n_s} \quad (2.6)$$

where $\delta_k(0)$ is the value of the matter density perturbation at present time and the power law index n_s determines the relative distribution of power at different scales. Primordial density fluctuations are usually assumed to be Gaussian in nature and with random phases; moreover observations suggest that $n_s \sim 1$, corresponding to a nearly scale-invariant spectrum (Harrison-Zeldovich spectrum).

With regard to the shape, two regions can be identified within the matter power spectrum: at super horizon scales the shape of the power spectrum is gauge dependent; at smaller scales, hence before matter domination, the amplitude of the matter fluctuation is damped compared to larger scales due to the fact that matter perturbations grow less during Radiation Dominated Era (RDE). The bend in the middle corresponds to the scale that entered the horizon at matter-radiation equality. Finally, the shape of the power spectrum depends on the content and nature of Dark Matter with a subdominant dependence on the baryon density and can be constrained through CMB, as well as through several other types of observations which also contribute to determine the amount of baryons and Dark Matter in the Universe. We will now briefly recall some of these measurements:

- Galaxy distribution: two main surveys for galaxy observation have been realized, able to give a three dimensional view of large scale structures in the Universe. The 2-degree Field (2dF) Galaxy Redshift Survey has measured nearly 230.000 redshifts allowing to constrain the power spectrum for $k > 0.02 h \text{ Mpc}^{-1}$ with 10% accuracy [88]. The measured density power spectrum fits with a CDM model with $\Omega_m h = 0.168 \pm 0.016$ and a baryon fraction $\Omega_b/\Omega_m = 0.185 \pm 0.046$ [138]; the neutrino contribution is estimated to be $\Omega_\nu/\Omega_m < 0.13$ at 95% confidence level [88]. In fig.(2.5) we can see an example of map of the galaxy distribution, in which each pixel covers a patch of 0.1 degrees and the brighter the pixels the more galaxies are there. The Sloan Digital Sky Survey (SDSS) has measured the three dimensional power spectrum $P(k)$ using over 200.000 galaxies in a quarter of the sky providing constraints which tighten limits on Ω_Λ and h independently of CMB and 2dF data [125]. Note, however, that galaxy surveys measure the galaxy power spectrum $P_g(k)$ which needs to be related to $P_k \equiv P_{CDM}(k)$ via a constant multiplying factor b called the linear

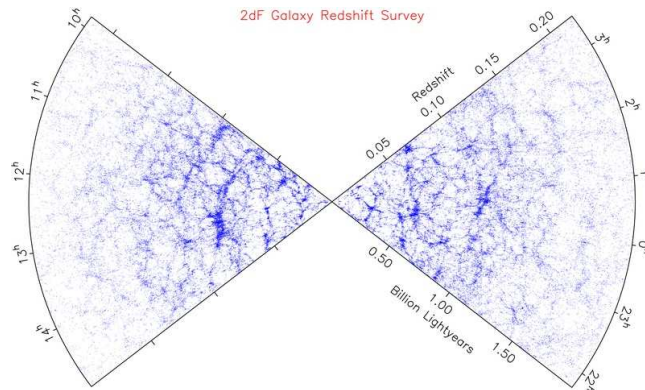


Figure 2.5: Map of the galaxy distribution produced by 2dF in June 2003.

The figure is from [137].

bias, which does not depend on the scale as long as we work at scales where the anisotropies are linear ($k/h \leq 0.15 Mpc^{-1}$), while at smaller scales the pattern is modified by galaxy peculiar velocities. In fig.(2.6) one dimensional likelihoods for the two major surveys are compared.

- Rotation curves of spiral galaxies: though the observational evidence for a flat Universe is quite recent, the need for a Dark Matter component in the Universe was originally pointed out in 1933 by Zwicky, by realizing that the velocities of individual galaxies located within the Coma cluster are larger than expected: the cluster can only be gravitationally bound if its total mass exceeds the sum of the masses of its component galaxies. Velocity curves have been compiled for over 1000 spiral galaxies thanks to the Doppler shift associated to the radio emission (21 cm line) from neutral hydrogen. The orbital velocity raises linearly from the center outward and then remains flat, even at distances large enough for there to be no luminous galactic component (fig. 2.7). This is in contrast with the decaying behavior $v_{rot} = (GM/r)^{1/2}$ expected if all the mass were virialized and associated with light. A possible explanation is that the galaxy bulk and thin disk is surrounded by non luminous matter⁴ (Dark Matter) whose mass increases as $M \propto r$.

⁴The total mass of an individual galaxy is still uncertain since a turn around to the $v \propto r^{-1/2}$ at large radii has not yet been observed; only recently, a group from the SDSS claims the detection of the edge of the dark matter halo, where the rotational curve falls off [123].

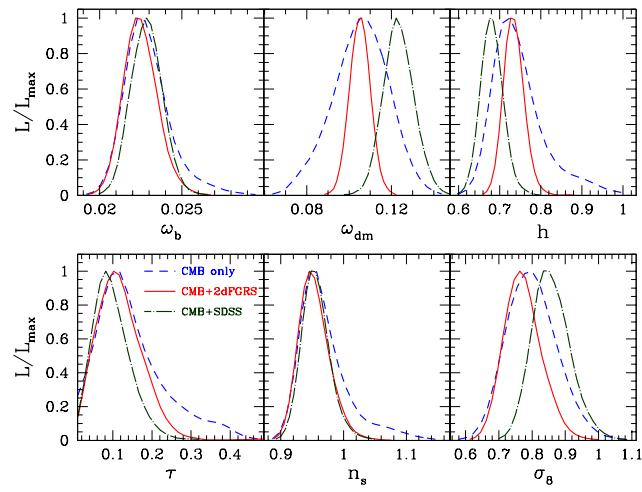


Figure 2.6: Marginalized one-dimensional likelihoods in the basic-six parameter space described in [122]: curves are shown for CMB data only (dashed lines), CMB plus the 2dF (solid lines) and CMB plus the SDSS (dot-dashed lines).

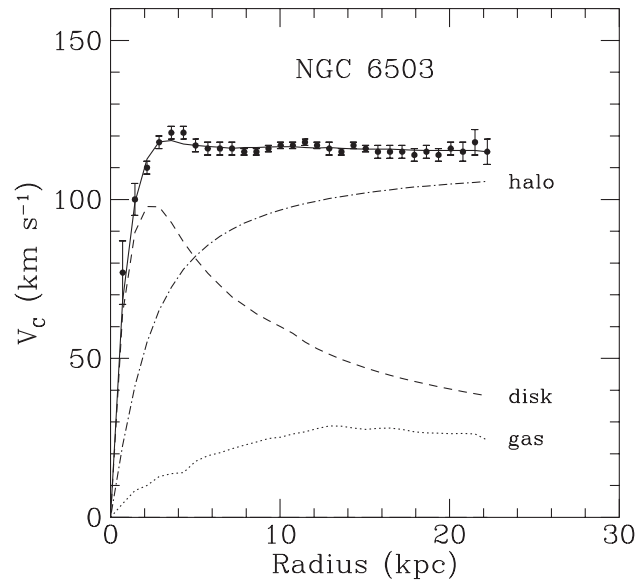


Figure 2.7: Rotation curve of the spiral galaxy NGC 6503 as established from radio observations of hydrogen gas in the disk [14]. The dashed line shows the rotation curve expected from the disk material alone, the dot-dashed line from the dark matter halo alone. The figure is from [115].

- Clusters of galaxies: the number density of clusters⁵ depends on the size of primordial density perturbations and is used to constraint the σ_8 amplitude, which sets the size of the mass fluctuation in spheres of radius $8h^{-1}$ Mpc, a region containing about the right amount of material to form a cluster. Observations mainly come from the X-ray emission from hot gas in the cluster, whose temperature can be used to estimate the mass of the cluster. The σ_8 parameter, equal to $0.78^{+0.30}_{-0.06}$ at 95% CL [88] mainly depends on the Dark Matter density (favouring low matter density), with a sub-dominant dependence on the Dark Energy density. If clusters well represent the mass distribution in the Universe, at least within a 20% systematic error, they can help finding an estimate of the baryonic content, mainly present in the form of X-ray emitting gas and in stellar galaxies present in clusters. The following approximated relation holds:

$$\Omega_m \sim \frac{\Omega_b}{0.08h^{-1.5} + 0.01h^{-1}} \quad (2.7)$$

and if we consider the BBN estimate on $\Omega_b h^2 \approx 0.02$, then $\Omega_m h^2 \approx 0.25$.

- Lyman Alpha⁶ forest: the presence of clouds of neutral hydrogen gas in the intergalactic medium is detected, since the gas absorbs light from distant objects like quasars.
- Gravitational lensing: the image of a galaxy observed in the background is deformed due to mass fluctuations along the line of sight, generating strong or weak lensing according to the amplitude of the deformation. Weak lensing is now widely used to measure the mass power spectrum and measurements are mainly sensitive to Ω_M and the amplitude σ_8 .
- Baryonic oscillations [63]: while Dark Matter primordial perturbation grow in place, baryonic perturbations expand outward in a spherical wave, reaching a shell of radius ~ 150 Mpc at recombination. Though both perturbations combine to the formation of large scale structure, the Dark Matter ones are dominant and the baryonic shell appears as weak oscillations in the CMB as well as in the matter power spectrum. Both SDSS [127] and 2dF [138], using totally different samples, have recently claimed the detection of the first acoustic peak of baryon oscillations at the 4σ level and, if confirmed, this would give another hint for the existence of Dark Matter since a fully baryonic model produces an effect much larger than the observed one.

⁵A cluster is a collection of galaxies held together by mutual attraction up to $10^{15} M_\odot$.

⁶The Lyman-alpha is the spectral line at 1216 \AA in the far ultraviolet corresponding to the transition of an electron between the two lowest energy levels of a hydrogen atom.

2.1.3 Type Ia supernovae

The first evidence of cosmic acceleration came with measurements from type Ia Supernovae (SNe Ia)⁷. Since their light has travelled a large fraction of the Universe before being observed, we can expect it to be a possible indicator of the geometry of the Universe and of the rate of expansion. This can actually be realized relating the distance of the source to $H(z)$.

Theoretically, if we had a set of sources (standard candles) of known intrinsic luminosity L , one could use the observed flux F to estimate the luminosity distance $d_L \equiv \sqrt{L/4\pi F}$, which is related to the expansion via the Hubble parameter $H(z)$:

$$d_L = (1+z) \int \frac{dz'}{H(z')} \quad (2.8)$$

Using eq.(1.37) we can relate d_L to the cosmological parameters:

$$d_L(z) = H_0^{-1}(1+z) \int_0^z [d\tilde{z}[\Omega_{r0}(1+\tilde{z})^4 + \Omega_{m0}(1+\tilde{z})^3 + \Omega_{\Lambda_0} + \Omega_{x_0} e^{3 \int_0^z (1+\omega_x(z')) \frac{dz'}{1+z'}}]^{-1/2}] \quad (2.9)$$

and, combining it with (1.38, 1.39, 1.40) we can rewrite d_L as [80]:

$$d_L(z) = \frac{1}{H_0} \left\{ z + \frac{1}{2}[1-q_0]z^2 - \frac{1}{3!}[1-q_0-3q_0^2+j_0]z^3 + o(z^4) \right\} \quad (2.10)$$

Although SNe Ia do not behave as perfect standard candles, in the sense that their luminosity curves deviate from a common pattern (fig. 2.8, left), it has been demonstrated that when the curve is corrected with a relation between the light curve shape and the luminosity at maximum brightness (brighter SNe last longer), the dispersion of the measured luminosities can be greatly reduced (fig.(2.8), right) [80]. A wide set of measurements has been performed independently by two groups: the Supernova Cosmology Project [131] and the High-z Supernova Search Team [78, 79, 80] and both found that SNe are dimmer than we would expect if the Universe were decelerating its expansion (fig.(2.9)), thus providing evidence for an accelerating Universe. Furthermore, a linear combination of Ω_m and Ω_Λ has been found and constrained [132]:

$$0.8\Omega_m - 0.6\Omega_\Lambda = -0.16 \pm 0.05 \quad (1\sigma) \quad (2.11)$$

⁷SNe Ia are due to the thermonuclear explosion of a carbon-oxygen white dwarf which accretes matter from a companion star in a binary system, until it passes the Chandrasekhar limit. The intensity of the emitted radiation takes about three weeks to reach its maximum brightness and then declines over a period of months.

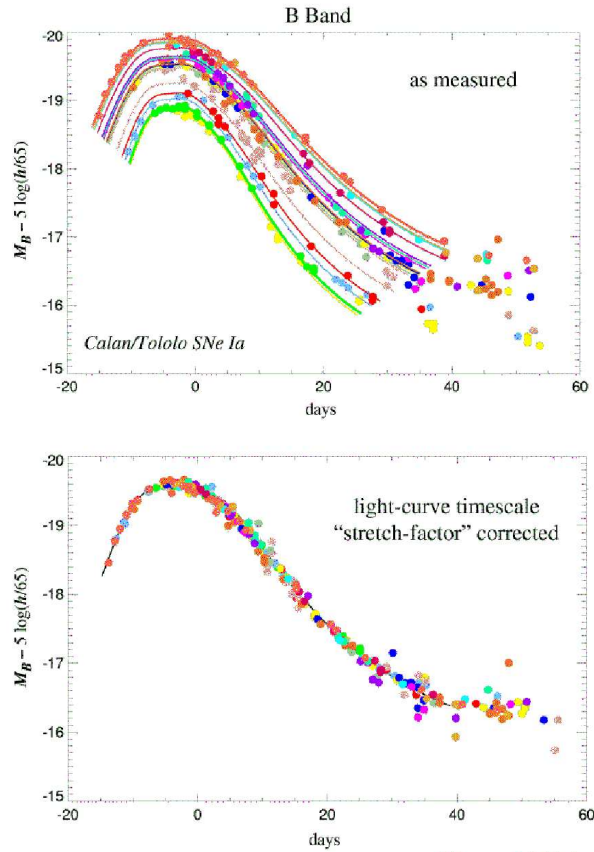


Figure 2.8: Light curves of Type Ia supernovae (L vs t): the relation between the absolute luminosity and the timescale is shown (upper panel). In the lower panel the timescale is multiplied by a stretch correcting factor.

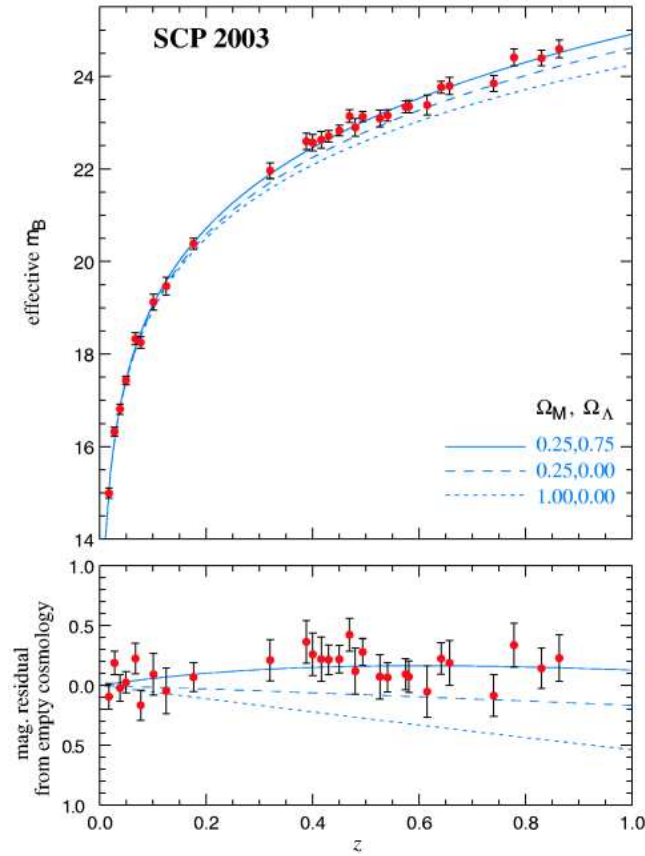


Figure 2.9: Upper panel: Hubble diagram in linear redshift scale [132]. The solid curve represents the best-fit flat-universe model, ($\Omega_m = 0.25, \Omega_\Lambda = 0.75$). Two other cosmological models are shown for comparison: ($\Omega_m = 0.25, \Omega_\Lambda = 0$) and ($\Omega_m = 1, \Omega_\Lambda = 0$). Lower panel: residuals of the averaged data relative to an empty universe.

For a flat Universe, this leads to $\Omega_\Lambda = 0.71 \pm 0.05$ and $\Omega_m = 0.29 \pm 0.05$ at 1σ . Using only the background equations, without solving the perturbed ones, SNIa data can provide the likelihoods for the parameters, as shown in fig.(2.10) in the well known plane $(\Omega_\Lambda, \Omega_m)$. Note that in SNIa data it

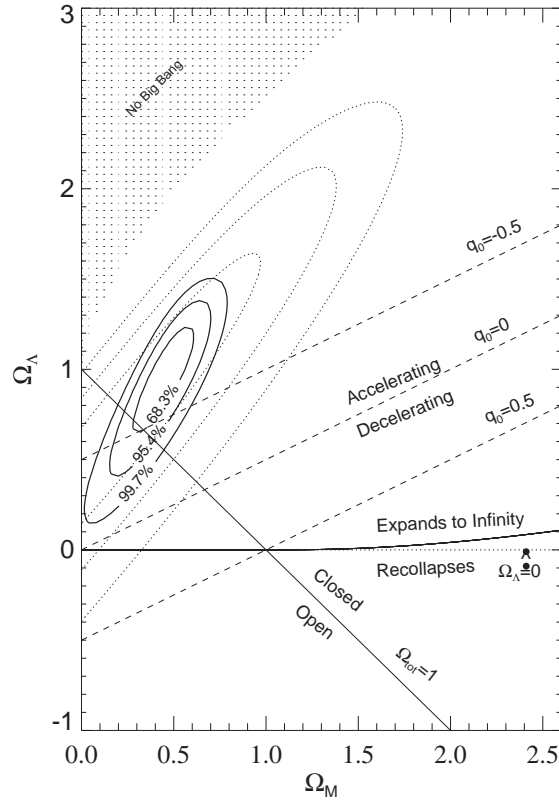


Figure 2.10: 2d likelihoods in the $(\Omega_\Lambda, \Omega_m)$ plane. The solid contours are the result from the gold sample of 157 SNe presented in [80]. The dotted contours are results from [79].

is difficult to go to redshifts higher than the ones already measured since not only supernovae get fainter but also, since only the region of the peak is really observed, it is harder to obtain the fit of the whole light curve, necessary since SNIa are not perfect standard candles. Despite the fact that several possible systematic effects may affect the accuracy of the SNe Ia as distance indicators (for example interstellar extinction in the host galaxy and in the Milky Way), there is yet no evidence that any of these systematic errors is significant to constrain parameters. Note also that even though SNe provide a strong support to the presence of a Λ /DE component accelerating the Universe, arguments for a significant Dark Energy contribution in the

Universe had been proposed long before SNe Ia observations, in order to explain the ages of globular clusters and the observed distribution of galaxies, clusters and voids.

Combining the experimental results All the experiments we have quickly recalled give impressively concordant results. Combined likelihood functions can be found in [125] both in one (fig.2.12) and in two (fig.2.11) dimensions, in which SDSS constraints are included in combination with other CMB experiments (WMAPext). A table similar to (2.1.1) can be found in [153] including WMAP+2dF results whose combination gives, for example, a value of $\Omega_m h = 0.18 \pm 0.02$ and a baryon fraction $\Omega_b/\Omega_m = 0.17 \pm 0.06$ [139]. Models with 10 parameters ($h, \Omega_m, \Omega_b, \Omega_\Lambda, \Omega_r, \Omega_\nu, \Delta, n, r, \tau$) can provide a

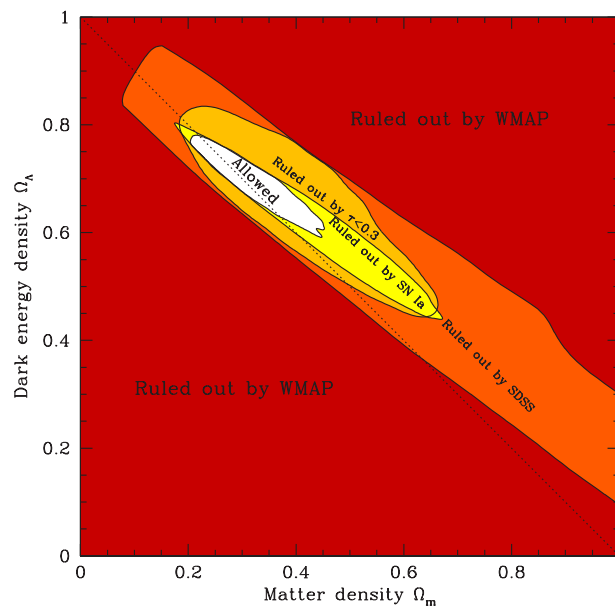


Figure 2.11: Constraints at 95% CL in the $(\Omega_m, \Omega_\Lambda)$ plane. Shaded dark red/grey region is ruled out by WMAP alone for a choice of parameters illustrated in [125]. The light red/grey region is ruled out when adding SDSS data. The figure also shows the regions ruled out when $\tau < 0.3$ is assumed and when adding data from SNIa. Models on the diagonal dotted line are flat models, those below are open and those above are closed.

good fit to the complete set of data available at present: however, since

observations are consistent with spatial flatness and inflation models automatically generate spatial flatness, it is possible to set $\Omega = 1$. In addition, there is no observational evidence for the existence of tensor perturbations and so r could be set to zero. WMAP alone is the most powerful experiment so far, able to give, alone, an estimate of most of the considered parameters: under the assumption that the primordial perturbations are adiabatic with a power-law spectrum, $\Omega_m = 1$ can be ruled out from CMB alone; the Ω_Λ parameter, though, is still obtained as a derived quantity in the analysis, performed assuming a flat Universe. Note however that WMAP and the Hubble space telescope can prove alone the acceleration of the Universe even without the need of controversial data from SNIa.

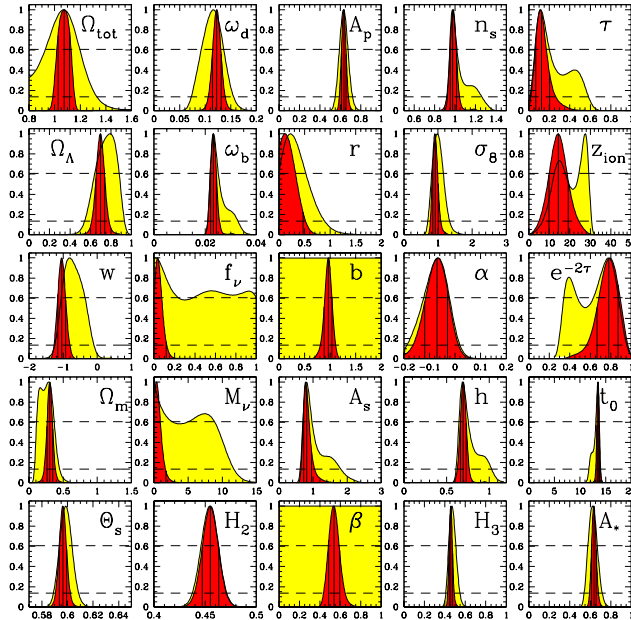


Figure 2.12: One dimensional likelihood functions for individual cosmological parameters are shown, using WMAP alone (light grey/yellow) and including SDSS data (dark grey/red). Each distribution has been obtained marginalizing over all other quantities as illustrated in [125].

Confirmation of the presence of Dark Energy has recently come from another independent detection which concerns cross correlation between CMB maps and LSS surveys. As we have discussed in the comments which follow

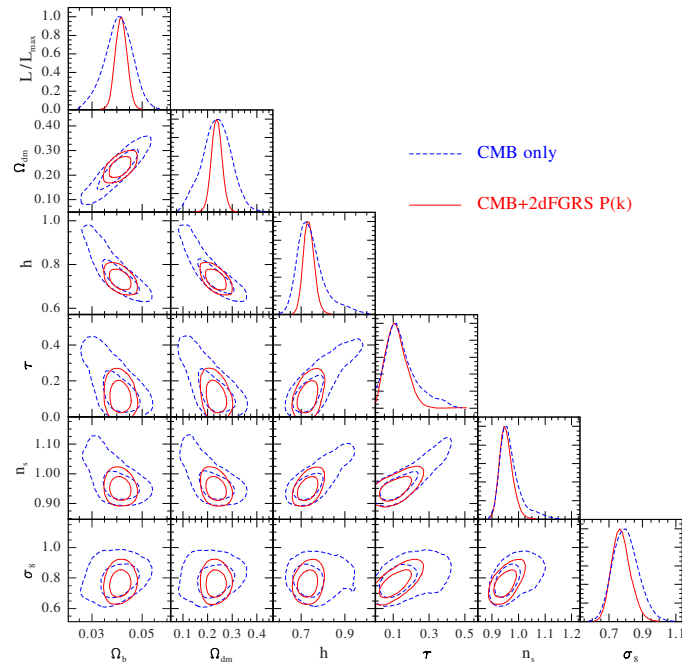


Figure 2.13: Marginalized likelihoods for the cosmological parameters in the basic-six model described in [122]: the plot shows CMB data only (dashed lines) and CMB plus 2dF (solid lines). The diagonal shows the 1-d likelihood for individual parameters; the other panels show the 2-d likelihood contours for pairs of parameters, obtained by marginalizing over the other parameters.

eq.(1.207), when Dark Energy dominates over the other components, matter gravitational potentials evolve, causing an additional redshift or blueshift on CMB photons as they travel through; at large scales this LISW effect is well visible in the CMB spectrum. The local origin of the LISW effect creates the expectation of a non-null cross correlation between CMB and LSS, due to the fact that the same gravitational potential created by galaxies also affects CMB anisotropies. The amplitude and sign of the cross correlation depend only on Ω_{DE} , Ω_k and h and therefore cross correlation represents a further indication of the presence of Dark Energy. Different surveys and methods have been used to perform this measurement [25] [124] [152] [141] the latter of which shows the maximum signal, at 3σ detection, when cross correlation between the radio galaxy survey NVSS [101] and WMAP is considered.

In conclusion, several evidences confirm that the amount of the total matter density is not more than 30% so that, in order for the Universe to be flat, we need to have an extra component counting for the remaining 70%. The simplest and yet possible choice consists in a pure cosmological constant Λ . This model is referred to as Λ CDM whose basic ingredients are given by $\Omega_b \sim 0.04$, $\Omega_c \sim 0.26$, $\Omega_\Lambda \sim 0.70$ and a Hubble constant $h \sim 0.7$. The spatial geometry is very close to flat (and often assumed to be precisely flat), and the initial perturbations are Gaussian, adiabatic, and nearly scale-invariant. There is yet no clear evidence of evolution of the Dark Energy density and future experiments will also aim to set constraints on the cosmic equation of state $\omega(z)$, which is so far in agreement with a cosmological constant (fig.2.14).

Even though there is not a single experiment which provides alone all the estimated values of the parameters, there is no other model like the Λ CDM model which agrees simultaneously with the whole set of observations and this explains why, although Λ CDM main ingredients are still unknown, the Λ CDM model is almost universally accepted by cosmologists as the best description of present data and it represents, up to now, the standard cosmological model and the essence of concordance cosmology.

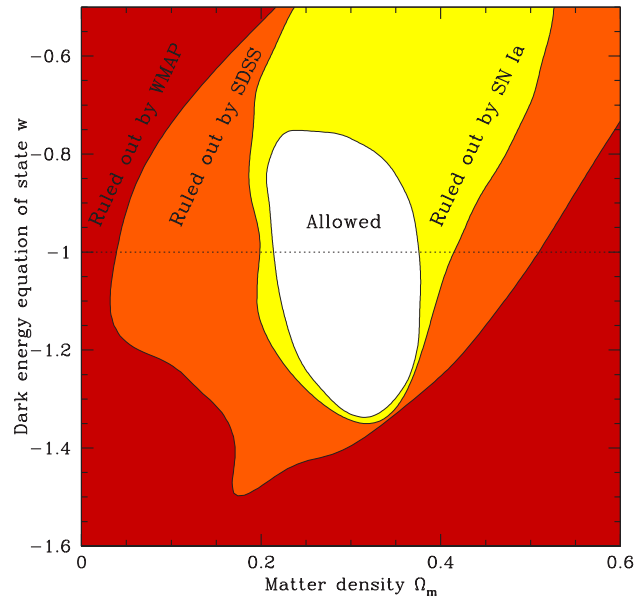


Figure 2.14: Constraints at 95% CL in the (Ω_m, ω_{DE}) plane, where ω_{DE} is the Dark Energy equation of state. The shaded dark red/grey region is ruled out by WMAP alone for a choice of parameters illustrated in [125]. The light red/grey region is ruled out when adding SDSS data. The figure also shows the region ruled out when adding data from SNIa (yellow/very light grey).

Chapter 3

Quintessence scalar field

3.1 Dark energy as a minimally coupled scalar field

A minimal generalization of Λ consists in a scalar field $\phi(x)$ called Quintessence (Q) which interacts only with itself and, minimally, with gravity. The idea of a dynamical component, viewed as a possible alternative to a cosmological constant, has its origins both in particle physics and in cosmology: while the former looked for a dynamical cancellation of the vacuum energy density, the latter tried to reconcile the need for a flat universe with the small mass density indicated by galaxy peculiar velocities without incurring in the fine-tuning and coincidence problems: on both sides the intent was to justify the smallness of Λ in the present epoch as a consequence of the age of the Universe ($t_0 \sim 13 \times 10^9$ yrs), old enough for the field potential to decay towards zero and naturally decrease with time similarly to what matter and radiation do. The guess of a scalar field was mainly inspired by the inflationary scenario, in which, in order to account for the homogeneity of the cosmic microwave background, a scalar field (the inflaton) is responsible for the accelerated expansion which occurred in the very early stages of the evolution of the Universe. Analogously, the quintessence field needs to account for the accelerating expansion that started when the Universe was about two-third of the present size. Furthermore, the choice of a scalar field represents the simplest way to introduce new physics beyond the well-tested standard model.

The simplest quintessence model is characterized by the action:

$$S = \int \sqrt{-g} d^4x \left(\frac{1}{2} g^{\mu\nu} \partial_\mu \phi \partial_\nu \phi + V(\phi) \right) \quad (3.1)$$

where $V(\phi)$ is a scalar potential and g is the usual determinant of the metric tensor $g_{\mu\nu}$. By deriving with respect to the metric we get the corresponding

energy momentum tensor, given by:

$$T^\mu{}_\nu \equiv \partial^\mu \phi \partial_\nu \phi - \delta_\nu^\mu \left(\frac{1}{2} \partial^\alpha \phi \partial_\alpha \phi + V(\phi) \right) \quad (3.2)$$

As we will see in the next paragraph, the field ϕ usually depends on both temporal and spatial coordinates; however, since the homogeneous background field $\bar{\phi}(\eta)$ of $\phi(x)$ only depends on η , the energy momentum tensor (3.2) can be substantially simplified

$$\bar{T}_\nu^\mu(\eta) = \begin{pmatrix} -\rho & 0 \\ 0 & \delta_j^i p \end{pmatrix} \quad (3.3)$$

reducing to that of a perfect fluid (1.15) with energy and pressure given by

$$\rho_{\bar{\phi}} = \frac{1}{2a^2} \bar{\phi}'^2 + V(\bar{\phi}) \quad (3.4)$$

$$p_{\bar{\phi}} = \frac{1}{2a^2} \bar{\phi}'^2 - V(\bar{\phi}) \quad (3.5)$$

where the bar indicates that we are considering background quantities. The energy conservation equation for the scalar field is equal to the one written in (1.21); we recall it here for convenience

$$\frac{\rho'_{\bar{\phi}}}{\rho_{\bar{\phi}}} = -3\mathcal{H}(1 + \omega_\phi) \quad (3.6)$$

together with the Friedmann equation (1.16) in the case of a flat Universe:

$$\mathcal{H}^2(\eta) = \frac{8\pi G}{3} a^2 \left(\rho_{fluid} + \frac{1}{2a^2} \phi'^2 + V(\phi) \right) \quad (3.7)$$

which can also be rewritten as

$$H^2 = \frac{8\pi G}{3} \sum_i \rho_{i0} e^{3 \int_0^z \frac{1+\omega_i(z')}{1+z'} dz'} \quad (3.8)$$

where we have made the Hubble parameter dependence on ω_Q explicit. The equation of motion for the field (Klein Gordon equation) can be obtained either deriving the action with respect to the field ϕ or directly from the continuity equation (3.6):

$$\ddot{\bar{\phi}} + 3H\dot{\bar{\phi}} + V_{,\bar{\phi}} = 0 \quad (3.9)$$

where the dot derivatives are with respect to the cosmic time and $V_{,\bar{\phi}} \equiv \partial V / \partial \bar{\phi}$; if derivatives are calculated with respect to the conformal time the Klein Gordon equation reads as:

$$\bar{\phi}'' + 2\mathcal{H}\bar{\phi}' + a^2 V_{,\bar{\phi}} = 0 \quad (3.10)$$

The steepness of the potential drives the field, which is on the other hand slowed down by the Hubble friction.

The quintessence scalar field is also characterized by a sound velocity defined as usual and equal to [87]:

$$c_{s\phi}^2 \equiv \frac{p'_{\phi}}{\rho'_{\phi}} = \frac{\phi' [3\mathcal{H}\phi' + 2a^2V_{,\phi}]}{3\mathcal{H}(1 + \omega_{\phi})(\phi'^2 + a^2V)} \quad (3.11)$$

Using (3.6) we can also express the sound velocity of the scalar field in terms of its equation of state¹:

$$c_{s\phi}^2 = \omega_{\phi} - \frac{1}{3\mathcal{H}} \frac{\omega'}{1 + \omega'} \quad (3.12)$$

If the field potential $V(\phi)$ is Taylor expanded to the quadratic order in the field $\phi(x)$ about the homogeneous mean background $\bar{\phi}(\eta)$, we get the mass of the field:

$$m_{\phi}^2 = V''(\bar{\phi}) \quad (3.13)$$

Within the context of a minimally coupled model (as for example the inverse power-law model we will recall soon ahead in this Chapter), the quintessence field results to be very light, with a mass of approximately $m_{\phi}(t_0) \sim 10^{-33}$ eV; the tiny value of the mass is due to the requirements that $V(\phi)$ varies slowly with the field value and that the current value of $V(\phi)$ must be observationally acceptable. [116].

One of the most significant parameters for ϕ is the equation of state defined in (1.20) which, for a minimally coupled quintessence field, is equal to

$$\omega_Q = \frac{\frac{1}{2}\dot{\phi}^2 - V}{\frac{1}{2}\dot{\phi}^2 + V} \quad (3.14)$$

Note that in the limit in which the field is a cosmological constant, $\dot{\phi} = 0$ and hence we recover $\omega_{\Lambda} = -1$. One of the key observational features of Dark Energy is then that $\omega_Q \neq -1$. In principle, the quintessence equation of state ω_Q is not a constant but can vary with time; despite the fact that experiments are mainly sensitive to some average value weighted over recent epochs and that present observations are so far consistent with a cosmological constant, ω_Q is usually considered as a free parameter [88] whose limit has been shown in tab.(2.1.2) as reported by WMAP [153]; a subsequent analysis [125] which includes SDSS data, constraints ω_Q within the range

$$-1.19 < \omega_Q < -0.83 \quad (3.15)$$

¹The sound velocity is not a well defined concept for classical scalar fields [87] since it can change sign.

if the ratio between tensor and scalar modes is fixed to $r = 0$ or

$$-1.11 < \omega_Q < -0.77 \quad (3.16)$$

if tensor modes are included. Though highly constrained, some information could come when parametrizing the equation of state in terms of the scale factor, in such a way that, for example, $\omega_Q(a) = \omega_{Q_0} + \omega'_Q a$. In the plane ω'_Q, ω_Q Dark Energy models are not yet well constrained [33].

Usually ω_Q is restricted to the case $\omega_Q \geq -1$ to avoid violation of the weak energy condition².

The dependence of the quintessence energy density on the redshift (or equivalently on the scale parameter) can easily be expressed in terms of the equation of state ω_ϕ by integrating the continuity equation (3.6):

$$\rho_{\bar{\phi}} = \rho_{\bar{\phi}_0} e^{3 \int_0^z \frac{1+\omega_\phi(z')}{1+z'} dz'} = \rho_{\phi_0} e^{[-3 \int_0^a d \ln a' [1+\omega_\phi(a')]]} \quad (3.17)$$

equal to $\bar{\rho}_\phi \sim a^{-3(1+\omega_\phi)}$ if ω_ϕ is a constant. As a consequence, the time evolution of ω_ϕ determines the time evolution of quintessence by altering the slope of $\rho_{\bar{\phi}}(a)$. As we see from eq.(3.14) and (1.19), if the field slowly rolls in the potential or, in other words, if its pressure is sufficiently negative to have repulsive gravitational effects, then the field will accelerate the expansion of the universe soon after it starts dominating over ordinary matter³. In minimally coupled models the scalar field does not play a significant role in the evolution of the Universe up to about $z \sim 2$ and has its main effect only in recent times when it comes to dominate. This happens earlier for quintessence models compared to Λ CDM models since

$$a_{\Lambda DE} = \left(\frac{\rho_{m_0}}{\rho_{\Lambda_0}} \right)^{1/3} > a_{Q DE} = \left(\frac{\rho_{m_0}}{\rho_{Q_0}} \right)^{1/3|\omega_Q|} \quad (3.18)$$

Note that in principle, using (3.14), one could think of reconstructing the kinetic energy, the potential and the field, directly from the dependence of the equation of state on the scale factor:

$$T(a) \equiv \frac{1}{2} \dot{\phi}^2 = \frac{1}{2} \rho_\phi(a) [1 + \omega_\phi(a)] \quad (3.19)$$

$$V(a) = \frac{1}{2} \rho_\phi(a) [1 - \omega_\phi(a)] \quad (3.20)$$

$$\phi(a) = \int d \ln a H^{-1} \sqrt{\rho_\phi(a) [1 + \omega_\phi(a)]} \quad (3.21)$$

²The weak energy condition states that the energy density measured by any observer in his rest frame is always non-negative; models in which the scalar field is characterized by an equation of state $\omega_\phi < -1$ have been recently investigated too within a variety of possibilities: braneworld models [121], scalar-tensor models [128], phantom models [29].

³We recall that in order to provide an acceleration to the Universe expansion, Dark Energy's equation of state needs to be negative and $\omega_\phi < -1/3$.

Nevertheless, a direct reconstruction results to be very difficult to achieve; hence, people have mainly tried to proceed phenomenologically to find potentials which are able to address the inevitable problems encountered in a cosmological constant framework. Before illustrating the most popular guesses for the quintessence potential, we will first discuss perturbations of the field, which account for its dependence on spatial coordinates.

3.1.1 Perturbations

In order to be meaningful, the quintessence scalar field is not really homogeneous but has perturbations depending on the coordinate point

$$\phi(\eta, \mathbf{x}) = \varphi(\eta) + \delta\phi(\eta, \mathbf{x}) \quad (3.22)$$

where we have redefined the background $\bar{\phi} \equiv \varphi(\eta)$ for convenience and we can rewrite

$$\delta\phi(\eta, \mathbf{x}) = \chi(\eta)Y_{\mathbf{k}}^{(0)}(\mathbf{x}) \quad (3.23)$$

where the set of functions $Y^{(0)}$ has been defined in (1.63). Note that the homogeneous and perturbed scenarios do not represent models in competition with each other: the scalar field must have fluctuations since any smooth time evolving $\Lambda(t)$ component is unphysical, being gauge dependent, not well defined and in contrast with the equivalence principle [28]. Usually, however, we don't see spatial fluctuations because the field $\phi(x)$ is very light and as a consequence, at least in minimally coupled scenarios, perturbations of the quintessence field move away very fast below the horizon so that relativistic pressure prevents them from clustering in potential wells.

Linear perturbation behavior is rather well understood; under a gauge transformation of type (1.74) with ϵ given by (1.77), the scalar field and its perturbation transform as in (1.76):

$$\tilde{\phi}(x) = \phi(x) + \varphi'(\eta)T_{\mathbf{k}}(\eta)Y_{\mathbf{k}}^{(0)}(\mathbf{x}) \quad (3.24)$$

$$\tilde{\chi}(\eta) = \chi(\eta) - \varphi'(\eta)T_{\mathbf{k}}(\eta)Y_{\mathbf{k}}^{(0)}(\mathbf{x}) \quad (3.25)$$

so that the combination

$$X = \chi - k^{-1}\sigma\varphi' \quad (3.26)$$

is gauge invariant [87]. Since in the Newtonian/longitudinal gauge $\sigma = 0$, we have that $X^{\text{long}} = \chi$. Perturbing the energy momentum tensor (3.2) to the first order and using (1.81, 3.22, 3.26), it is possible to obtain the various components of the perturbed tensor [56, 87], here specified in the longitudinal gauge and written in terms of the gauge invariant metric perturbation Ψ

defined in (1.102):

$$\delta T_0^{0(\text{longit})} = a^{-2} \left[\Psi \varphi'^2 - \chi' \varphi' - V_\phi \chi \right] Y^{(0)} \quad (3.27)$$

$$\delta T_j^{i(\text{longit})} = -a^2 \delta_j^i \left[\varphi'^2 \Psi - X' \varphi' + a^2 V_\phi X \right] Y^{(0)} \quad (3.28)$$

$$\delta T_j^0(\text{longit}) = -a^2 k \varphi X Y_j^{(0)} \quad (3.29)$$

$$\delta T_0^i(\text{longit}) = -a^2 k \varphi' X Y^i{}^{(0)} \quad (3.30)$$

where⁴ V_ϕ is the derivative of the potential $V(\phi)$ with respect to ϕ and δT_ν^μ has been defined as in (1.108). Note also that perturbations of the quintessence field only involve scalar contributions. Comparing these expressions with the ones in (1.115) we can easily derive

$$(\bar{\rho}_\phi + \bar{p}_\phi) v^{(\phi)} = a^{-2} k \varphi' X \quad (3.31)$$

where $v^{(\phi)}$ is the velocity perturbation of the quintessence field. Substituting the expressions of the background energy density (3.4) and pressure (3.5) it's easy to obtain:

$$v^{(\phi)} = \frac{kX}{\varphi'} \quad (3.32)$$

Note also that in the longitudinal gauge $v_{\text{long}}^{(\phi)} = V^{(\phi)}$ where $V^{(\phi)}$ is the gauge invariant velocity perturbation defined in (1.122) not to be confused with the potential $V(\phi)$.

Analogously, the expression for the density perturbation of the quintessence field can be obtained combining eq.(1.115, 1.123, 3.4, 3.5, 3.27) (see [56, 87]):

$$\Delta_g^{(\phi)} = \bar{\rho}_\phi^{-1} a^{-2} \left[\varphi' X' + a^2 V_{,\phi} X - \varphi'^2 \Psi - 3\varphi^2 \Phi \right] \quad (3.33)$$

$$= (1 + \omega_\phi) \left[3\Phi - \Psi + X' \varphi'^{-1} \right] + X V'(\phi) \bar{\rho}_\phi^{-1} \quad (3.34)$$

The gauge invariant entropy perturbation is equal to

$$\Gamma_\phi = \bar{p}_\phi^{-1} \left[(1 - c_s^2) \bar{\rho}_\phi \left(\Delta_g - 3\bar{\rho}_\phi^{-1} a^{-2} \varphi'^2 \Phi \right) - 2V_{,\phi} X \right] \quad (3.35)$$

while the anisotropic perturbation Π vanishes in minimally coupled models. Finally, the perturbed equation of motion for the quintessence field is given by

$$X'' + 2\mathcal{H}X' + (k^2 + a^2 V_{,\phi\phi})X = \varphi' (\Psi' - 3\Phi') - 2a^2 V_{,\phi}(\phi) \Psi \quad (3.36)$$

where the gravitational source on the right hand side (depending on the gauge invariant scalar metric perturbations Ψ and Φ) can only be neglected

⁴Tensor components in (3.27) are not gauge invariant, even though they are written in terms of gauge invariant variables.

for modes far inside the horizon. In the synchronous gauge eq.(3.36) becomes [28, 48]

$$X'' + 2\mathcal{H}X' + (k^2 + a^2V_{,\phi\phi})X = -\frac{1}{2}h'X' \quad (3.37)$$

where h is the trace of the spatial metric perturbation [92]. Finally, note that even in the case of a background cosmological constant with $\omega_Q = -1$, in which $V_\phi = 0$ and $\phi = \text{const}$ is a solution of the Klein Gordon equation, eq.(3.36) becomes $X'' + 2\mathcal{H}X' + (k^2 + a^2V_{,\phi\phi})X = 0$ so that scalar field fluctuations could still be present and give a dynamical behavior to what appears to be a constant [10].

3.2 Tracking solutions

As we have seen in Chapter 2, up to present the cosmological constant is still compatible with observations; therefore, the first aim of a quintessence model should be that of overcoming the serious problems related to Λ in order to motivate the choice for a valid alternative. An interesting and very popular subclass of models which has made the first steps in this direction was first proposed in [116] and then developed later on within Quintessence theories by [156, 134]. This class is usually referred to as ‘tracker field models’ and it first appeared to solve one of the most compelling issues, i.e. that of the fine tuning of the initial conditions, fixed in order to have a value of the field energy density and of the equation of state today in agreement with observations. The powerful peculiarity of these models is that, irrespectively of the initial conditions, the field rolls down to the right place. In other words, though starting from a large set of initial conditions for ϕ and $\dot{\phi}$, tracking scalar fields evolve and eventually converge into a common path which behaves as an attractor: the latter is a solution of the Klein Gordon equation (3.10) characterized by an almost constant equation of state for the field, constrained in the range $-1 < \omega_Q < \omega_B$, where ω_B is the background equation of state [134]. In this models the value of the quintessence energy density today (fig. 3.2) as well as that of the equation of state ω_Q (fig. 3.2) become naturally the required one, avoiding the fine-tuning problem within a range of tens of orders of magnitude. In particular, quintessence could have been initially of the same order of ordinary matter.

The new issue within this framework has then consisted for long in looking for those potentials that admit attractor solutions; the condition proposed in [134] depends on the value of a key parameter for minimal coupled quintessence models, referred to as Γ and defined as

$$\Gamma \equiv \frac{V''V}{(V')^2} \quad (3.38)$$

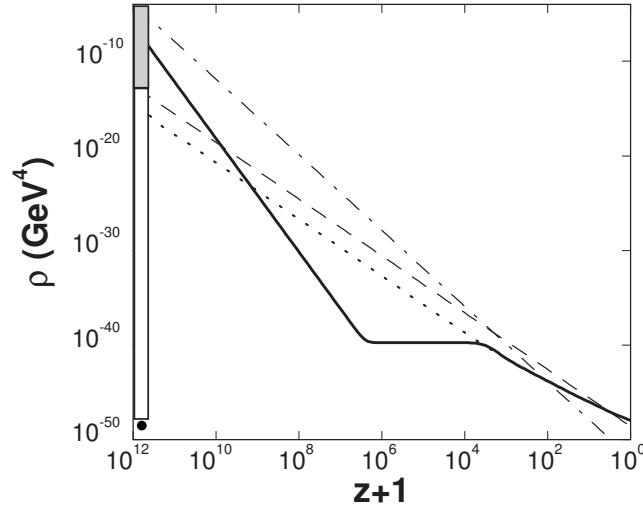


Figure 3.1: Quintessence energy density versus redshift in the case of a tracker field. The solid thick curve represents the case in which Q begins from a value greater than the tracker solution value (overshoot), decreases rapidly and freezes, eventually reaching the tracker solution. Both the white (undershoot) and the grey (overshoot) bars on the left represent the allowed range of initial values of the field that lead to the attractor, spanning more than 100 orders of magnitude. The small black circle represents the unique initial condition required in the case of a cosmological constant. The figure is from [134].

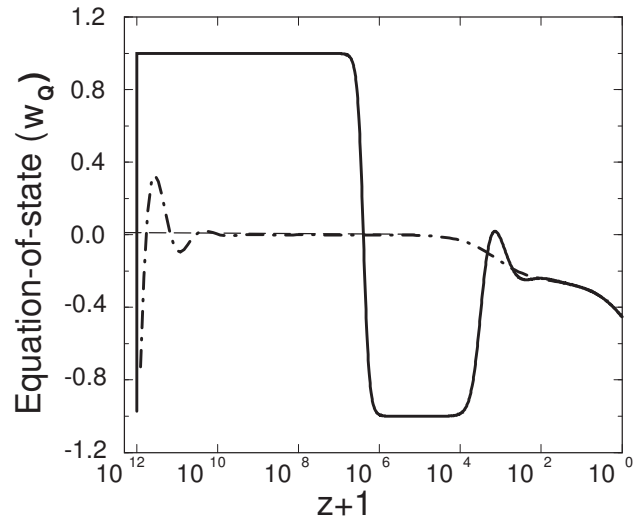


Figure 3.2: Equation of state ω_Q versus redshift in the case of a tracker fields. Starting from different initial conditions, ω_Q converges, after a few oscillations, to the tracker solution. All the curves are for $V(Q) = M^4/Q^6$. The solid curve corresponds to the thick solid curve in the previous figure; the thin curve with $\omega_Q \sim 0$ is the tracker solution; the dash-dotted curve represents a slightly undershooting solution. The figure is from [134]

When

$$\Gamma > 1 ; \omega_Q < \omega_B ; \Gamma \sim \text{const} \quad (3.39)$$

or

$$\Gamma < 1 ; \omega_B < \omega_Q < \frac{1}{2}(1 + \omega_B) ; \Gamma \sim \text{const} \quad (3.40)$$

then solutions of the Klein Gordon equation converge to a tracker solution; here the subscript B stands for the background and V is the potential in which the quintessence field rolls. Moreover, a complete analysis has been performed in [90] on potentials which admit scaling solutions, that is to say solutions in which the scalar field energy density scales as

$$\rho_\phi \propto a^{-n} \quad (3.41)$$

when the background scales as

$$\rho_{\text{fluid}} \propto a^{-m} \quad (3.42)$$

equivalently defined as models in which the scalar field potential and kinetic energies stay in fixed proportion.

We will now review briefly three of the most popular choices for the $V(\phi)$ potential: the exponential, the inverse power-law, and the SUGRA potentials.

3.2.1 Exponential potential

The exponential potential [147, 116, 69] is given by

$$V(\phi) = V_0 e^{-\lambda\phi/M_{Pl}} \quad (3.43)$$

where λ is a constant. This potential allows quintessence to have attractor solutions in which, however, the scalar field energy density always scales in time exactly as the background; as a consequence, since $\Omega_Q \propto (1 + \omega_Q)/\lambda^2$ [148], quintessence equation of state results to be always $\omega_Q = \omega_B$. This means that $\omega_Q = \omega_{CDM} = 0$ today which is in contrast with the need of an accelerating Universe. This scenario changes in models in which Dark Energy is coupled to Dark Matter [4]: in this case both the coupling and λ need to vary in order to fix $\Omega_{Q_0} = 0.7$ today; however either quintessence doesn't manage to dominate today over the background or coupled quintessence dominates directly over radiation, with no matter domination era at all.

3.2.2 Ratra-Peebles potential

Another interesting suggestion for the potential is the inverse power law (Ratra-Peebles potential) [116, 117, 27]

$$V(\phi) = A \left(\frac{M_P}{\phi} \right)^\alpha \quad (3.44)$$

where $\alpha > 0$, the overall factor A has the dimension of a mass to the power of $(\alpha + 4)$ and A is chosen in such a way that

$$A \sim \Omega_{\phi_0} \rho_{c0} \quad (3.45)$$

where ρ_{c0} is the present critical density. Though this fixes the right value today for the energy density of the field, the initial conditions for the evolution equations do not need to be fine tuned, due to the tracking: if the scale factor expands as a power law $a \propto t^n$, then the Klein Gordon equation (3.9) has scaling solutions of the type

$$\phi \propto t^{2/(2+\alpha)} \quad (3.46)$$

with energy density

$$\rho_{\phi} \propto t^{-2\alpha/(2+\alpha)} \quad (3.47)$$

whose ratio with respect to the background energy density increases in time as $\rho_{\phi}/\rho_B \propto t^{4/(2+\alpha)}$ when taking into account that matter and radiation scale as in (1.44) and (1.49) respectively. As long as $\alpha > 0$ the scalar field energy density decays in time more slowly than the background until, at some point, it dominates over the other components in the Universe leading to an accelerating expansion. As for the equation of state, its value today is related to the α parameter through the relation:

$$\omega_{Q_0} = -\frac{2}{\alpha + 2} \quad (3.48)$$

A slowly changing potential characterized by small values of its first and second derivatives also explains the fact that the mass of the field is very small, as previously mentioned. Note, however, that in this case the mass is a derived quantity that evolves with the expansion and not a fixed fine tuned value as in the case of a potential of the type $V = m_q^2 \phi^2/2$ [106]. Moreover, once the condition (3.45) is fixed, the transition from matter dominated to Dark Energy dominated eras happens to occur right at $z \sim 1 - 2$, as required by observations and without imposing further constraints.

Constraints on the inverse power law potential (as well as on other quintessence models) imposed by CMB and Supernovae observations have been investigated in [31]. In particular, the α parameter is constrained to values $\alpha < 1 - 2$ in consistence with previous analysis [11] so that flatter potentials seem to be favored by data. The most direct implication of flattening $V(\phi)$ is that the basin of attraction of the tracker field, that is to say the allowed range of initial conditions able to lead to the attractor, shrinks of about ten orders of magnitude when passing from $\alpha = 6$ to $\alpha = 0.5$; if on one side this allows to have smaller values of the quintessence equation of state ω_Q in agreement with recent data, on the other hand the potential resembles more and more to that of a cosmological constant [18], enhancing the fine tuning and losing the main appeal of tracking trajectories.

3.2.3 SUGRA

An example of models in which the quintessence equation of state is very near to -1 today but in which $\omega_Q \neq -1$ in the past is provided by supergravity inspired (SUGRA) models [26, 27]. In this case the potential has the form:

$$V(\phi) = A \left(\frac{M_P}{\phi} \right)^\alpha \exp \left[4\pi (\phi/M_P)^2 \right] \quad (3.49)$$

where A has the dimension of a mass to the power of $(\alpha + 4)$. In (3.49) an inverse power law potential is corrected by an exponential which has mainly effect at very small redshifts, in the final stages of the Universe, and is irrelevant when $\phi \ll M_{Pl}$. This implies that the insensitivity to the initial conditions that characterizes the inverse power law potential is preserved within a range of 100 orders of magnitude, as it has been checked in [26]; then, in recent times, the exponential tracks these potentials to values of the equation of state lower than in the inverse power law potential with a very low dependence on the α parameter.

Finally, we would like to note that, though appealing to overcome the fine-tuning problem preserving a negative equation of state, all tracker models are still affected by fine tuning in the post-tracking regime, in order to fix the dark energy abundance today. This is obtained when tuning the constant A in the potential, both in (3.44) and in (3.49).

3.3 Effects on cosmological perturbations

The presence of Dark Energy changes the expansion of the Universe through the extra contribution in the Friedmann equation (1.37); this has effect on the curvature of the Universe which in turn modifies the luminosity distance (2.8) influencing, as we have seen, the way SNIa appear to us as well as the amplitude of CMB fluctuations and gravitational lensing effects, which depend on the geometry of the Universe. In particular, when we consider quintessence models, the luminosity distance gets contracted with respect to Λ CDM models as we see from (2.8).

We will now review the basic effects of Dark Energy on CMB and LSS in the simple case of a minimally coupled scalar field.

3.3.1 CMB

Dark Energy influences the CMB spectrum in three regions, which involve the first peak, the large angular scales and the small angular scales (fig. 3.3) [30] [31]. In particular, the first peak location depends on the geometry of

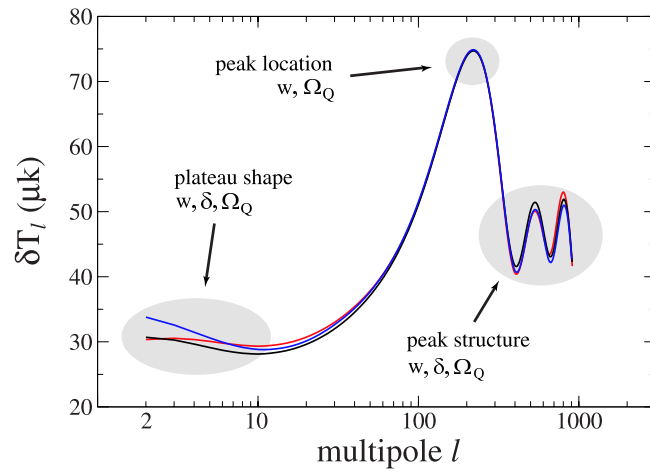


Figure 3.3: CMB spectrum for three different quintessence models. The red ($\omega_Q = -0.5$) and blue ($\omega_Q = -1.2$) curves, though equal to CMB, can be distinguished by SNe data. The black curve ($\omega_Q = -0.8$), although consistent with the SNe data and with the location and height of the first peak as determined by WMAP, is rejected by CMB at the 3σ level. Figure from [31].

the Universe and on the distance from the last scattering surface: the latter depends on the amount of Dark Energy today and on the equation of state ω_Q analogously to what happens for the luminosity distance in eq.(2.8). Fig.(3.4) shows the influence that quintessence has on CMB for different values of Ω_Q and of the equation of state ω_Q both whether it has a constant value and if it varies in time. All plotted models correspond to flat cosmolo-

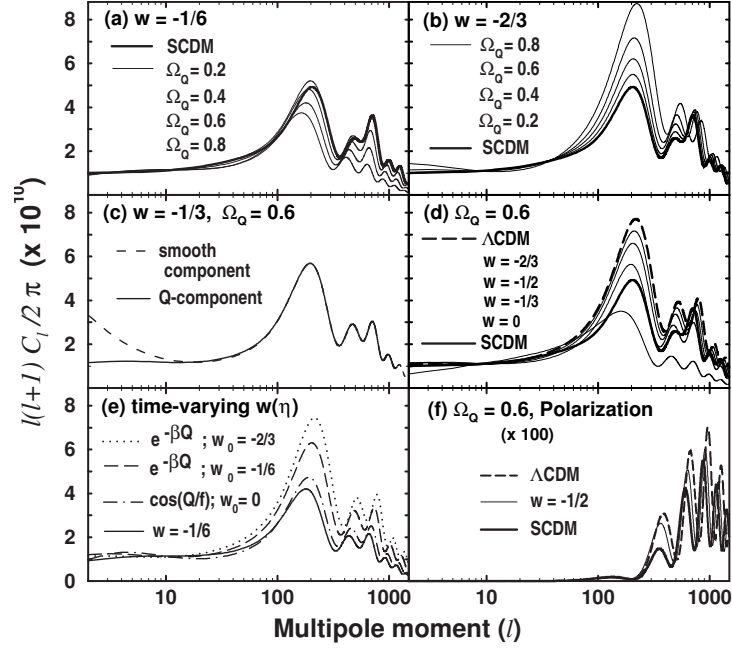


Figure 3.4: CMB power spectrum as a function of Ω_Q (a,b) and ω (d). Thin lines represent Λ CDM models. Panel (c) compares a smooth component to the case in which fluctuations are included. In panel (e) the equation of state varies with time and is obtained from the specified potential (an exponential and a cosine). Panel (f) shows the effect of quintessence on CMB polarization. The figure is from [28].

gies, therefore the location of the first peak is approximately at the same value of l .

A second region which is affected by both Ω_Q and ω_Q is the plateau at low multipoles. Here the shape of the spectrum is distorted by the ISW effect described in the comments following eq.(1.207); the ISW effect is due to the fact that the cosmic expansion stretches the gravitational potentials so

that CMB photons require less (more) energy climbing out of an overdense (underdense) region than they acquire falling in it. The main contribution is given by the LISW which depends on how the expansion is modified by the quintessence domination and therefore changes according to Ω_Q and ω_Q . The more the equation of state of the quintessence field changes, the more the effect is enhanced. We recall here that the LISW effect is visible in the cross-correlation of the CMB with LSS at angular scales $\Theta \leq 10^\circ$.

The plateau at low l 's is also affected by Quintessence fluctuations sound speed [31]: as Ω_Q grows in time, quintessence density fluctuations are attracted by overdensities due to the presence of Dark Matter and baryons [30]; despite the fact that, as we have seen before, minimally coupled quintessence is characterized by fast fluctuations which do not allow the scalar field to cluster, some models like k-essence models [7] or extended quintessence models [110] can admit a lower value of the quintessence fluctuation sound speed: as Dark Energy clusters, it deepens the gravitational wells, thus balancing the flattening of the potential due to the ISW effect; in this case new features like dips and bumps can alter the plateau shape at low multipoles.

When comparing quintessence (QCDM) models to Λ CDM and open models, the ISW of the former models is shifted to higher multipoles. This is due to the fact that the expansion is faster in QCDM than in the other models; as a consequence, quintessence dominates before Λ (see eq. 3.18) and before the curvature term of an open model. When this occurs the horizon is therefore smaller and since the LISW has mainly effect on scales comparable to the sound horizon, the peak of the LISW effect in QCDM moves to smaller scales and to higher multipoles; this effect goes up to the scale of the horizon at last scattering and tends to enhance the amplitude of the first peak. When the equation of state ω_Q gets smaller and nearer to -1 , quintessence dominates on matter later and later; however, the transition occurs more rapidly and ω_Q has a bigger overall change so that the ISW effect is more pronounced.

Finally, note that when fluctuations of the quintessence scalar field are included, the ISW contribution is enhanced, thus increasing the degeneracy among different models [146].

At small angular scales and at high multipoles the shape of the spectrum is greatly influenced by the amount of quintessence at last scattering [32]. The oscillations of the baryon-photon fluid at recombination and therefore the peaks in the CMB spectrum are damped by the presence of a non-clustering component like a minimal coupled quintessence scalar field, even though the quintessence field at last scattering is only few percent of the total energy density.

Finally, from (3.8) we see that for a fixed value of the energy densities today, QCDM models with $\omega_Q > -1$ are characterized by a larger value of H^{-1} in the past with respect to Λ CDM models. This effect influences linear perturbations and since the angular scale $\Theta \propto H^{-1}$, the peaks in the CMB

spectrum are shifted towards higher multipoles (projection effect).

3.3.2 LSS

Large scale structures are deeply influenced by the content of the Universe and both the shape and the amplitude of the matter power spectrum change when considering Λ CDM or QCDM models instead of standard CDM models (SCDM) in which $\Omega_m = 1$ [48, 12, 54]. First of all, Λ CDM and QCDM models shift the overall spectrum to larger scales: this is due to the fact that, as we have seen in par.(2.1.2), the bend in the power spectrum depends on the equivalence point, which in turn is given by $a_{eq} = \bar{\rho}_{r0}/\bar{\rho}_{m0}$ (see eq. 1.46). Therefore, if Ω_m is smaller, as it happens both in Λ CDM and in QCDM with respect to SCDM, a_{eq} is delayed and scales which enter the horizon at the equivalence point are therefore bigger, no matter whether we have a dynamical quintessence field or a cosmological constant. A key difference between the two latter models is however that while Λ is spatially homogeneous at all scales, Q has fluctuations and can in principle cluster above a certain length scale. The effects of fluctuations on the power spectrum have been investigated in [94] for different values of ω_Q , though the equation of state has been strongly constrained since then and there is very little chance to measure such a modification.

In particular, Λ CDM and QCDM models differ in the amplitude of the spectrum, as we can see in fig.(3.5). The first effect is given by the change in the growth factor D_+ defined in (2.5) according to which structures form earlier in QCDM with respect to Λ CDM models in agreement with (3.18) and with the δ evolution shown in fig. (3.6). Characterized by a higher δ , QCDM predicts more structures at higher redshift and, for a chosen z , older and hence more complex and concentrated structures than in the case of a cosmological constant. This same effect is also evident on density profiles of Dark Matter halos, which change too according to the earlier quintessence domination with respect to Λ CDM models [12]: the parameters describing the halo formation change and the halos themselves are denser due to their earlier formation.

The amplitude of the power spectrum, which is related to δ via $P(k) \propto \delta^2$, is smaller in Λ CDM than in QCDM, unless COBE normalization is considered ⁵ (fig.3.5, left panel).

⁵COBE normalization fixes the amplitude of the power spectrum at its maximum scale; this implies fixing the gravitational potential and consequently the value of the product $\Omega_m \delta$ [48] which combined with the change in the growth factor gives $\delta \propto \Omega_m^{p-1}$ with $p_\Lambda \sim 0.2$ and $p_Q \sim 0.56$ so that the amplitude of the spectrum $P(k)$ for QCDM is suppressed; codes like CMBfast now use *WMAP* normalization, which consists in multiplying the CMB and matter spectra by an overall factor which assures the best fit to the WMAP

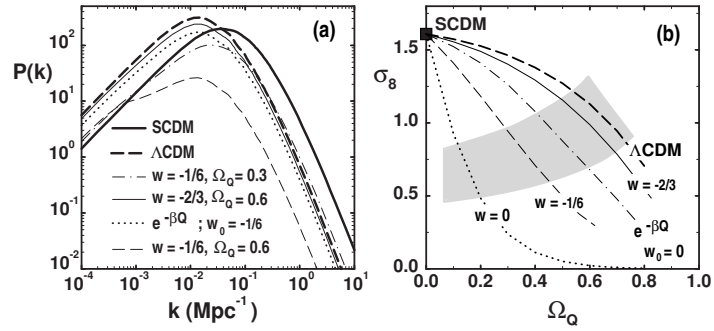


Figure 3.5: The left panel shows the matter density power spectrum $P(k)$ as a function of k for different models. The right panel plots the σ_8 parameter vs Ω_Q for different values of the quintessence equation of state [28].

This effect, however, is balanced by the opposite change in the σ_8 parameter, which is suppressed as ω_Q increases (fig.3.5, right panel).

If COBE normalization is used, the amplitude of the power spectrum is further suppressed by the ISW effect: this is due to the fact that $P(k)$ is influenced by the change in time of the gravitational potential whose dynamics tends to enhance the anisotropy at large scales; for a fixed COBE normalization, the amplitude at maximum scale is fixed so that the overall power spectrum is suppressed. In QCDM the potential usually changes more than in Λ CDM so that the ISW is more pronounced and the power spectrum (when COBE normalized) is more suppressed.

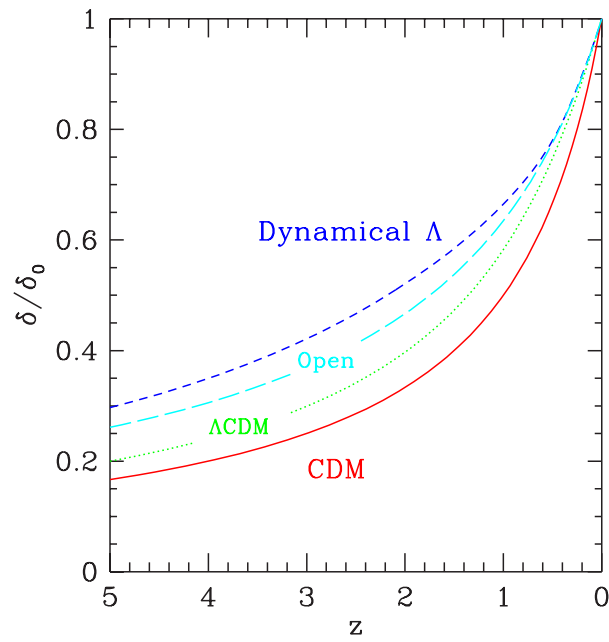


Figure 3.6: Evolution of the density fluctuation amplitude versus redshift z , normalized to its present amplitude, $\delta(z)/\delta_0$. The models shown are standard CDM with $\Omega_{CDM} = 1$ (solid red), Λ CDM with $\Omega_\Lambda = 0.6$ (dotted green), an open CDM model with $\Omega_m = 0.4$ (short dashed light blue), and the dynamical quintessence model with $\Omega_\phi = 0.6$ (long dashed dark blue). The figure is from [48].

Chapter 4

Generalized Cosmologies

4.1 Scalar-tensor theories

As we have seen in the previous Chapter, minimally coupled models represent a first interesting alternative to the cosmological constant and become particularly appealing when proposing attractor solutions as a mean to address the fine tuning problem. Nevertheless, the stringent difficulties which still affect these models when the experimental requirement of a small equation of state is taken into account, encourage to pursue new ways of approaching the Dark Energy issue. In particular, it seems essential to understand how the scalar field behaves when the possibility of an interaction between Dark Energy and other existing components in the Universe is considered. At this purpose, one possibility is to alter the minimal interaction with gravity to which we have restricted our analysis up to now. Starting from the original Brans-Dicke idea (see [74] and references therein) of connecting a scalar field to gravity, one could be tempted to simply interpret the presence of Dark Energy and the recent cosmic acceleration entirely in terms of a signature of a modification of gravity and of General Relativity (GR). With this aim in mind we have worked within the context of scalar-tensor (ST) theories defined as generalized theories of gravity in which the metric tensor interacts with a scalar field via an explicit coupling to the Ricci scalar [144]. These theories represent one of the most natural alternative to General Relativity [67], where conservation laws are preserved together with the constancy of non gravitational constants. In particular, in ST theories the gravitational interaction is not only mediated by a spin-2 graviton related to the metric but also by one or more spin-0 scalar fields. The latter naturally arise in the most promising attempts of quantizing gravity like extra dimension and superstring theories, where the metric components correspond to the so called “moduli” scalar fields, though scalar fields can be obtained in several ways and their existence doesn’t imply the presence of extra dimensions.

In the following we restrict our analysis to the case in which a single scalar field is considered in addition to the ones included in the standard matter terms. In particular, we will review how the background and perturbation equations change in generalized theories of gravity, delineating the framework of scalar-tensor theories and following what have been done in [110, 109]. Then, in the next chapter, we will see in details what happens when the extra scalar field is interpreted as Dark Energy in the context of Extended Quintessence (EQ) [108].

4.1.1 Action and rescaling

Generalized theories of gravity are described by the following action, first introduced in a cosmological context by [84]:

$$S = \int d^4x \sqrt{-g} \left[\frac{1}{2\kappa} f(\phi, R) - \frac{1}{2} Z(\phi) g^{\mu\nu} \partial_\mu \phi \partial_\nu \phi - V(\phi) + \mathcal{L}_{\text{fluid}}[\psi_m; g_{\mu\nu}] \right] \quad (4.1)$$

where g is the determinant of the background metric, R is the Ricci scalar, $\kappa = 8\pi G_*$ and G_* denotes the bare gravitational coupling constant¹ [67].

The scalar field ϕ is supposed to couple only to gravity through the function $f(\phi, R)$ and not to matter fields. The latter are described by the classical fluid lagrangian:

$$\mathcal{L}_{\text{fluid}} = -i\bar{\psi} g^{\mu\nu} \gamma_\nu \nabla_\mu \psi + m\bar{\psi}\psi \quad (4.2)$$

which only depends on matter fields and on the metric $g_{\mu\nu}$, and not on the scalar field ϕ , ensuring that the weak equivalence principle is exactly satisfied².

Functions $Z(\phi)$ and $V(\phi)$ specify the kinetic and potential energies respectively of ϕ and together with $f(\phi, R)$ determine the dynamics of the field. Note however that one can always redefine the scalar field so that $Z(\phi) = 1$ thus reducing the scalar field kinetic energy to the canonical form. This is performed thanks to the following change of variables [77]:

$$\chi = K(\phi) \quad (4.3)$$

where we have introduced the scalar field χ and

$$Z(\phi) \equiv k^2(\phi) \quad \text{with} \quad k(\phi) = \frac{\partial K(\phi)}{\partial \phi} \quad (4.4)$$

¹In the following we will use the convention $M_P^2 \equiv 1/G_*$ and we will define the reduced Planck mass as $M^2 \equiv M_P^2/8\pi$ so that $1/2\kappa = M^2/2$.

²The weak equivalence principle states the universality of free fall of laboratory-size objects.

Action (4.1) then becomes:

$$S = \int d^4x \sqrt{-g} \left[\frac{1}{2\kappa} f[K^{-1}(\chi), R] - \frac{1}{2} g^{\mu\nu} \partial_\mu \chi \partial_\nu \chi - V[K^{-1}(\chi)] \right] + \int d^4x \sqrt{-g} \mathcal{L}_m[\psi_m; g_{\mu\nu}] \quad (4.5)$$

The coupling function $f(\phi, R)$ is often rewritten in terms of a function $F(\phi)$ depending only on the field and defined as

$$F(\phi) \equiv \frac{1}{\kappa} \frac{\partial f}{\partial R} \quad (4.6)$$

In particular, we will assume that the coupling is a simple product of the latter function times the Ricci scalar:

$$f(\phi, R) \equiv \kappa F(\phi) R \quad (4.7)$$

Two popular parametrizations are $f(\phi, R) \equiv F(\phi) R = \phi R$ and $Z(\phi) = w(\phi)/\phi$ (Brans - Dicke) or the choice $Z(\phi) = 1$ with $F(\phi)$ arbitrary.

Action (4.1) is written in the so called Jordan or Weyl frame (WF) in which the scalar field ϕ is coupled to gravity via $f(\phi, R)$ while matter is universally and minimally coupled to gravity via the ordinary metric $g_{\mu\nu}$ with respect to which lengths and times are defined and actually measured. In the case in which (4.7) holds, it can be, however, sometimes clearer and more convenient to rewrite the action and the derived equations in the so called Einstein frame (EF) in which the scalar field is minimally coupled to gravity. The change of reference frame can be achieved via a conformal transformation of the metric joined to a redefinition of matter fields [144] [67] [147] [58]:

$$g_{\mu\nu} = A^2(\phi) \tilde{g}_{\mu\nu} \quad (4.8)$$

$$g^{\mu\nu} = A(\phi)^{-2} \tilde{g}^{\mu\nu} \quad (4.9)$$

$$\psi = A^{-3/2}(\phi) \tilde{\psi} \quad (4.10)$$

$$\gamma_\nu(x) = \tilde{\gamma}_\alpha e_\nu^\alpha(x) \quad (4.11)$$

$$\epsilon_\nu^\alpha(x) = A(\phi) \tilde{\epsilon}_\nu^\alpha(x) \quad (4.12)$$

where ϵ_ν^α is the Levi-Civita tensor³ [145] and we have used the $\tilde{}$ to identify quantities in the EF and distinguish them from those in the WF present in action (4.1). The conformal scaling factor $A(\phi)$ is related to the coupling function according to the following relation:

$$A^2(\phi) = \frac{M^2}{F(\phi)} \quad (4.13)$$

³The Levi-Civita tensor is defined such as $\epsilon^{\alpha\beta\gamma\delta} = \{+1 \text{ if } \{\alpha\beta\gamma\delta\} \text{ is an even permutation of } \{0123\}; -1 \text{ if } \{\alpha\beta\gamma\delta\} \text{ is an odd permutation of } \{0123\}; 0 \text{ otherwise}\}$

where $M \equiv M_{Pl}/8\pi$ is the reduced Planck mass. In terms of this conformal transformation the determinant of the metric and the Ricci scalar respectively transform as:

$$\sqrt{-g} = \sqrt{-\tilde{g}} A(\phi)^4 \quad (4.14)$$

$$R = A(\phi)^{-2} \left\{ \tilde{R} - 6 \tilde{g}^{\mu\nu} (\ln A)_{;\nu} (\ln A)_{;\mu} \right\} \quad (4.15)$$

When applying the Weyl scaling to the action (4.1) we obtain:

$$\tilde{S} = \tilde{S}_\phi + \tilde{S}_{\text{fluid}} \quad (4.16)$$

where

$$\tilde{S}_\phi = \int d^4x \sqrt{-\tilde{g}} \left[\frac{M^2 \tilde{R}}{2} - \left(\frac{3M^2}{A_{,\phi}^2} + \frac{1}{2} \right) A^2(\phi) \tilde{g}^{\mu\nu} \partial_\mu \phi \partial_\nu \phi + \right. \quad (4.17)$$

$$\left. - A^2(\phi) V(\phi) \right]$$

$$\tilde{S}_{\text{fluid}} = - \int d^4x \sqrt{-\tilde{g}} \left[\frac{3i}{2} \frac{A_{,\phi}(\phi)}{A(\phi)} \tilde{\psi} \tilde{g}^{\mu\nu} \tilde{\gamma}_\nu (\nabla_\mu \phi) \tilde{\psi} + i \tilde{\psi} \tilde{g}^{\mu\nu} \tilde{\gamma}_\nu \nabla_\mu \tilde{\psi} + \right. \quad (4.18)$$

$$\left. + mA(\phi) \tilde{\psi} \tilde{\psi} \right]$$

where $A_{,\phi}$ stands for the derivative of $A(\phi)$ with respect to ϕ and we have put $Z(\phi) = 1$ for simplicity. If we define the function σ as:

$$\sigma(\phi) = -M \ln A(\phi) \quad (4.19)$$

we can rewrite \tilde{S}_ϕ and \tilde{S}_{fluid} as

$$\tilde{S}_\sigma = \int d^4x \sqrt{-\tilde{g}} \left[\frac{M^2 R}{2} - \left(3 + \frac{e^{-2\sigma/M}}{2[\sigma_\phi(\phi)]^2} \right) \sigma^{;\mu} \sigma_{;\mu} - W \right] \quad (4.20)$$

$$\tilde{S}_{\text{fluid}} = - \int d^4x \sqrt{-\tilde{g}} \left[\frac{3i}{2M} \sigma_\phi \tilde{\psi} \tilde{\gamma}^\mu (\nabla_\mu \phi) \tilde{\psi} + i \tilde{\psi} \tilde{\gamma}^\mu \nabla_\mu \tilde{\psi} + \eta(\phi) \tilde{\psi} \tilde{\psi} \right] \quad (4.21)$$

where we have defined

$$W \equiv V e^{4\sigma/M} \quad (4.22)$$

$$\eta(\phi) \equiv m e^{-\sigma(\phi)/M} \quad (4.23)$$

Coupling a scalar field to gravity as in (4.1) is therefore equivalent to coupling the scalar field universally to all matter fields: in other words the conformal transformation leads to a theory in which the scalar field is minimally coupled to gravity, as in General Relativity, but in which, however, the action differs from GR in the fluid part. Matter fields are now explicitly coupled to the scalar field ϕ through the conformal factor $A(\phi)$ which alters the kinetic

term of the scalar field and makes the fluid masses depend on ϕ via $\eta(\phi)$; note that this dependence affects all matter fluids in a universal manner, coupling the scalar field to both baryonic and dark matter.

The kinetic term in (4.17) can also be reduced to the standard form by performing a redefinition of the field ϕ :

$$\phi^2 \equiv M^2 A^{-2}(\varphi) \quad , \quad (4.24)$$

This corresponds to defining a new scalar field φ in which the conformal factor $A(\varphi)$ has to be now calculated. A standard kinetic term is then obtained by imposing the condition [38, 66]

$$\alpha_{\text{weyl}}^2(\varphi) = \frac{1}{Z(\phi)/M^2 + 6} \quad (4.25)$$

where α_{weyl} is defined as

$$\alpha_{\text{weyl}}(\varphi) \equiv \frac{d \log A(\varphi)}{d\varphi} \quad . \quad (4.26)$$

Equivalently, one can rescale ϕ defining φ from the condition [67, 118]:

$$\left(\frac{d\varphi}{d\phi}\right)^2 \equiv \frac{3}{4} \left(\frac{d \ln 1/A^2(\phi)^2}{d\phi}\right) + \frac{Z(\phi)A^2(\phi)}{2} \quad (4.27)$$

where the fluid part of the action has to be calculated in $S_m [\tilde{\psi}_m, A^2(\varphi)\tilde{g}_{\mu\nu}]$.

In [144] it is also shown that the equivalence between scalar-tensor theories with $\mathcal{L} \sim f(\phi, R)/2\kappa + \mathcal{L}_{\text{fluid}}[\psi_m, g_{\mu\nu}]$ and General Relativity plus scalar matter fields described by the lagrangian $\mathcal{L} \sim R/2\kappa + \mathcal{L}_{\text{fluid}}[\psi_m, A^2(\varphi)\tilde{g}_{\mu\nu}]$ extends to higher-order gravity lagrangians in which $\mathcal{L} \sim f(R) + \mathcal{L}_{\text{fluid}}[\psi_m, g_{\mu\nu}]$.

Choosing either one of the Weyl or Einstein frames is matter of convenience. We will usually work in the WF, which will be better suited for our purposes but we will also check the consistency of our results by finally translating them in terms of Einstein-frame quantities.

4.1.2 Background

We will now proceed in illustrating both the background and linear perturbations in scalar-tensor theories. All formalism will be developed in the WF, starting from (4.1) and following [110][87].

A first remark concerns Einstein equations, which can still be expressed in the usual form (1.1) though now the conserved stress energy tensor includes both the contribution of matter fields and the one coming from the scalar field:

$$T_{\mu\nu} = T_{\mu\nu}^{\text{fluid}} + T_{\mu\nu}(\phi) \quad (4.28)$$

In particular, the scalar field stress-energy tensor assumes the form:

$$T_{\mu\nu}(\phi) = T_{\mu\nu}^{mc}(\phi) + T_{\mu\nu}^{nmc}(\phi) + T_{\mu\nu}^{\text{grav}}(\phi) \quad (4.29)$$

where the various contributions are given by

$$T_{\mu\nu}^{mc}(\phi) = Z(\phi) \left[\phi_{;\mu}\phi_{;\nu} - \frac{1}{2}g_{\mu\nu}\phi^{;\lambda}\phi_{;\lambda} \right] - V(\phi)g_{\mu\nu} \quad (4.30)$$

$$T_{\mu\nu}^{nmc}(\phi) = \frac{f/\kappa - RF}{2}g_{\mu\nu} + F_{;(\mu\nu)} - g_{\mu\nu}\square F \quad (4.31)$$

$$T_{\mu\nu}^{\text{grav}}(\phi) = \left(\frac{1}{\kappa} - F \right) G_{\mu\nu} \quad (4.32)$$

The apices *mc*, *nmc* and *grav* identify respectively the usual minimal coupling contribution (kinetic plus potential energies), the non-minimal coupling term (depending on the coupling function and on the Ricci scalar) and the gravitational term (which contains the Einstein tensor).

The absence of an explicit coupling between matter fields and ϕ assures that both contributions in (4.28) also conserve separately:

$$\nabla^\mu T_{\mu\nu}^{\text{fluid}} = \nabla^\mu T_{\mu\nu}(\phi) = 0 \quad (4.33)$$

leading to the usual conservation equations for the energy densities (1.21) for matter, radiation and the scalar field components, as long as the latter has energy density and pressure given by the following expressions [110]:

$$\rho_\phi^{\text{cons}} = Z(\phi)\frac{\phi'^2}{2a^2} + V(\phi) + \frac{RF - f/\kappa}{2a^2} - \frac{3}{a^2}\mathcal{H}F' + 3\frac{\mathcal{H}^2}{a^2}\left(\frac{1}{\kappa} - F\right) \quad (4.34)$$

$$p_\phi^{\text{cons}} = Z(\phi)\frac{\phi'^2}{2a^2} - V(\phi) - \frac{RF - f/\kappa}{2a^2} + \frac{1}{a^2}(\mathcal{H}F' + F'') - \frac{2\mathcal{H}' + \mathcal{H}^2}{a^2}\left(\frac{1}{\kappa} - F\right) \quad (4.35)$$

where we have assumed a spatially flat Universe. The latter terms on the right hand side represent additional terms present in the two latter expressions when the non minimal coupling is ‘active’ i.e. when the function $F \neq 1/\kappa$, differing from the value it has today and from the one it has in minimal coupling theories.

The Klein Gordon equation, written in the case of minimal coupling in (3.10), gets an extra contribution and becomes

$$\phi'' + 2\mathcal{H}\phi' + \frac{1}{2Z(\phi)}\left(Z_{,\phi}\phi'^2 - \frac{a^2}{\kappa}f_{,\phi} + 2a^2V_{,\phi}\right) = 0 \quad (4.36)$$

If (4.7) holds and we choose $Z = 1$ for simplicity, then eq. (4.36) becomes:

$$\phi'' + 2\mathcal{H}\phi' + a^2V_\phi = \frac{a^2}{2}F_{,\phi}R \quad (4.37)$$

Furthermore, Friedmann equation, written as (3.7) in the case of a minimal coupling models, in scalar-tensor theories becomes equal to:

$$\mathcal{H}^2 = \left(\frac{a'}{a}\right)^2 = \frac{1}{3F} \left(a^2 \rho_{fluid} + \frac{1}{2} \phi'^2 + a^2 V - 3\mathcal{H}F' \right) \quad (4.38)$$

while the acceleration equation is given by:

$$\mathcal{H}' = \mathcal{H}^2 - \frac{1}{2F} \left(a^2 (\rho_{fluid} + p_{fluid}) + \phi'^2 + F'' - 2\mathcal{H}F' \right) \quad (4.39)$$

Formally, one could still rewrite equations (4.38) and (4.39) as:

$$\mathcal{H}^2 = \frac{a^2}{3F} (\rho_{fluid} + \tilde{\rho}_\phi) \quad (4.40)$$

$$\mathcal{H}' = \mathcal{H}^2 - \frac{a^2}{2F} (\rho_{fluid} + p_{fluid} + \tilde{\rho}_\phi + \tilde{p}_\phi) \quad (4.41)$$

provided we define a generalized formal energy density $\tilde{\rho}_\phi$ and a generalized pressure \tilde{p}_ϕ as:

$$\tilde{\rho}_\phi = \frac{\phi'^2}{2a^2} + V(\phi) - \frac{3\mathcal{H}F'}{a^2} \quad (4.42)$$

$$\tilde{p}_\phi = \frac{\phi'^2}{2a^2} - V(\phi) + \frac{F''}{a^2} + \frac{\mathcal{H}F'}{a^2} \quad (4.43)$$

Also, one can still define the energy density and pressure for the scalar field in the usual manner

$$\rho_\phi = \frac{\phi'^2}{2a^2} + V(\phi) \quad (4.44)$$

$$p_\phi = \frac{\phi'^2}{2a^2} - V(\phi) \quad (4.45)$$

though these quantities are not conserved anymore, i.e. they do not obey the relation $\dot{\rho}_\phi + 3H(\rho_\phi + p_\phi) = 0$. Expressions (4.44) and (4.45) can be generally very different from (4.34) and (4.35), mostly because of the terms in the conserved formulations which are multiplied by $(1/\kappa - F)$: those are proportional to the cosmological critical density via \mathcal{H}^2 and they are active whenever the theory differs from General Relativity. Although that difference is small to match the observational constraints, the presence of \mathcal{H}^2 makes it relevant. This may have important consequences for the dynamics of the Dark Energy density perturbations, leading to effects like gravitational dragging [110] about which we will briefly discuss ahead in this Chapter.

For our analysis, it is also relevant to write down the explicit form of the Ricci scalar in terms of the cosmological content

$$R = -\frac{1}{F} \left[-\rho_{fluid} + 3p_{fluid} + \frac{\phi'^2}{a^2} - 4V + 3 \left(\frac{F''}{a^2} + 2\frac{\mathcal{H}F'}{a^2} \right) \right], \quad (4.46)$$

as well as its expression in terms of the Hubble parameter:

$$R = -\frac{6}{a^2} (\mathcal{H}' + \mathcal{H}^2) \quad (4.47)$$

Finally, if no explicit interaction with matter fields is considered and therefore eq.(1.21) holds for all components in the Universe, then the sound velocity of the scalar field ϕ is equal to:

$$c_{s_\phi}^2 = \omega_\phi - \frac{1}{3\mathcal{H}} \frac{\omega'_\phi}{1 + \omega_\phi} \quad (4.48)$$

4.1.3 Linear Perturbations

We now proceed perturbing the conservation equations (4.33) for each cosmological component ‘ a ’ in the Universe [84, 110]:

$$\delta T_{(a)j;\nu}^\nu = 0 \quad (4.49)$$

In particular, the time and spatial components of the conservation equations for the field, that is to say $\nabla^\mu T_{\mu 0}(\phi) = 0$ and $\nabla^\mu T_{\mu j}(\phi) = 0$, correspond to the following equations respectively [87]:

$$(\rho_\phi \delta_\phi)' + 3\mathcal{H}(\rho_\phi \delta_\phi + p_\phi \pi_{L_\phi}) + h_\phi(kv_\phi + 3H'_L) = 0 \quad (4.50)$$

$$[h_\phi(v_\phi - B)]' + 4\mathcal{H}h_\phi(v_\phi - B) - kp_\phi \pi_{L_\phi} - kh_\phi A + \frac{2}{3}kp_\phi \pi_{T_\phi} = 0 \quad (4.51)$$

where we have defined

$$h_\phi = \rho_\phi + p_\phi \quad (4.52)$$

Also, $\delta \equiv \delta\rho/\rho$ is the density perturbation, v_ϕ is the velocity perturbation defined in (1.112), π_{T_a} is the amplitude of the perturbation for the anisotropic pressure defined in (1.111) and gauge invariant by itself and π_{L_a} is the diagonal component of the stress energy tensor perturbation; moreover, A , B and H_L are three of the four metric perturbation parameters defined in (1.86, 1.87, 1.88) and the subscript ϕ indicates that quantities refer to the field ϕ . Again, if eq.(1.21) holds for all components in the Universe, then (4.48) can be used to rewrite eq.(4.50) and eq.(4.51) in the form:

$$\frac{d}{d\eta} \left(\frac{\delta_\phi}{1 + \omega_\phi} \right) + kv_\phi + 3H'_L + 3\mathcal{H} \frac{\omega_\phi}{1 + \omega_\phi} \Gamma_\phi = 0 \quad (4.53)$$

$$(v'_\phi - B') + \mathcal{H}(v_\phi - B)(1 - 3c_{s_\phi}^2) - k \frac{\omega_\phi}{1 + \omega_\phi} \pi_{L_\phi} + \frac{2}{3}k \frac{\omega_\phi}{1 + \omega_\phi} \pi_{T_\phi} - kA = 0 \quad (4.54)$$

where Γ_ϕ has been defined in (1.127).

The perturbed Klein Gordon equation reads:

$$\begin{aligned}
(\delta\phi)'' &+ \left(2\mathcal{H} + \frac{Z_{,\phi}\phi'}{Z}\right) (\delta\phi)' + \\
&+ \left[k^2 + \left(\frac{Z_{,\phi}}{Z}\right)_{,\phi} \frac{\phi'^2}{2} + \left(\frac{-a^2 f_{,\phi}/\kappa + 2a^2 V_{,\phi}}{2Z}\right)_{,\phi} \right] \delta\phi = \\
&= \phi' A' - \left(3\mathcal{H}\phi' + \frac{-a^2 f_{,\phi}/\kappa + 2a^2 V_{,\phi}}{2Z}\right) A + \\
&+ \phi' (3\mathcal{H}A - 3H'_L - kB) + \frac{1}{2Z\kappa} f_{,\phi R} \delta R
\end{aligned} \tag{4.55}$$

with

$$\begin{aligned}
\delta R &= -\frac{2}{a^2} (3\mathcal{H}A - 3H'_L - kB)' Y - \frac{6}{a^2} \mathcal{H} (3\mathcal{H}A - 3H'_L - kB) Y + \\
&+ \frac{2}{a^2} (k^2 - 3\mathcal{H}' + 3\mathcal{H}^2) AY + \frac{4}{a^2} k^2 \left(H_L + \frac{1}{3}H_T\right) Y
\end{aligned} \tag{4.56}$$

Finally, from the definition of the entropy perturbation (1.127) one can obtain the following useful relation:

$$p_\phi \Gamma_\phi = \delta p_\phi - c_s^2 \delta \rho_\phi \tag{4.57}$$

where $\delta p_\phi \equiv p_\phi \pi_{L_\phi}$ and $\delta \rho \equiv \rho \delta \phi$.

For each cosmological component, the perturbed stress energy tensor has the form seen in (1.113, 1.114, 1.115, 1.116). In particular, when perturbing $T_\mu^\nu(\phi)$ in (4.29) one gets again three contributions

$$\delta T_\mu^\nu(\phi) = \delta T_\mu^{\nu mc}(\phi) + \delta T_\mu^{\nu nmc}(\phi) + \delta T_\mu^{\nu grav}(\phi) \tag{4.58}$$

whose explicit formulation for each component can be found in [110] and is

given by:

$$\delta T_0^{0mc}(\phi) = \left[-Z_{,\phi} \frac{\phi'^2}{2a^2} \delta\phi + \frac{Z}{a^2} (A\phi'^2 - \phi' \delta\phi') - V_{,\phi} \delta\phi \right] Y \quad (4.59)$$

$$\begin{aligned} \delta T_0^{0nmc}(\phi) &= \left[-\frac{3}{a^2} A\mathcal{H}F' + \frac{3}{a^2} \mathcal{H}\delta F' + \frac{1}{2\kappa} f_{,\phi} \delta\phi + \right. \\ &+ \left(\frac{k^2}{a^2} - \frac{R}{2} \right) \delta F + \\ &+ \left. \frac{3}{a^2} \mathcal{H} \left(-A + \mathcal{H}^{-1} \frac{B}{3} + \mathcal{H}^{-1} H'_L \right) F' \right] Y \end{aligned} \quad (4.60)$$

$$\begin{aligned} \delta T_0^{0grav}(\phi) &= \frac{3}{a^2} \mathcal{H}^2 \delta F Y + \left(\frac{1}{\kappa} - F \right) \frac{2}{a^2} [3\mathcal{H}^2 A - \mathcal{H}kB + \\ &- 3\mathcal{H}H'_L - k^2 \left(H_L + \frac{H_T}{3} \right)] Y \end{aligned} \quad (4.61)$$

$$\delta T_j^{0mc}(\phi) = \frac{k}{a^2} (Z\phi' \delta\phi) Y_j \quad (4.62)$$

$$\delta T_j^{0nmc}(\phi) = \frac{k}{a^2} (\delta F' - \mathcal{H}\delta F - AF') Y_j \quad (4.63)$$

$$\delta T_j^{0grav}(\phi) = \frac{2}{a^2} \left(\frac{1}{\kappa} - F \right) \left(k\mathcal{H}A - kH'_L - \frac{k}{3} H'_T \right) Y_j \quad (4.64)$$

$$\delta T_j^{imc}(\phi) = \frac{1}{a^2} \left[Z\phi' \delta\phi' + \frac{Z_{,\phi}}{2} \phi'^2 \delta\phi - a^2 V_{,\phi} \delta\phi - AZ\phi'^2 \right] Y \delta_j^i \quad (4.65)$$

$$\begin{aligned} \delta T_j^{inmc}(\phi) &= \frac{1}{a^2} \left[\frac{1}{2\kappa} f_{,\phi} \delta\phi + 2F'\mathcal{H} \left(-A + \frac{B}{3\mathcal{H}} + \frac{H'_L}{\mathcal{H}} \right) + \right. \\ &+ \left. \left(\frac{R}{2} + \frac{2}{3} k^2 \right) \delta F + \mathcal{H}\delta F' + \delta F'' - F'A' - 2F''A \right] Y \delta_j^i + \\ &+ \frac{k^2}{a^2} \left[\delta F + (kB - H'_T) \frac{F'}{k^2} \right] Y_j^i \end{aligned} \quad (4.66)$$

$$\begin{aligned} \delta T_j^{igrav}(\phi) &= \frac{1}{a^2} (2\mathcal{H}' + \mathcal{H}^2) \delta F Y \delta_j^i + \\ &+ \frac{2}{a^2} \left(\frac{1}{\kappa} - F \right) \left[(2\mathcal{H}' + \mathcal{H}^2) A + \mathcal{H}A' - \frac{k^2}{3} A - \frac{k}{3} B' + \right. \\ &- \left. \frac{2}{3} k\mathcal{H}B - H''_L - 2\mathcal{H}H'_L - \frac{k^2}{3} \left(H_L + \frac{H_T}{3} \right) \right] Y \delta_j^i + \\ &+ \frac{1}{a^2} \left(\frac{1}{\kappa} - F \right) \left[-k^2 A - k(B' + \mathcal{H}B) + H''_T + \right. \\ &+ \left. \mathcal{H} (2H'_T - kB) - k^2 \left(H_L + \frac{H_T}{3} \right) \right] Y_j^i \end{aligned} \quad (4.67)$$

where $\delta F = F_{,\phi} \delta\phi + F_{,R} \delta R$.

Notice that in general the stress energy tensor contains both an isotropic

stress perturbation π_{L_ϕ} and an anisotropic stress perturbation π_{T_ϕ} whose existence is a peculiar feature of non minimally coupled models; indeed, as we have seen in par. 3.1.1, the anisotropic stress perturbation vanishes in the minimal coupling case [87]. Moreover, the gravitational contributions, both for the density component δT_0^0 and for the spatial contributions δT_i^0 and δT_j^i contain terms which multiply $(1/\kappa - F)$ and are respectively proportional to δG_0^0 , δG_i^0 and δG_j^i . As we have already commented in the case of the background, when the non minimal coupling is ‘active’ and $F \neq 1/\kappa$, gravity gives an extra contribution. In particular, if the gravitational term dominates over the others, the energy density perturbation of the scalar field is dragged by the total density fluctuation through the δG_0^0 term, forcing the scalar field to behave as the dominant component in the Universe. Note also that Einstein equation (1.136) indicates that the gravitational potential Φ is fed by the gauge invariant density perturbation Δ which needs to be summed up over all cosmological components so that:

$$\rho\Delta \equiv \sum_a \rho_a \delta_a + 3 \sum_a \rho_a (1 + \omega_a) \frac{\mathcal{H}}{k} (v_a - B) \quad (4.68)$$

As a consequence, each cosmological component can generate a potential well affecting the behavior of the density perturbations of the other components. In particular, the scalar field itself can generate a gravitational well which alters δ_m ; in turn matter itself can alter the gravitational potential, acting as a back reaction effect on the scalar field energy density perturbation through the δG_0^0 term in the gravitational contribution of δT_0^0 . This effect, known as ‘gravitational dragging’ [110], is also evident from the explicit expression of δ_{ρ_ϕ} which can be again split into three pieces:

$$\delta_{\rho_\phi} = \delta_{\rho_\phi}^{mc} + \delta_{\rho_\phi}^{nmc} + \delta_{\rho_\phi}^{grav} \quad (4.69)$$

The latter term receives contribution from the coupling to gravity while the first two terms are fed not only by metric perturbations but also by proper perturbations $\delta\phi$ of the scalar field. As a consequence, even when $\delta_\phi = 0$ one can have $\delta_{\rho_\phi} \neq 0$.

Gravitational dragging can indeed be very significant since the contribution in δ_{ρ_ϕ} of energy density coming from other components could lead the field ϕ to show non linear features which may grow themselves into clumps as a consequence of matter perturbations injection. Eventually, whether Dark Energy density perturbations managed to be present also on sub-horizon scales, there would be the need of a modification of the N-body codes involved in the description of structure formation, which would then have to take into account the possibility of the presence of Dark Energy in Dark Matter haloes. An example of such a scenario has been investigated in [110] for a particular non minimal coupling model.

As we have announced, in the next Chapter we will study in more details the case in which scalar-tensor theories are considered in a cosmological

framework, thus interpreting the scalar field ϕ as the Dark Energy contribution to the Universe in extended quintessence theories [108, 8]. First, however, we end this chapter with a review of the most recent bounds imposed by observations on scalar tensor theories.

4.2 Experimental constraints

As we can see from action (4.1), scalar-tensor theories propose the existence of a varying gravitational constant $1/F(\phi)$ whose strength depends on a scalar field; seen in the Einstein frame, this corresponds to a universal coupling to matter fields whose masses depend on ϕ . In both cases, when dealing with such theories, we always need to keep an eye on the bounds put by experiments on the variation of the gravitational constant and on the coupling to matter. In particular, a field as light as usually ϕ is, cannot be coupled too strongly to baryonic matter since it would produce a long range fifth force which is not observed [116]. Deviations from GR have been constrained in various sets of experiments, including solar-system experiments where precision measurements have been performed, binary-pulsar tests whose orbit is in perfect agreement with GR, observations which involve the early Universe, from BBN to CMB radiation; finally, future detection of Gravitational Waves would be an important test for GR.

Note however, that nowadays tests mainly concern scales up to the Solar System, while very few tests have been performed on astrophysical scales and no really direct proof has been given at cosmological scales.

A detailed review on recent constraints can be found in [66] (see also [67, 118, 149, 133]) to which we will refer in the next few paragraphs.

4.2.1 Solar system

Tests on solar system scales mainly concern the presence of a long range fifth force as well as tests on the universality of free fall. The effect of the scalar field on the gravitational force which acts on bodies in the solar system is negligible if the mass of the scalar field is so large that its effect is on scales much smaller than the distances between the bodies. In this case, on solar-system scales, the theory is essentially equivalent to General Relativity [149]. However, though there exist models in which the quintessence field is massive [71], quintessence field is usually very light so that its effect is highly constrained by experiments. Deviations from GR can be parametrized by two main parameters, γ and β , the only two parameters that change within

the original set of ten quantities originally denoted by Eddington [62]:

$$\gamma - 1 \equiv -2 \frac{\alpha_0^2}{1 + \alpha_0^2} = \frac{F_\phi^2}{ZF + 2F_\phi^2} \quad (4.70)$$

$$\beta - 1 \equiv \frac{1}{2} \frac{\alpha_0^2}{(1 + \alpha_0^2)^2} \beta_0 = \frac{1}{4} \frac{FF_\phi}{2ZF + 3F_\phi^2} \frac{d\gamma}{d\phi} \quad (4.71)$$

where the first expressions refer to quantities in the EF (4.17) and the second terms are the equivalent expressions in the WF (4.1). Note that GR corresponds to the case $\beta = 1 = \gamma$. In particular, α_0 and β_0 are defined in terms of the conformal factor $A(\phi)$ defined in (4.8) and are related to its first and second derivatives:

$$\alpha \equiv \frac{d \ln A(\phi)}{d\phi} \quad \beta = \frac{\ln A(\phi)}{d\phi^2} \quad (4.72)$$

so that

$$\ln A(\phi) \equiv \alpha_0(\phi - \phi_0) + \frac{1}{2} \beta_0(\phi - \phi_0)^2 + o(\phi - \phi_0)^3 \quad (4.73)$$

The subscript 0 indicates that quantities are calculated for $\phi = \phi_0$, which is the present background value of the scalar field.

The γ parameter is related to the exchange of a scalar field in the interaction between two matter fields (*from*(4.70) $\gamma - 1 \propto \alpha_0^2$) while the β parameter is related to the exchange of two scalar fields between three matter bodies ($\beta - 1 \propto \alpha_0^2 \beta_0$ *from* 4.71) [66]. The most stringent bound comes, up to now, from the Cassini spacecraft [16]:

$$\gamma - 1 = (2.1 \pm 2.3) \times 10^{-5} \quad (4.74)$$

which impressively improves previous bounds from the Very Long Baseline Interferometry⁴; a bound on a combination of both γ and β parameters has also been found by the perihelion shift of Mercury and the Lunar Laser Ranging (see [66] and references therein):

$$|2\gamma - \beta - 1| < 3 \times 10^{-3} \quad (4.75)$$

$$4\beta - \gamma - 3 < (-0.7 \pm 1) \times 10^{-3} \quad (4.76)$$

Hence, solar system experiments indicate that α_0 (and thus the coupling between matter and ϕ) needs to be small, while β_0 can be quite large (matter could be strongly coupled to two scalar fields).

The bound (4.74) can be rewritten in terms of the ω_{JBD} parameter, often used in the WF and defined as:

$$\omega_{JBD} \equiv F \left(\frac{dF}{d\phi} \right)^{-2} = -\frac{1}{\gamma - 1} \geq 4 \times 10^4 \quad (4.77)$$

⁴A review of bounds before Cassini can be found in [133].

Today's value of the effective Newtonian constant G_{eff} defined as

$$G_{\text{eff}}(\phi) \equiv \frac{M^2 G}{F(\phi)} = A^2(\phi) G \quad (4.78)$$

differs by less than 0.02% from the one measured in laboratories in a Cavendish like experiment and defined as

$$G_{N_{\text{eff}}} = \frac{GM^2}{F_0} \frac{16\pi M^2 F_0 + 4/M^2 (F'_0)^2}{16\pi M^2 F_0 + 3/M^2 (F'_0)^2} G A_0^2 (1 + \alpha_0^2) \quad (4.79)$$

where the two contributions in the second expression refer to the exchange between two matter fields of a graviton and of a scalar field respectively. Nevertheless, G_{eff} and $G_{N_{\text{eff}}}$ can have been very different in the past. Also, the experimental limit on the variation of the gravitational constant

$$|\dot{G}_{\text{eff}}/G_{\text{eff}}| < 6 \times 10^{-12} \text{yr}^{-1} \quad (4.80)$$

does not imply a bound on \dot{F}/F or equivalently on \dot{A}/A and even if G_{eff} is almost constant, $F(\phi)$ (or equivalently $A(\phi)$) can vary⁵. We also note that the the bare gravitational coupling constant indicated as G_* in (4.1) differs from the one measured in the Cavendish like experiments by corrections which are negligible in the limit $\omega_{JBD} \gg 1$ [67].

4.2.2 Binary pulsars

Other tests come from the orbital motion of binary pulsars [133], which consist in rapidly rotating neutron stars which emit a beam of radio waves. The measurement of the arrival times of their pulses can be used both to measure the masses of the two pulsars orbiting around each other and to test General Relativity, therefore constraining scalar-tensor theories. In particular they limit the β_0 parameter to have values which are not very negative [66]:

$$\beta_0 > -4.5 \quad (4.81)$$

4.2.3 Cosmological observations

It may not be straightforward to extend limits obtained on solar system scales to cosmological scales, as it was pointed out recently [44]. Indeed, observations probe regions well within our Galaxy, which is a self-gravitating virialized system: in physical theories where fundamental constants vary, the latter may acquire local values which are different from their large scale,

⁵For example if $A(\phi) = \cos \phi$, then $G_{\text{eff}} = G_*(\cos^2 \phi + \sin^2 \phi) = G_*$ [67].

cosmologically effective ones. For this reason, cosmology is likely to become a source of constraints for the underlying theory of gravity in a complementary way with respect to the solar system. In [3] constraints have been derived on a Jordan Brans Dicke theory both from CMB anisotropies and galaxy power spectrum data, obtaining a 95% marginalized probability lower bound on the Jordan Brans Dicke parameter

$$\omega_{JBD} > 120 \quad (4.82)$$

The latter represents a complementary result with respect to the very strong bound (4.74) which probes completely different scales.

Moreover, while solar system and binary pulsars experiments give only bounds on the slope of the $A(\phi)$ function in (4.17), the whole shape of the latter can be reconstructed via cosmological observations. In particular, it was shown in [67] that both the $V(\phi)$ potential and the $A(\phi)$ coupling function can be reconstructed once both the luminosity distance $d_L(z)$ and density fluctuation $\delta_m(z) = \delta\rho/\rho$ are known as functions of z .

4.2.4 Big Bang Nucleosynthesis

The most direct cosmological probe of the value of the scalar field ϕ during radiation domination is the Big Bang Nucleosynthesis (BBN). At this purpose, an important tool is represented by the amount of light nuclides produced when the photon temperature was in the range $0.01 \div 10$ MeV, which is rather sensitive to the value of the Hubble parameter during that epoch, as well as to its time dependence. In particular the ${}^4\text{He}$ mass fraction Y_p strongly depends on the temperature at which weak processes which keep neutrons and protons in chemical equilibrium freeze out. Changing the value of \mathcal{H} affects the neutron to proton number density ratio at the onset of the BBN, which is the key parameter entering the final value of Y_p and more weakly in the Deuterium abundance. For a fixed baryon density parameter $\Omega_b h^2 = 0.023 \pm 0.001$ in the range suggested by WMAP data [153], the amount of both ${}^4\text{He}$ and Deuterium nuclei increases monotonically with \mathcal{H} . Recent reviews on BBN can be found in [49, 50, 129].

The most accurate measurement of primordial Deuterium number density, normalized to Hydrogen, X_D , is obtained from DI/HI column ratio in Quasi Stellar Objects (QSO) absorption systems at high redshifts. The most recent estimate [86] gives

$$X_D^{exp} = (2.78_{-0.38}^{+0.44}) \times 10^{-5} \quad , \quad (4.83)$$

and is in good agreement with the theoretical expectation for a standard scenario with three active neutrinos and a baryon density given by the WMAP result [129]; the latter is

$$X_D^{th} = (2.44_{-0.17}^{+0.19}) \times 10^{-5} \quad , \quad (4.84)$$

where the (1σ) theoretical uncertainty accounts for both the propagated error due to the several rates entering the BBN nuclear reaction network as well as the 5% uncertainty on ω_b . On the other hand the ${}^4\text{He}$ mass fraction Y_p obtained by extrapolating to zero the metallicity measurements performed in dwarf irregular and blue compact galaxies is still controversial and possibly affected by large systematics. There are two different determinations [70, 85] which are only compatible by invoking the large systematic uncertainty quoted in [70]

$$Y_p = 0.238 \pm (0.002)_{stat} \pm (0.005)_{sys} , \quad (4.85)$$

$$Y_p = 0.2421 \pm (0.0021)_{stat} . \quad (4.86)$$

Both results are significantly lower than the theoretical estimate [129]

$$Y_p^{th} = 0.2481 \pm 0.0004 , \quad (4.87)$$

where again we use $\omega_b = 0.023$ and the small error is due to the uncertainty on the baryon density and, to a less extent, to the error on experimental determination of the neutron lifetime. As in [129] we will consider a more conservative estimate for the experimental ${}^4\text{He}$ abundance obtained by using the results of [104]

$$Y_p^{exp} = 0.245 \pm 0.007 . \quad (4.88)$$

As we have seen in the analysis of the background, scalar-tensor theories affect the value of \mathcal{H} both introducing an extra contribution in the Friedmann equation (4.38) and by changing the effective gravitational constant so that $G \sim 1/F$ appears as a multiplying factor in (4.38). As a consequence, BBN can be used to constrain the coupling parameters entering in the model. In particular, if the generalized Dark Energy density defined in (4.42) is negligible with respect to the background radiation at BBN

$$\tilde{\rho}_{DE} \ll \rho_r \quad (4.89)$$

Friedmann equation can be rewritten as

$$\mathcal{H}^2 \sim \frac{a^2}{3F} \rho_r = \frac{\mathcal{H}_{GR}^2}{8\pi GF} \quad (4.90)$$

where the radiation energy density is given by

$$\rho_r = \frac{\pi^2}{30} g_* T^4 \quad (4.91)$$

and we have defined

$$\mathcal{H}_{GR}^2 \equiv \frac{8\pi G}{3} a^2 \rho_r \quad (4.92)$$

The effect of a varying gravitational constant can then be estimated interpreting it in terms of a modification δg_* of the number of degrees of freedom

of relativistic particles g_* , whose expected value at BBN is $g_* = 10.75$ [118]. In this case, the effective Hubble parameter would then be written as:

$$\mathcal{H}^2 = \frac{8\pi G}{3} a^2 \frac{\pi^2}{30} (g_* + \delta g_*) T^4 \quad (4.93)$$

$$= \mathcal{H}_{GR}^2 + \frac{\delta g_*}{g_*} \mathcal{H}_{GR}^2 \quad (4.94)$$

Setting (4.90) equal to (4.94) we have:

$$\frac{\delta g_*}{g_*} \equiv \frac{F_0 - F(\phi_{BBN})}{F(\phi_{BBN})} \quad (4.95)$$

where ϕ_{BBN} is the value of the field at BBN and $F_0 = 1/8\pi G$ is the value of the coupling today, equal to the one assumed in General Relativity.

Consequently, eq.(4.95) allows us to rewrite a constrain on the number of degrees of freedom in terms of a bound on the coupling function. If we allow, for example, g_* to vary of an amount of 20% we have

$$\left| \frac{\delta g_*}{g_*} \right| \leq 0.2 \quad (4.96)$$

and consequently

$$0.8 \leq \left| \frac{F_0}{F(\phi_{BBN})} \right| = \left| \frac{A^2(\phi_{BBN})}{A_0^2} \right| \leq 1.2 \quad (4.97)$$

where $F(\phi)$ is the coupling function in the Weyl frame and $A(\phi)$ is the conformal factor in the Einstein frame. We will see an application of this bound in the next Chapter for a specific model.

Chapter 5

A general approach to Extended Quintessence cosmologies

5.1 Dark Energy as a modification of gravity

Dark energy dynamics in scalar-tensor cosmologies has recently arised a broad interest due to the temptation to interpret quintessence in terms of a gravity modification [91]. This purpose was first suggested in [55] where scalar-tensor theories were used in order to have a decaying, asymptotically null, contribution to vacuum energy thanks to a massless scalar field non minimally coupled to the Ricci scalar; nevertheless, the interesting range of the proposed dynamics was in strong contradiction with observational constraints on the variation of the gravitational constant [120]. Since then, a similar framework, described by action (4.1) has been exploited in a wide variety of works: several appealing features which characterize these models have been object of many analysis concerning both the background and cosmological perturbations as well as constraints imposed by experiments [2, 8, 13, 34, 43, 68, 84, 96, 108, 110, 111, 118, 136, 140]. Such scenarios, in which the non minimal coupled scalar field ϕ acts as a Dark Energy component at recent times, go under the name of Extended Quintessence (EQ).

In EQ theories the motion of the field is strongly modified by gravitational effects: in particular, the direct coupling of the field itself to the Ricci scalar makes the field undergoing an enhanced dynamics at early times known as R-boost; also, the field trajectory behaves as an attractor for several choices of the coupling, extending to EQ the most appealing property of tracker models, i.e. that of having attractor solutions which try to solve the problem of fine tuning of the initial conditions. As we have already

pointed out, recent analysis [125] exclude a large fraction of cosmological parameters values, allowing to partly constrain theoretical models; tracker quintessence models which predict $\omega_\phi \geq -0.7$ are now excluded, so that only models in which $\omega_\phi \sim -1$ remain acceptable. Moreover, as ω_ϕ gets closer to -1 the basin of attraction in the early universe of minimal coupling models shrinks, threatening the basis of the whole quintessence picture [18]. Interestingly, it was recently argued that in these conditions coupling Dark Energy to other entities may be very relevant, especially at early times, possibly saving the existence of attractors for the initial field dynamics [96]. Indeed, extended quintessence scenarios allow to have models in which ω_ϕ today is very near to -1 but in which $\omega_\phi \neq -1$ in the past [8]. We will see that this feature can be obtained regardless of the initial conditions, thanks to the presence of attractors. In particular, while in minimally coupled quintessence models attractors are usually called scaling [90] or tracking [134] solutions, the corresponding trajectories in extended quintessence come from the non-minimal coupling and are called *R*-boost solutions [8].

Finally, minimal coupling models are usually ruled out if the Dark Energy equation of state $\omega_\phi < -1$, whose value is strangely in fair agreement with the observations. On the contrary, several authors [19] [65] [99] [107] [136] have shown that certain Extended Quintessence scenarios can cross the cosmological constant value and reach $\omega_\phi < -1$ without incurring in the problems encountered by phantom models.

5.2 R-boost

A major achievement of Extended Quintessence concerns the early universe dynamics of the quintessence scalar field. For small values of the scale parameter $a(t)$, during RDE, the dominant term in the expression for the Ricci scalar (4.46) is the one including $(\rho_{fluid} - 3p_{fluid})$. Since $\omega_r \equiv p_r/\rho_r = 1/3$, radiation gives a null contribution; nevertheless, as soon as one or more sub-dominant non-relativistic species exists, the Ricci scalar gets a non-zero contribution $R \sim \rho_{nrm}/F$ that scales as non relativistic matter. Hence, R tends to diverge as $1/a^3$, becoming increasingly relevant at early times

$$R \simeq \frac{1}{F} \frac{\rho_{mnr0}}{a^3} \quad \text{for } a \rightarrow 0 \quad (5.1)$$

The parameter ρ_{mnr0} above indicates the energy density of the species which are non-relativistic at the time in which the dynamics is considered. Note that the remaining terms in (4.46) are negligible with respect to (5.1) for $a(t)$ sufficiently small. As a consequence, the term proportional to R in the Klein Gordon equation (4.37) acts as a new source for the quintessence motion, activating an effective purely gravitational potential in the equation that originates only from non-minimal coupling. This term drives the motion

of the field at early times and is the dominant contribution in the Klein Gordon equation. In particular, the true potential $V(\phi)$ has a negligible effect during all RDE and it becomes relevant only at recent times. The resulting motion of the field is the R -boost, an effect first shown in [8]. In the following sections we will see that, in the early universe, the R -boost trajectory behaves as an attractor generated only by a modification of gravity and not by a particular choice of the true potential $V(\phi)$. In this context, the R -boost effect has recently acquired a crucial importance since it can remove the fine tuning in the early universe even if the potential is constrained to be almost flat in order to be consistent with the observations.

Despite the discussed interest in the topic, most of the results obtained in EQ theories have been performed within induced gravity theories or non minimal coupling theories, in which the coupling function has respectively the following expressions:

$$F(\phi) = \xi\phi^2 \quad (5.2)$$

$$F(\phi) = \frac{1}{16\pi G} + \xi\phi^2 \quad (5.3)$$

which differ from each other by the term $1/16\pi G$, equal to the value the coupling should have at present. Nevertheless, there is not a priori a particularly motivated form of the coupling to gravity and the possibilities among which it can be selected cover a wide range. A general treatment of Extended Quintessence theories was therefore still missing. Our aim will consist in providing a general classification of scalar-tensor theories which guarantee the existence of attractor solutions to the Klein Gordon equation [113]. With this purpose in mind, we will not fix a specific expression for the coupling $F(\phi)$. On the contrary, we will try to identify the possible forms of the coupling which give rise to R -boost trajectories behaving as attractors in the early Universe.

As a further step, later ahead in this Chapter, we will choose a specific expression for the coupling $F(\phi)$, different from the ones usually used in the past: in this framework we will investigate the effect of such a coupling both on the background and on perturbations, pointing out the differences with other choices of $F(\phi)$.

Before proceeding, however, in the classification of scalar-tensor theories according to the attractor features of the field trajectory, we briefly recall here the relevant equations describing the cosmological expansion assuming a Friedmann Robertson Walker (FRW) background metric. In the following we will operate in the framework of scalar-tensor theories described in the previous Chapter, containing both a scalar field ϕ coupled to gravity through the function $F(\phi)$ and a contribution of perfect fluid components with pressure and energy density generically indicated with p_{fluid} and ρ_{fluid} ; in particular we rewrite here for convenience the action and the equations

which will turn useful for the subsequent analysis:

$$S = \int d^4x \sqrt{-g} \left[\frac{1}{2} F(\phi) R - \frac{1}{2} \phi^{;\mu} \phi_{;\mu} - V(\phi) + \mathcal{L}_{fluid} \right] \quad (5.4)$$

$$H^2 = \left(\frac{\dot{a}}{a} \right)^2 = \frac{1}{3F} \left(\rho_{fluid} + \frac{1}{2} \dot{\phi}^2 + V(\phi) - 3H\dot{F} \right) \quad (5.5)$$

$$\ddot{\phi} + 3H\dot{\phi} = \frac{1}{2} F_{,\phi} R - V_{,\phi} \quad (5.6)$$

where we have used (4.7) and we have chosen $Z(\phi) = 1$ in (4.1). For flat cosmologies, the distance is specified by (1.3) in term of the cosmic time t or by (1.6) in terms of the conformal time variable η , related to the cosmic time via the transformation (1.4).

5.3 Scaling solutions in scalar-tensor cosmologies

In order to proceed to the analysis, we will closely follow what has been done in [90] in the case of minimal coupling, where the authors have classified the allowed forms of the true potential $V(\phi)$ in order to have attractors in the form of scaling solutions. With the latter we mean that we are interested in solutions of the Klein Gordon equation which scale as a power of the scale factor. In particular, assuming that in the Friedmann equation the terms involving the scalar field are negligible with respect to the fluid energy density

$$\rho_{fluid} \gg \tilde{\rho}_\phi \quad , \quad (5.7)$$

which is true in the epoch of early Universe we are interested in, and that the fluid scales as

$$\rho_{fluid} \propto a^{-m} \quad , \quad (5.8)$$

we want to find the forms of the coupling $F(\phi)$ which admit solutions of the equation (5.6) of the form

$$\tilde{\rho}_\phi \propto a^{-n} \quad , \quad (5.9)$$

where m and n are two integer positive defined numbers.

Note that we have considered the generalized energy density defined in (4.42) which, as stated in the previous Chapter, is different from the conserved one (4.34). Nevertheless, the present aim is to look for trajectories of the scalar field as a function of time, determined by the effective gravitational potential in the Klein Gordon equation. In the energy density, this contribution is entirely kinetic [8], which therefore is the relevant energy density component for our purpose, as we see in detail in the next section. In other words, we are interested in attractor paths which solve the Klein Gordon equation for the field, which is unique regardless of the definition of the energy density. In this perspective, it is convenient to refer to the

generalized energy density $\tilde{\rho}_\phi$, which has a direct intuitive meaning for the dynamics of cosmological expansion, as it regroups the scalar field terms which compete with ρ_{fluid} in the Friedmann equation (5.5).

Assuming that the approximation (5.1) for the Ricci scalar is still valid and since the potential $V(\phi)$ in eq.(5.6) has no relevant effect up to recent times, we can rewrite the Klein Gordon equation in the following way:

$$\ddot{\phi} + 3H\dot{\phi} = \frac{1}{2} \frac{\rho_{mnr0}}{a^3} \frac{F_\phi}{F} \quad (5.10)$$

Assuming that the perfect fluid is the dominant component, Friedmann equation (5.5) allows us to calculate the behavior with time of the scale factor $a(t)$ as

$$a = \left(\frac{t}{t_*} \right)^{2/m}, \quad (5.11)$$

where t_* stands for a fixed reference time in the RDE and we neglected any initial condition, assuming to work with t large enough with respect to t_* . In eq.(5.11) we have assumed that the time dependence of F in the Friedmann equation is modest enough not to affect significantly the dependence on the scale factor of the right hand side of equation (5.5). Also, the last two terms in the Friedmann equation must be small in order to satisfy the condition (5.7). However, we will still verify a posteriori that these assumptions are plausible. Substituting in eq.(5.10) we get:

$$\ddot{\phi} = -\frac{6}{m} \frac{1}{t} \dot{\phi} + \frac{1}{2} \rho_{mnr0} \left(\frac{t_*}{t} \right)^{6/m} \frac{F_\phi}{F} \quad (5.12)$$

At this stage the energy density of the field ϕ is mainly given by its kinetic contribution, acquired through slow rolling onto the effective gravitational potential in the Klein Gordon equation. Thus $\rho_\phi \simeq \dot{\phi}^2/2$ and assuming the desired scaling behavior (5.9) we obtain ϕ time dependence

$$\dot{\phi} \propto t^{-n/m} \quad (5.13)$$

We will now proceed by distinguishing the two cases $m = n$ or $m \neq n$.

5.3.1 Case $m = n$

If $m = n$ then $\dot{\phi} \propto t^{-1}$ and integrating this expression we get

$$\phi = A \ln \frac{t}{t_*} + \phi_* \quad (5.14)$$

where A is a constant with the dimensions of a field, i.e. proportional to the Planck mass $m_P = 1/\sqrt{G}$ in our units. Substituting (5.14) and its first and second derivatives in eq.(5.12) we obtain the following expression

$$\frac{F_\phi}{F} = \frac{2A}{\rho_{mnr0}} \frac{1}{t_*^2} \left(\frac{6}{m} - 1 \right) e^{[2(\frac{3}{m}-1)\frac{\phi-\phi_*}{A}]} \quad (5.15)$$

If $m \neq 3$, the condition on the coupling, obtained by integrating eq.(5.15), is

$$F = F_* e^{[B(e^{C(\phi-\phi_*)}-1)]} \quad , \quad (5.16)$$

where

$$B = \frac{A^2}{\rho_{mnr0}} \frac{1}{t_*^2} \frac{6-m}{3-m} \quad , \quad C = \frac{2}{A} \left(\frac{3}{m} - 1 \right) \quad (5.17)$$

and F_* is the value the coupling has at t_* . Note that the combination $\rho_{mnr0} t_*^2$ has a direct interpretation in terms of the abundance of the non-relativistic components at the t_* time; indeed $\rho_{mnr0} t_*^2 \propto (a_*/a_0)^3 \rho_{mnr*}/H_*^2$.

If $m = 3$, which is the case of a Universe dominated by ordinary matter, eq.(5.15) becomes

$$\frac{F_\phi}{F} = \frac{2A}{\rho_{mnr0}} \frac{1}{t_*^2} \quad (5.18)$$

and the form of the allowed coupling is

$$F = F_* e^{\left[\frac{2A}{\rho_{mnr0}} \frac{1}{t_*^2} (\phi - \phi_*) \right]} \quad (5.19)$$

Notice that in minimal coupling theories the case $m = n$ corresponds to a scenario in which the Dark Energy scales as the dominant component, thus never achieving acceleration unless such regime is broken by some physical mechanism, as in the case of quintessence with exponential potential [147, 90]. On the other hand, in scalar-tensor theories of gravity the case $m = n$ is fully exploitable in its context, since it has been obtained precisely with the assumption (5.7) and neglecting the true potential V in the Klein Gordon equation (5.6). Actually, its relevance is on the capability to provide an attractor mechanism when the dark energy is sub-dominant, independently on the form of the potential energy driving acceleration today. Indeed, it does not exclude a different behavior of the ϕ field at present time, when the potential V starts to have a dominant effect on the dynamics of ϕ .

5.3.2 Case $m \neq n$

Integrating eq.(5.13) in the case $m \neq n$ we get:

$$\phi = \tilde{A} \left(t^{1-\frac{n}{m}} - t_*^{1-\frac{n}{m}} \right) + \phi_* \quad , \quad (5.20)$$

where \tilde{A} has the dimensions of a time derivative of a field. Substituting this expression in eq.(5.12), together with its first and second derivatives, we obtain the following condition

$$\frac{F_\phi}{F} = \frac{\tilde{C}}{\tilde{A}} \left(\frac{\phi - \phi_*}{\tilde{A}} + t_*^{1-\frac{n}{m}} \right)^{\tilde{B}} \quad , \quad (5.21)$$

where

$$\tilde{C} = \frac{2\tilde{A}^2}{\rho_{mnr0}} \frac{1}{t_*^{6/m}} \frac{(m-n)(6-n)}{m^2} \quad \tilde{B} = \frac{6-m-n}{m-n} \quad . \quad (5.22)$$

As in Section 5.3.1, note the combination $\rho_{mnr0} t_*^{6/m} \propto (a_*/a_0)^3 \rho_{mnr*}/H_*^{6/m}$. Again we have to distinguish the two cases in which the exponent \tilde{B} is equal or not to -1 .

For $\tilde{B} = -1$ the condition (5.21) gives, after integration, polynomials of ϕ of the type:

$$F = F_* \left[1 + \frac{\phi - \phi_*}{\tilde{A}} t_*^{\frac{n}{m}-1} \right]^{\tilde{C}} \quad (5.23)$$

Notice that if the solution (5.20) is exactly a power law of the time t , namely $\tilde{A} t_*^{1-\frac{n}{m}}$, the coupling (5.23) becomes exactly a power law as well, as in induced gravity models (see e.g. [108] and references therein). Therefore, this class of gravity theories admits scaling solutions: however, those may arise in the radiation dominated era only, as $\tilde{B} = -1$ with $m = 4$ induces $n = 3$ while the same condition with $m = 3$ is not satisfied regardless of the value of n . For $\tilde{B} \neq -1$ the result of the integration of eq.(5.21) is

$$F = F_* e^{\left[\frac{\tilde{C}}{1+\tilde{B}} \left[\left(\frac{\phi - \phi_*}{\tilde{A}} + t_*^{1-\frac{n}{m}} \right)^{\tilde{B}+1} - \left(t_*^{1-\frac{n}{m}} \right)^{\tilde{B}+1} \right] \right]} \quad (5.24)$$

Expression (5.24) is general for values of $\tilde{B} \neq 0$ and includes exponential functions with general coupling constant \tilde{A} contained in \tilde{C} and defined in (5.20).

The case, $m = 4 = 2n$ yielding $\tilde{B} = 0$, also corresponds to the R-boost solution exploited in [8] in the radiation dominated era. The reason why our formalism does not show that the form of the non-minimal coupling in that case, $F = 1/2\kappa + \xi\phi^2$, is compatible with such a solution, is the following. For small values of the coupling constant ξ , the field dynamics is correspondingly reduced. Eventually one enters the regime in which the second term on the right hand side of (5.20) dominates over the first one, yielding a scalar field value as a function of time which is effectively constant; this is a clearly transient phase, as eventually such regime is broken, but before that the relation (5.21) remains approximately true. Although this is formally not a scaling solution as that found in the exponential case [112], the values of ξ may be chosen so small that for interesting initial conditions on ϕ , its variation due to the R-boost is not relevant at all interesting epochs in the radiation dominated era, keeping the solution $m = 4 = 2n$ effectively valid also for the coupling considered in [8]. We may refer to the solutions of the Friedmann and Klein Gordon equations in these scenarios as *transient* scaling solutions, meaning that they hold until the true R-boost dynamics takes over moving the field value away from its initial condition. Note finally that the same reasoning applies in general in all cases where F is the sum

of a constant plus a positive power of the field, normalized by a coupling constant.

5.3.3 Summary and consistency criteria

We have found, up to now, all possible choices of the coupling F which can have scaling solutions verifying (5.7) - (5.9), in the sense that there are no other forms of the coupling admitting scaling behavior in scalar-tensor theories of gravity; for some of them, like in the non-minimal coupling considered in [8], transient scaling solutions are admitted in the time interval preceding the epoch in which the R-boost motions moves the field away from its initial condition. We have found exponential forms of the coupling [112] for general choices of m , n and the \tilde{B} exponent in (5.24); also, we have seen that (5.23) allows polynomials of ϕ . Eq.(5.16) also suggests that a family for the coupling F might be allowed, in the case $m = n$, namely made by exponentials of exponentials. Though no other coupling can allow for scaling solutions, we have by now no guarantee that the general solution of all these expressions for the coupling will indeed have an attractor behavior and this is what we are going to investigate in the next section.

Before moving to that, let us briefly check the consistency of the scaling solutions we found with the assumptions we made. They are essentially three, concerning equations (5.5), (4.46) and (5.11). It is important to note that the variation of F induces corrections which are small in the limit $\omega_{JBD} \gg 1$. For example, $\dot{F}/F = \dot{\phi}F_\phi/F \propto \dot{\phi}/\sqrt{\omega_{JBD}}$; therefore, even if the field dynamics may be important as in (5.13), the coupling constant may be chosen small in order to yield a small variation in time of F . More precisely, it is easy to see that the kinetic contribution in (5.5) is the lowest order term in $1/\omega_{JBD}$; all the others, involving a change in F , yield terms like $F_\phi\dot{\phi}$, which are of higher order due to the presence of F_ϕ , which brings another $1/\sqrt{\omega_{JBD}}$. Indeed, it is important to stress again that the R-boost dynamics is caused primarily by a non-zero Ricci scalar, diverging in the early universe if at least one non-relativistic species is present, and not only to the underlying scalar-tensor gravity theory. Thus in the limit of a small coupling, all the three approximations mentioned above are satisfied. However, it is interesting to push the analysis a little further here, by computing the scaling of the terms in (5.5, 4.46) coming from the scalar-tensor coupling. Concerning the last term in (5.5), which may be written as $-HF_\phi\dot{\phi}/F$, using (5.12) and (5.13) it may be easily verified that it scales as $1/t^{\frac{2m+2n-6}{m}}$; when compared with the first term in the right hand side of (5.5), it yields the condition $n < 3$ both in matter and radiation dominated eras. Note that if one ignores the issue related with the coupling strength mentioned above, this relation is quite stringent, confining all the scaling solution in scalar-tensor theories of gravity to possess a shape not steeper than a^{-3} . The same criteria lead to

$n < 3$ and $n < 2$ in the matter and radiation dominated eras, respectively, for neglecting the last two terms in the right hand side of (4.46). Also in this case, this requirement may be bypassed by working in a small scalar-tensor coupling regime.

We now turn to study which scaling solutions represent attractors for the field dynamics.

5.4 Attractors

Our purpose here is to check whether the various forms of the coupling F found in the previous section lead to attractor solutions to the Klein Gordon equation (5.10). With this aim, we will investigate whether the particular solutions found for the cases $m = n$ and $m \neq n$ are indeed attractors or not. Following the criteria developed in [90], we will proceed by linearizing the Klein Gordon equation with small exponential perturbations around the critical point, represented, as we will see, by our particular solution. At a linear level, the attractor behavior will be guaranteed whenever the perturbation will converge to zero with time. We shall also investigate numerically a few cases without linearization.

With the following change of variable

$$u = \frac{\phi}{\phi_e} \quad (5.25)$$

where ϕ_e is the exact particular solution of eq.(5.12), eq.(5.10) can be rewritten as

$$\ddot{u}\phi_e + \dot{u} \left[2\dot{\phi}_e + 3H\phi_e \right] = \frac{\rho_{mnr0}}{2a^3} \frac{F_\phi}{F} (1 - u) \quad . \quad (5.26)$$

We will now distinguish what happens in the two cases discussed in the previous section, for $m \neq n$ and $m = n$.

5.4.1 Attractor behavior for $m \neq n$

As we have discussed in the previous section, in the case $m \neq n$ the coupling needs to satisfy eq.(5.21) and the exact solution ϕ_e depends on time as in eq.(5.20). For simplicity in the following we will consider $t \gg t_*$ in such a way that the t_* term in eq.(5.20) can be neglected; also, for t large enough, the initial condition ϕ_* can be neglected too and eq.(5.20) reduces to $\phi = \tilde{A} t^{1-\frac{n}{m}}$, where \tilde{A} is an arbitrary constant as defined in eq.(5.20). Substituting the first and second derivatives of ϕ_e in eq.(5.10) we get

$$\frac{\rho_{mnr0}}{2a^3} \frac{F_\phi}{F} = \frac{(6-n)(m-n)}{m^2} \frac{\phi_e}{t^2} \quad (5.27)$$

Using this expression in eq.(5.26) and with the change of variable

$$\tau = \ln \frac{t}{t_*} \quad , \quad (5.28)$$

we obtain

$$u'' + \frac{m - 2n + 6}{m} u' = \frac{(6 - n)(m - n)}{m^2} (1 - u) \quad , \quad (5.29)$$

where the derivatives are calculated with respect to τ . As we can see, this equation admits a critical point for $u = 1$ and $u' = 0$. If we consider a perturbation δu around the critical point, such that $u = 1 + \delta u$ we can rewrite eq.(5.29) as

$$\delta u'' + \frac{m - 2n + 6}{m} \delta u' = -\frac{(6 - n)(m - n)}{m^2} \delta u \quad (5.30)$$

which is a homogeneous differential equation of the second order in τ with constant coefficients. The generic expression of the perturbation δu is thus a combination of exponential terms ($\delta u = c_1 e^{\lambda_1 \tau} + c_2 e^{\lambda_2 \tau}$) where c_1 and c_2 are arbitrary constants and $\lambda_{1,2}$ are equal to

$$\lambda_{1,2} = -\frac{m - 2n + 6}{2m} \pm \frac{|m - 6|}{2m} \quad . \quad (5.31)$$

It is easy to see that the eigenvalues are real and negative for $n < \min\{6, m\}$. As a consequence, for these values of the parameters, the perturbation will go to zero with time and the solution of the Klein Gordon equation (5.29) will converge to $u = 1$ making $\phi = \phi_e$ to behave as a stable attractor.

The numerical solution of equation (5.29), in full generality and without linearization, is shown in fig.(5.1) for a somewhat large set of initial conditions. On the left side the time dependences of u and u' are shown, in the case ($m = 4, n = 2$). Different curves correspond to different initial conditions for u and u' and they all converge to the stable attractor solution ($u = 1, u' = 0$). On the right side it is shown the u' vs u plot for the same choices of initial conditions of the left hand side plot.

5.4.2 Attractor behavior for $m = n$

In the case $m = n$ the exact solution ϕ_e depends on time as in eq.(5.14) thus we have

$$\frac{\rho_{mnr0}}{2a^3} \frac{F_\phi}{F} = \frac{A}{t^2} \left(\frac{6}{m} - 1 \right) \quad , \quad (5.32)$$

where A is the same as in expression (5.14). With the change of variable (5.28) the Klein Gordon equation becomes:

$$u'' + u' \left(\frac{2A}{\phi_e} + \frac{6 - m}{m} \right) = \frac{A}{\phi_e} \frac{6 - m}{m} (1 - u) \quad . \quad (5.33)$$

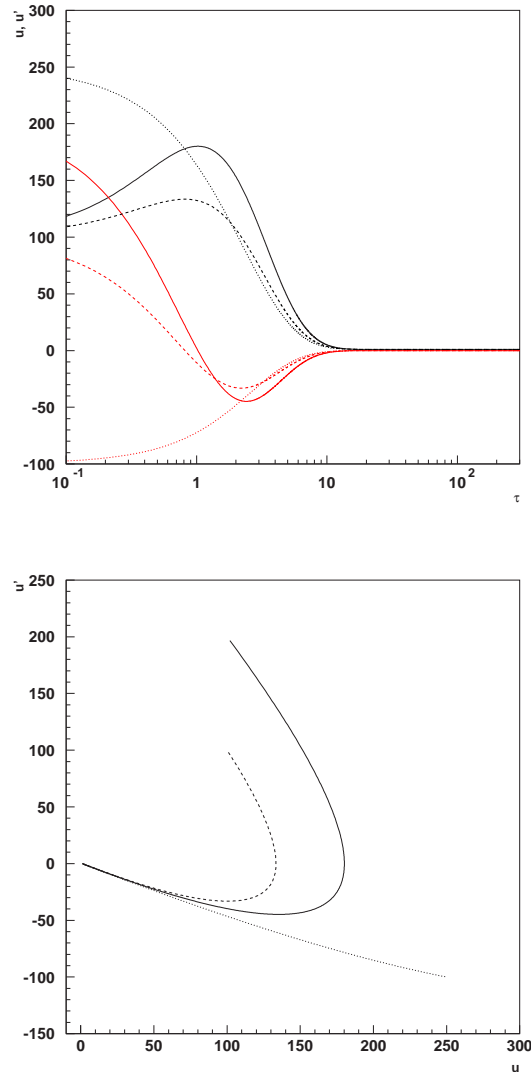


Figure 5.1: Numerical solutions of eq.(5.29) are shown: on the left side u (black) and u' (red) are plotted versus τ , in the case ($m = 4, n = 2$) and converge to the stable attractor solution ($u = 1, u' = 0$). Different curves correspond to different initial conditions for u and u' : $(u_0, u'_0) = (100, 200)$ (solid), $(100, 100)$ (dashed), $(250, -100)$ (dotted). The τ scale is logarithmic. On the right side u' vs u is plotted for the same initial conditions.

Note that, unlike what happens in the previous case, the coefficients in eq.(5.33) depend on time through $\phi_e(t)$. Nevertheless, ($u = 1$, $u' = 0$) still behaves as a critical point for the equation and we are still allowed to consider a generic perturbation δu to the critical point such that $u = 1 + \delta u$. Eq.(5.33) then becomes:

$$\delta u'' + \delta u' \left(\frac{2A}{\phi_e} + \frac{6-m}{m} \right) = -\frac{A}{\phi_e} \frac{6-m}{m} \delta u \quad . \quad (5.34)$$

However, we are now dealing with a homogeneous differential equation of second order in which the coefficients vary with time:

$$\delta u'' + P(\tau)\delta u' + Q(\tau)\delta u = 0 \quad , \quad (5.35)$$

where

$$P(\tau) = \frac{2A}{A\tau + \phi_*} + \frac{6-m}{m} \quad (5.36)$$

$$Q(\tau) = \frac{A}{A\tau + \phi_*} \cdot \frac{6-m}{m} \quad (5.37)$$

In order to find the expression of the perturbation δu we consider the following change of variables:

$$\delta u = \delta z e^{-\frac{1}{2} \int P(\tau) d\tau} \quad (5.38)$$

in terms of which eq.(5.34) can be rewritten (if $\delta u \neq 0$) as:

$$\delta z'' + \left[Q(\tau) - \frac{1}{2}P'(\tau) - \frac{1}{4}P^2(\tau) \right] \delta z = 0 \quad . \quad (5.39)$$

It is easy to check that for our values of P and Q we get

$$\delta z'' - \frac{(6-m)^2}{4m^2} \delta z = 0 \quad (5.40)$$

whose generic solution is

$$\delta z = c_1 + c_2 e^{\frac{(6-m)^2}{4m^2} \tau} \quad , \quad (5.41)$$

where c_1 and c_2 are arbitrary constants. Substituting this expression in (5.38) we get the form of the perturbation δu :

$$\delta u = \frac{c_1 k}{\tau + \frac{\phi_*}{A}} e^{-\frac{(6-m)}{2m} \tau} + \frac{c_2 k}{\tau + \frac{\phi_*}{A}} e^{\alpha \tau} \quad , \quad (5.42)$$

where k is a constant and $\alpha = \frac{3(2-m)(6-m)}{4m^2}$. It's then immediate to see that the generic perturbation goes to zero for $2 < m < 6$, a range including both

radiation ($m = 4$) and matter ($m = 3$) dominated backgrounds, thus making ϕ_e a stable attractor.

The numerical solution of equation (5.33) is shown in fig.(5.2) for a somewhat large set of initial conditions. On the left side the time dependences of u and u' are shown, in the case ($m = 3, n = 3$) and for the test values $A = M_{Pl}$ and $\phi_0 = M_{Pl}$: different curves correspond to different initial conditions for u and u' and they all converge to the stable attractor solution ($u = 1, u' = 0$). On the right side it is shown the u' vs u plot for the same choices of initial conditions of the left hand side plot.

In conclusion, focusing on scalar-tensor theories as a viable model to connect Dark Energy and gravity, we have explored the possible choices of the coupling between a scalar field and the Ricci scalar, in order to select those expressions which give rise to scaling solutions for the Klein Gordon equation, in the form (5.9). Our analysis resulted in selecting three classes of couplings, namely functions of the exponential form (5.19), polynomial functions (5.23), and the exponential of polynomial (5.24), depending on the coefficient m characterizing the scaling (5.8) and on the value of \tilde{B} on (5.22).

Our analysis recovers all the possibilities to have a scaling behavior. Most importantly, it has been found that these solutions actually possess stable attractor properties, which is an extremely appealing feature in view of the old fine-tuning problem of minimally-coupled Quintessence models. In particular, we have shown that all the scaling solutions of the form (5.9) with $n < 3$ and 4 in the matter and radiation dominated era, respectively, represent attractors. Clearly, this enforces the case for extending the theory of gravity beyond General Relativity, and opens a window on the solution of “initial values” problem. Cosmological models, characterized by the non-minimal couplings we have selected out, will deserve further investigation.

5.5 Exponential coupling

We will now provide a comprehensive analysis of cosmologies involving an exponential coupling of the extended quintessence scalar field to gravity. The latter case may be relevant for string cosmology, where the dilaton appears as an exponential which multiplies the fundamental lagrangian [76], although in the usual formulation the coupling multiplies all terms of the lagrangian and not just the Ricci scalar. We will work again in the framework described by the action (5.4) . However, we now fix the $F(\phi)$ coupling to have the following expression:

$$\omega(\phi) = 1 \quad , \quad \frac{f(\phi, R)}{2\kappa} = \frac{F(\phi)R}{2} = \frac{R}{16\pi G} \exp \left[\frac{\xi}{M} (\phi - \phi_0) \right] \quad , \quad (5.43)$$

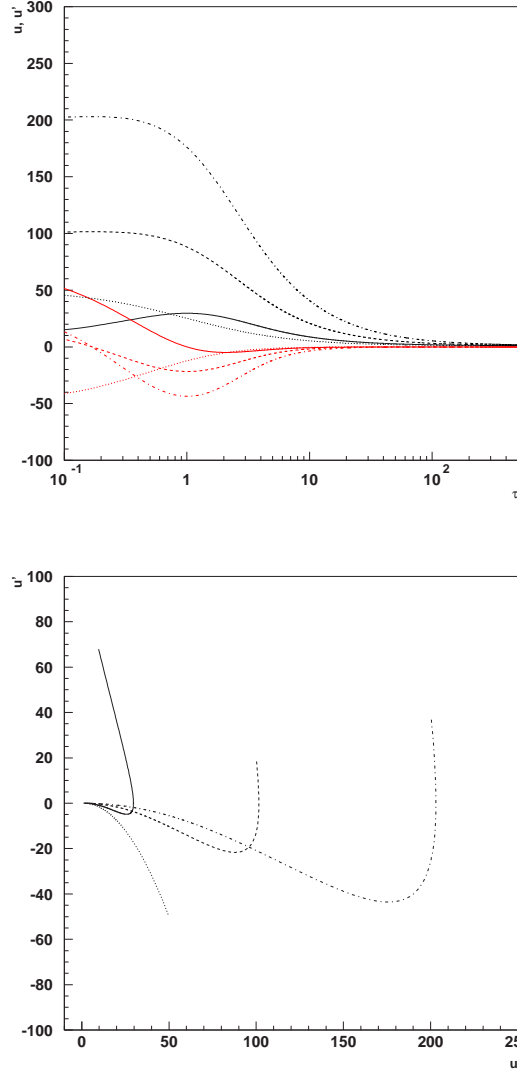


Figure 5.2: Numerical solutions of eq.(5.33) are shown: on the left side u (black) and u' (red) are plotted versus τ , in the case $(m = 3, n = 3)$ and converge to the stable attractor solution $(u = 1, u' = 0)$. Different curves correspond to different initial conditions for u and u' : $(u_0, u'_0) = (9, 70)$ (solid), $(100, 20)$ (dashed), $(50, -50)$ (dotted), $(200, 40)$ (dot-dashed). We have chosen the test values $A = M_{Pl}$ and $\phi_0 = M_{Pl}$. The τ scale is logarithmic. On the right side u' vs u is plotted for the same initial conditions.

where ξ is a dimensionless coupling, ϕ_0 is the present value for the ϕ field, introduced to make explicit that at present $F(\phi_0) = 1/8\pi G$.

Hence, action (5.4) assumes the following expression:

$$S = \int d^4x \sqrt{-g} \left[\frac{M^2}{2} e^{\frac{\xi(\phi-\phi_0)}{M_P}} R - \frac{1}{2} \phi^{;\mu} \phi_{;\mu} - V(\phi) + \mathcal{L}_{fluid} \right] \quad (5.44)$$

The Jordan-Brans-Dicke parameter in this scenario is

$$\omega_{JBD} = F \left(\frac{dF}{d\phi} \right)^{-2} = \frac{8\pi}{\xi^2} \exp \left[-\frac{\xi}{M_P} (\phi - \phi_0) \right] \quad (5.45)$$

whose present value is $\omega_{JBD0} = 8\pi/\xi^2$.

Note that we expect the exponential coupling to have attractor solutions since it corresponds to one of the expressions found in the previous section¹.

5.5.1 R-boost for an exponential coupling

In the following we derive the R -boost in the case of an exponential coupling. We shall write an analytic expression for that, both in matter dominated and radiation dominated eras, which is manifestly independent on the initial conditions; that represents an important new aspect with respect to earlier works [8], in which the initial field value appeared explicitly in the R -boost energy density. Moreover, exploiting a perturbative analysis [90], we demonstrate that such solution represents an attractor. Also, we shall see that the energy density corresponding to the R -boost depends on the value of ω_{JBD} .

We shall compare what we find here with previous models of extended quintessence, based on a quadratic coupling between the dark energy and the Ricci scalar, and with a case of minimally coupled quintessence (QCDM). In order to satisfy the constraint (5.45) the constant ξ is obtained through (5.45) by fixing $\omega_{JBD0} = 10^5$. The remaining cosmological parameters are chosen consistently with the concordance model (see *e.g.* [153]). The present dark energy density is 73% of the critical density, $\Omega_\phi = 0.73$, with a Cold Dark Matter contribution of $\Omega_{CDM} = 0.226$, three families of massless neutrinos, baryon content $\Omega_b = 0.044$ and Hubble constant $H_0 = 72$ Km/sec/Mpc. The quintessence potential is an inverse power law

$$V(\phi) = \frac{m^{4+\alpha}}{\phi^\alpha}, \quad (5.46)$$

¹We mention here that the analysis of the exponential case has been actually performed in [112] before the classification we have illustrated in the previous section, which can be found in [113].

with α close to zero in order to have ω_ϕ close to -1 at present (see *e.g.* [9] and references therein). We choose the initial conditions at $1+z=10^9$; in typical runs, with $\omega_\phi = -0.9$ at present, the value of the field today is $\phi_0 = 0.35M$; the dynamics induced by the potential V and the R -boost makes $\phi \ll \phi_0$ at early stages; the condition on ω_{JBD0} sets the value of the coupling constant $\xi = 1.6 \times 10^{-2}$. As a consequence, the BBN bounds (5.97) or (5.98) are largely satisfied.

Before proceeding in our analysis, we also note that, in order to derive the evolution of perturbations for our model and to study its impact on the observations as described ahead in this work, we have implemented the DEfast code, based on CMBfast [46] and originally written to study quintessence scenarios in which the Dark Energy scalar field is minimally [109] or non-minimally [108, 8] coupled to the Ricci scalar. After taking a set of cosmological parameters as an input, the code returns the CMB spectra (both for temperature and for polarisation) and the matter power spectrum. This is performed considering a dynamical and fluctuating scalar field, playing the role of the Dark Energy and/or of the Brans Dicke like field, together with the other cosmological components. We have implemented DEfast by adding the possibility of investigating the case in which the coupling of the scalar field to the Ricci scalar depends exponentially on the field [112].

We will now derive the Dark Energy dynamics before the onset of acceleration.

5.5.2 Radiation dominated era (RDE)

With our choice of the coupling (5.43) the Klein Gordon equation (5.6) for the field can be rewritten as

$$\ddot{\phi} + 3H\dot{\phi} - \frac{1}{2} \frac{\xi}{M} \frac{\rho_{mnr0}}{a^3} + V_{,\phi} = 0 \quad (5.47)$$

or equivalently, in terms of the conformal time η , defined in (1.4), as

$$\phi'' + 2\mathcal{H}\phi' - \frac{1}{2} \frac{\xi}{M_P} \frac{\rho_{mnr0}}{a} + a^2 V_{,\phi} = 0 \quad , \quad (5.48)$$

where we have used (5.1) to write the Ricci scalar in terms of the non relativistic matter contribution. For our purposes here we neglect the departure from general relativity in the RDE, *i.e.* we assume $F \simeq 1/8\pi G$ and we ignore all the contributions in the Friedmann equation except radiation. The above assumption is justified because we aim at deriving the R -boost dynamics at first order in $1/\omega_{JBD}$: a general analysis would yield corrections of higher order in $1/\omega_{JBD}$ in the effective gravitational potential appearing in the Klein Gordon equation. The expansion is given by

$$a \simeq C\eta \quad , \quad (5.49)$$

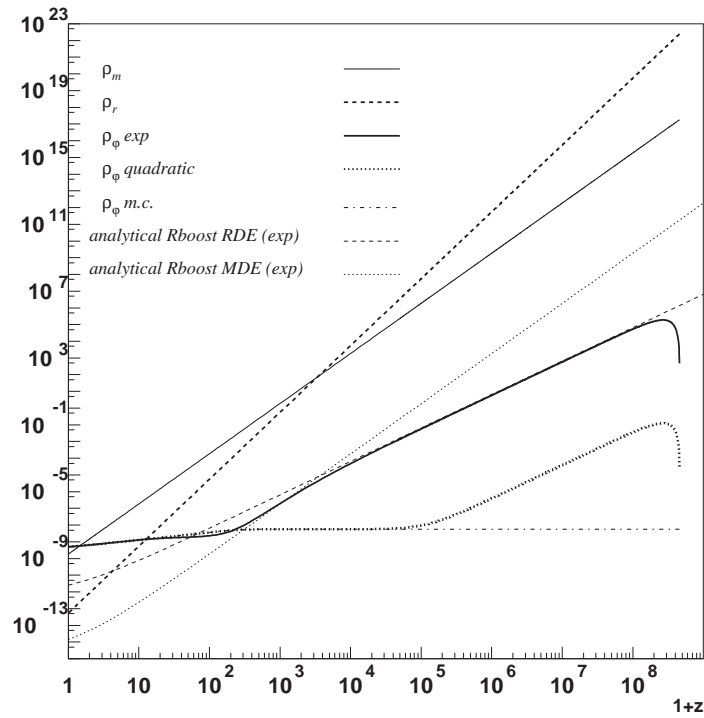


Figure 5.3: Energy density of matter (solid), radiation (heavy dashed) and ϕ for minimal (dot dashed), quadratic (heavy dotted) and exponential (heavy solid) coupling. Also shown the analytical behavior of the R-boost during radiation dominated era (dashed) and matter dominated era (dotted).

where $C = \sqrt{8\pi G\rho_{r0}/3}$ and ρ_{r0} represents the cosmological radiation density calculated at present; note that expression (5.49) corresponds to $a \sim t^{1/2}$ in (5.11). Since $\mathcal{H} \sim 1/\eta$, the equation of motion for ϕ reduces to

$$\phi'' + \frac{2}{\eta}\phi' - \frac{1}{2M} \frac{\xi}{C\eta} \rho_{mnr0} = 0 \quad , \quad (5.50)$$

which is solved by

$$\phi(\eta) = \frac{\xi}{4}\rho_{mnr0}\sqrt{\frac{3}{8\pi\rho_{r0}}}(\eta - \eta_{beg}) + \phi_{beg} \quad , \quad (5.51)$$

where ϕ_{beg} is the initial condition for ϕ . This solution corresponds to the slow roll phase which starts when the cosmological friction and effective gravitational potential effects in the equation of motion are comparable, yielding the R -boost equation

$$2\mathcal{H}\phi' \simeq \frac{a^2 R}{2} \frac{dF}{d\phi} \quad . \quad (5.52)$$

In this phase, the energy of the quintessence field is dominated by its kinetic contribution

$$\frac{1}{2} \left(\frac{d\phi}{dt} \right)^2 = \frac{3}{32} \frac{\rho_{mnr0}^2}{\rho_{r0}} \frac{1}{\omega_{JBD0}} (1+z)^2 \quad . \quad (5.53)$$

from which it is possible to derive that the R -boost solution is equivalent to a tracking one with equation of state $-1/3$. Expression (5.53) immediately tells us that the R -boost solution found during RDE in the case of an exponential coupling is characterized by an energy density scaling as $\rho_\phi \sim \dot{\phi}^2/2 \sim a^{-2}$, corresponding to the case $m = 4$ and $n = 2$ in (5.8) and (5.9) respectively. It is interesting to note that at first order in $1/\omega_{JBD}$ the R -boost energy density is related only to the present value of the Jordan-Brans-Dicke parameter. In Figure 5.3 we have plotted the energy density of the various cosmological components: besides matter and radiation we can observe the behavior of ϕ for minimal and extended quintessence, starting from zero initial kinetic energy. In the minimal coupling case the field behaves nearly as a cosmological constant until the true potential V starts to be relevant. In the extended quintessence case, instead, the field accelerates and soon enters the R -boost phase. In Figure 5.4 we show the absolute values of the four terms in the Klein Gordon equation (5.50). The potential term starts to be dominant only for $z \leq 10^2$; the friction term is zero at the beginning and then increases, joining the R -boost. The quintessence field accelerates until the sign inversion in ϕ'' occurs; then the field accelerates again for $z \sim 10^2$ when the potential V starts to have a relevant effect. The timing of the different phases of the trajectory depends on the details we have fixed, but the general behavior is model independent.

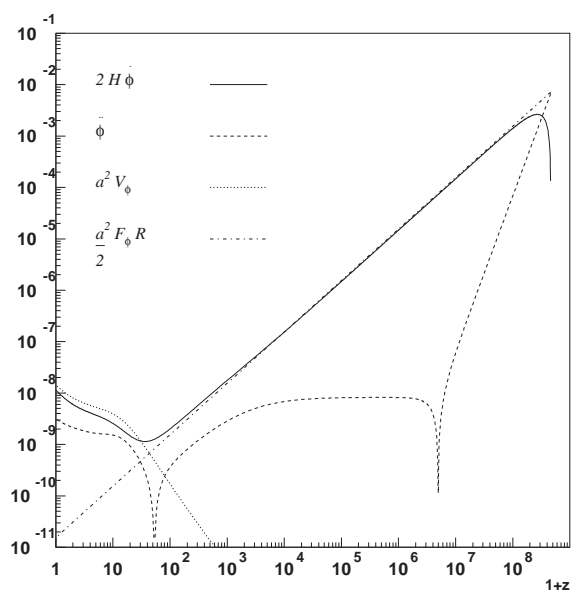


Figure 5.4: Absolute values of the four terms in the Klein Gordon equation (5.50) for an exponential coupling.

5.5.3 Matter dominated era (MDE)

In the matter dominated era, equation (5.52) still holds but the expansion parameter has a different behavior with time

$$a = \frac{2}{3}\pi G\rho_{mnr0}\eta^2 \quad . \quad (5.54)$$

As in the RDE case, we neglect the departure from general relativity to get the R -boost dynamics at the lowest order in $1/\omega_{JBD}$. The R -boost equation is

$$\phi' = \frac{3}{16\pi}\frac{\xi}{\eta}M \quad , \quad (5.55)$$

which is solved by

$$\phi = \frac{3}{16\pi}\xi M \log \frac{\eta}{\eta_{beg}} + \phi_{beg} \quad , \quad (5.56)$$

also shown in Figure 5.3. As a consequence, the behavior of the kinetic energy of the field changes, too

$$\frac{1}{2}\left(\frac{d\phi}{dt}\right)^2 = \frac{3}{32}\frac{1}{\omega_{JBD0}}\rho_{mnr0}(1+z)^3 \quad . \quad (5.57)$$

Hence, this case corresponds to the choice $m = 3$ and $n = 3$. If we now look at Figure 5.3 again, we notice that the R -boost has a bigger effect on ρ in the exponential case with respect to the quadratic coupling, also shown in the figure. In both cases ϕ receives a strong kick, which determines a major change in the dynamics with respect to the minimally coupled scenario. However, for an exponential coupling the path of the field departs from the standard one earlier with respect to the case of a quadratic coupling, reflecting the fact that the exponential coupling enhances the departure from general relativity as it depends exponentially on the field dynamics. We shall come back to this issue in the next Section.

5.5.4 Stability

The stability analysis we have carried out in the previous sections can be specified to the case of the exponential coupling. Following the method illustrated in this chapter and already exploited in [90], we now show that the R -boost solution found above is an attractor. We look for scaling solutions of the Klein Gordon equation, *i.e.* solutions in which the energy density of quintessence field scales as a power of the scale factor

$$\left(\frac{d\phi}{dt}\right)^2 \propto a^{-2} \quad , \quad (5.58)$$

in the RDE and

$$\left(\frac{d\phi}{dt}\right)^2 \propto a^{-3} \quad , \quad (5.59)$$

in the MDE, as found in (5.53, 5.57). The behavior of the background energy density is also given by a power of the scale factor. In particular

$$\rho_r \propto a^{-4} \quad , \quad \rho_m \propto a^{-3} \quad , \quad (5.60)$$

for radiation and non-relativistic matter respectively. As far as $a(t)$ is concerned, neglecting again the corrections of the order $1/\omega_{JBD}$ induced by $1/F$ in front of the right hand side of the Friedmann equation (5.5) as well as the other dark energy terms, one has

$$a^{RDE} \propto t^{1/2} \quad (5.61)$$

$$a^{MDE} \propto t^{2/3} \quad (5.62)$$

The corresponding time dependence of the field ϕ is given by

$$\phi_e^{RDE} = \phi_* \left(\frac{t}{t_*}\right)^{\frac{1}{2}} \quad , \quad (5.63)$$

$$\phi_e^{MDE} = \phi_* \log\left(\frac{t}{t_*}\right) \quad , \quad (5.64)$$

where the subscript ‘*’ stands for a given reference time and the subscript ‘e’ reminds us that this is the R -boost exact solution.

We verify that the R -boost solution is an attractor by rewriting the Klein Gordon equation (5.6), with the change of variables seen in (5.25) and (5.28). During RDE, we obtain

$$2\frac{d^2u}{d\tau^2} + 3\frac{du}{d\tau} + u - 1 = 0 \quad , \quad (5.65)$$

As we immediately see, this equation admits a critical trajectory for $u = 1$ and $u' = 0$, corresponding to the R -boost. Linearizing equation (5.65) by choosing small exponential perturbations around the critical point ($u = 1 + e^{\lambda\tau}$) and solving for the eigenvalues $\lambda_{1,2}$ we get

$$\lambda_1 = -1 \quad ; \quad \lambda_2 = -\frac{1}{2} \quad . \quad (5.66)$$

The fact that the eigenvalues are real and negative shows that the generic perturbation will be suppressed with time, thus flattening the trajectory on the critical one $\phi = \phi_e$.

Similarly, during MDE, the Klein Gordon equation (5.6) can be rewritten as

$$u'' + \left(\frac{2\phi_*}{\phi_e} + 1\right)u' = \frac{\phi_*}{\phi_e}(1 - u) \quad , \quad (5.67)$$

which again admits ($u = 1, u' = 0$) as a critical point. The perturbed equation reads now as follows:

$$\delta u'' + \frac{3 + \tau}{1 + \tau} \delta u' + \frac{1}{1 + \tau} \delta u = 0 \quad (5.68)$$

In this case, however, the coefficients depend explicitly on τ and hence the analytical resolution follows the procedure described in section (5.4.2). In particular, using the change of variables introduced in (5.38) eq.(5.68) can be rewritten as

$$\delta z'' - \frac{1}{4} \delta z = 0 \quad (5.69)$$

whose solution is

$$\delta z = c_1 + c_2 e^{\tau/4} \quad (5.70)$$

where c_1 and c_2 are two arbitrary constants. The latter expression corresponds to

$$\delta u \propto \frac{c_1}{1 + \tau} e^{-\tau/2} + \frac{c_2}{1 + \tau} e^{-\tau/4} \quad (5.71)$$

which implies that $\delta u \rightarrow 0$ so that the generic solution of the Klein Gordon equation tends to $u = \text{constant}$.

Summarizing, the simple choice of an exponential as a coupling between dark energy and Ricci scalar in the Lagrangian leads to the existence of an attractive R -boost solution in both matter and radiation dominated eras. This result agrees with the general treatment illustrated at the beginning of this chapter; in particular, the general classification allows us to recover the exponential coupling both for $m = n$ and for $m \neq n$; for $m = n = 3$, which is the case of matter domination, eq.(5.19) reduces to the exponential coupling if we define $A \equiv \frac{\xi}{M} \frac{t_*^2 \rho_{mnr0}}{2}$, where ξ is a dimensionless constant, in the regime $\phi \gg \phi_*$. Furthermore, the exponential case is included in 5.24 when $\tilde{B} = 0$ and thus $m + n = 6$ with $m \neq n$. If $m = 4$ and $n = 2$, hence in the case of radiation dominated era, we obtain again the expression of the coupling found in 5.24. The exponential case may be obtained exactly in the limit in which t_* and ϕ_* may be neglected in (5.20).

5.6 Weyl scaled exponential extended quintessence

In the case in which the coupling to gravity has the form of the exponential (5.43), action (5.44) can be rewritten using the Weyl scaling we have illustrated in section 4.1.1. In particular, the part of the action containing the scalar field terms reads as follows:

$$S_\phi^{exp} = \int d^4x \sqrt{-\tilde{g}} \left[\frac{M^2 \tilde{R}}{2} - \tilde{k}^2(\phi) \phi^{;\mu} \phi_{;\mu} - \tilde{U}^{exp}(\phi) \right] \quad (5.72)$$

where the non standard kinetic term is specified by

$$\tilde{k}^2(\phi) \equiv \left(\frac{3\xi^2}{32\pi} + \frac{e^{-\frac{\xi}{M_P}(\phi-\phi_0)}}{2} \right) \quad (5.73)$$

and the rescaled potential is equal to:

$$\tilde{U} \equiv V(\phi)e^{-\frac{2\xi}{M_P}(\phi-\phi_0)} \quad (5.74)$$

The fluid part of action (5.44) becomes:

$$S_{fluid}^{exp} = - \int d^4x \sqrt{-\tilde{g}} \left[\frac{3i\xi}{4M_P} \bar{\psi} \tilde{\gamma}^\mu (\nabla_\mu \phi) \tilde{\phi} + i \bar{\psi} \tilde{\gamma}^\mu \nabla_\mu \psi + \eta^{exp}(\phi) \bar{\psi} \psi \right] \quad (5.75)$$

where the mass of the matter fields is now a function of the scalar field ϕ via

$$\eta^{exp}(\phi) = m e^{-\frac{\xi}{2M_P}(\phi-\phi_0)} \quad (5.76)$$

A first immediate remark is that the model apparently looks quite complicated in the Einstein frame, where the scalar field, now characterized by a non standard kinetic energy and a different potential, is now coupled universally to all matter scalar fields. As we have pointed out, the choice of the frame is matter of convenience and we might equivalently choose one or the other according to the aim of our analysis. The case of a scalar-tensor theory with an exponential potential looks much more straightforward in the Weyl frame; nevertheless, it is indeed incredibly interesting to investigate the problem in the Einstein frame, in order to check the consistency of our results. Our aim will be therefore that of solving the background equations of our scalar-scalar model, in which ϕ is coupled to matter fields, just as if it were a completely independent coupled quintessence (CQ) model. Notice also that this procedure will guarantee a valuable test for the numerical code used to solve the exponential model in the Weyl frame; indeed, a successful independent comparison of the same model in two different frames, will encourage us to deeply trust the implementation of the DEfast code we have performed in the Weyl frame.

The coupling of the Dark Energy scalar field to matter can now be treated, in the Einstein frame, as illustrated in [87]. From now on, we will omit for simplicity the $\tilde{\cdot}$ used up to now to identify quantities in the Einstein frame. We will therefore consider a model described by the following action:

$$S^{exp} = \int d^4x \sqrt{-g} \left[\frac{M^2 R}{2} - k^2(\phi) \phi^{;\mu} \phi_{;\mu} - U(\phi) + \mathcal{L}_{kin,\psi} - m(\phi) \bar{\psi} \psi \right] \quad (5.77)$$

Here the potential is given by:

$$U(\phi) = V(\phi) e^{-4\frac{\beta}{M}(\phi-\phi_0)} = V_0 \left(\frac{\phi_0}{\phi} \right)^\alpha e^{-4\frac{\beta}{M}(\phi-\phi_0)} \quad (5.78)$$

where we have introduced the constant β defined as

$$\beta \equiv \frac{\xi}{2\sqrt{8\pi}} \quad (5.79)$$

in order to match the formalism usually used in coupled quintessence theories [4]; furthermore, we have written the potential $V(\phi)$ explicitly, using the same expression we had used in the Weyl frame (see eq.(5.46)) and indicating with the constant V_0 the value of the potential today, fixed in agreement with the amount of Dark Energy observed by experiments at the present epoch. The non standard kinetic function can be rewritten in terms of β as:

$$k(\phi) = \sqrt{6\beta^2 + e^{-2\frac{\beta}{M}}(\phi - \phi_0)} \quad (5.80)$$

Hence, the energy density and pressure of the quintessence scalar field read as:

$$\rho_\phi = \frac{1}{2a^2}k^2(\phi)\phi'^2 + U(\phi) \quad (5.81)$$

$$p_\phi = \frac{1}{2a^2}k^2(\phi)\phi'^2 - U(\phi) \quad (5.82)$$

where the derivative is performed with respect to the conformal time η ; the motion of the field is described by the Klein Gordon equation, now given by

$$k^2(\phi)\phi'' + 2k^2(\phi)\mathcal{H}\phi' + k(\phi)\frac{\partial k}{\partial\phi}\phi'^2 + a^2\frac{\partial U}{\partial\phi} = a^2\frac{\beta}{M}\rho_m \quad (5.83)$$

A comparison with equations 1.8, 1.11, 1.15 of [87] allows us to interpret the model as follows: we are now dealing with a ‘scalar-scalar’ coupling which corresponds to including a scalar source Q_a for each component interested by the coupling, satisfying the condition

$$\sum_a Q_a = 0 \quad (5.84)$$

and such that

$$T_{(a)\mu;\nu}^\nu = Q_{(a)\mu} \quad (5.85)$$

In particular, the scalar source for our case is defined as

$$Q_\phi = \frac{\beta}{M}\frac{\rho_m}{a} \quad (5.86)$$

$$Q_m = -Q_\phi \quad (5.87)$$

In this framework the energy density of matter and Dark Energy are not conserved separately anymore but they exchange each other the coupling source contribution:

$$\rho'_m + 3\mathcal{H}\rho_m = -\frac{\beta}{M}\rho_m\phi' \quad (5.88)$$

$$\rho'_\phi + 3\mathcal{H}(\rho_\phi + p_\phi) = +\frac{\beta}{M}\rho_m\phi' \quad (5.89)$$

while radiation, being decoupled from Dark Energy and matter fields, still satisfies the usual energy continuity equation:

$$\rho'_r + 3\mathcal{H}(\rho_r + p_r) = 0 \quad (5.90)$$

With regard to the cosmological expansion, the latter can be specified by the time dependence of the scale parameter:

$$a' = a^2 \sqrt{\frac{\rho}{3M^2}} \quad (5.91)$$

which corresponds to Friedmann equation $\mathcal{H}^2 = a\sqrt{\rho_{tot}/3M^2}$. Equations (5.81, 5.82, 5.83, 5.88, 5.90, 5.91) completely describe the background of our coupling quintessence model and can be numerically solved in order to obtain the energy density behavior of Dark Energy, matter and radiation as well as the evolution of the field ϕ itself. Results are shown in fig.(5.5). The comparison of this plot to the one shown in fig.(5.3) is astonishing, in the sense that the behavior of the energy densities is the same. We stress again that the two plots have been obtained in two completely independent manners:

1. the first one, shown in fig.(5.3), was derived considering the equations which characterize an extended quintessence model in which the Dark Energy scalar field is exponentially coupled to gravity; the coupling has been introduced in a pre-existing code named DEfast [8] which has been implemented to include the requested behavior. DEfast itself is a fortran77 code obtained as an implementation of CMBfast [46] by introducing non minimal coupled Extended Quintessence and which allows to solve perturbation equations for a chosen cosmological model;
2. the second plot, shown in fig.(5.5), was obtained considering the background equations of a coupled quintessence model, in which a Dark Energy scalar field with non standard kinetic energy is coupled to matter fields. This new framework was obtained applying Weyl scaling to the exponential extended quintessence model previously investigated; the equations were then numerically solved using a (much simpler) hand-made code.

Eventually, the comparison is incredibly satisfying, showing that the behavior of the energy densities is the same in both models; this result has several important implications.

First of all, Weyl scaling allowed us to test the DEfast code and its implementation, in which we can now be confident, in the sense that we have excluded the possibility that the found dynamics was in some way related to numerical instabilities of the code more than to the physics of the model.

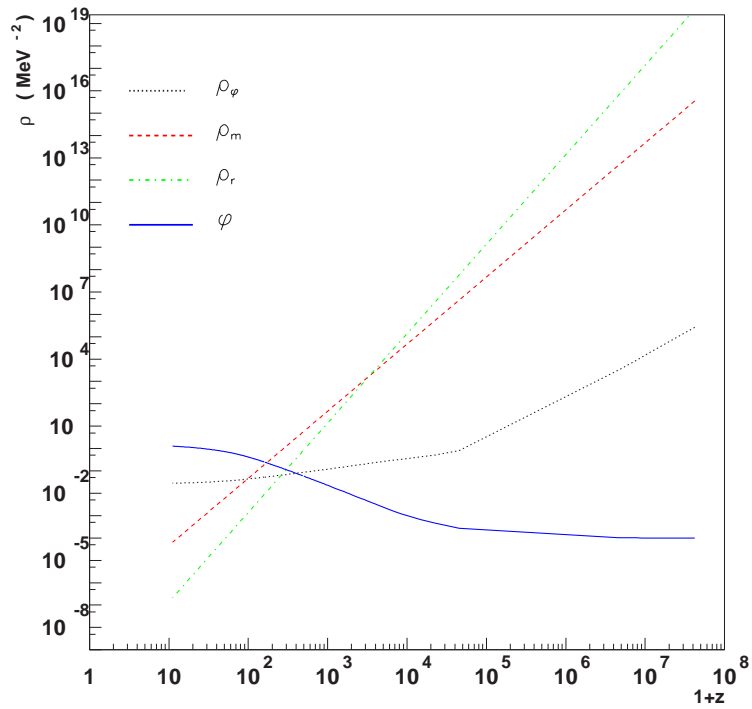


Figure 5.5: The behavior of the background of the coupling quintessence model obtained weyl scaling extended quintessence with an exponential potential is shown. The three curves refer to ρ_m (dashed), ρ_ϕ (dotted), ρ_r (dot-dashed), ϕ (solid).

Moreover, Weyl scaling allows us to make an easier comparison of scalar-tensor theories and extended quintessence models with scalar-scalar coupled quintessence models [4, 93, 95]; also, it opens the way to a future perturbation analysis which might be done in the Einstein frame, using numerical codes like CMBeasy [45] and its implementation to coupled quintessence models [73, 100] in order to constrain CQ theory with cosmology [5, 6].

Finally, the two EQ and CQ models we have illustrated are indeed equivalent. On one side, in the extended quintessence model, the gravitational coupling is responsible for the R-boost effect, enhancing the dynamics of the field during RDE; at that epoch the energy density of the field is mainly kinetic and doesn't depend on the choice of the potential neither on the initial conditions, the R-boost being an attractor solution. On the other side, the same effect can equally be guaranteed by coupling Dark Energy to matter. This enforces the need of a deeper understanding of Dark Energy interaction with other cosmological entities, whose reciprocal influence can be extremely relevant for the understanding of the dark sector dynamics [9, 93].

5.7 Effects on cosmological perturbations

In this section we analyze the observational impact of extended quintessence cosmologies. In order to do so, we will consider our exponential coupling model described in the previous sections (5.4) as a reference model and we will investigate its effect on the spectra of cosmological perturbations. This work will require the implementation of the Boltzmann code illustrated in par.(5.5.1). We find that observational effects are qualitatively consistent with those corresponding to a quadratic coupling, but quantitatively different. For our purposes, an analysis based on the CMB power spectrum only is sufficient. The scalar perturbations are Gaussian and described by a scalar power spectrum with spectral index $n = 0.96$, and no tensors, consistently with the cosmological concordance model [153].

Since the constant ξ is chosen to be positive and the field ϕ is smaller in the past with respect to ϕ_0 , $F < 1/8\pi G$ in the past. As a consequence, our model describes a cosmology in which the gravitational constant (and thus the Hubble parameter) is higher in the past than in the QCDM case. It follows that for a fixed ω_{JBD0} , we expect a larger amplitude of the effects induced by the behavior of F for the exponential case with respect to the quadratic coupling: indeed, the exponential is sensitive to the field dynamics also at the linear level, which dominates for small values of $\phi/\phi_0 - 1$. This can be seen in Figure 5.6, where we plot $H(z)$ for three cosmological models: two of them represent extended quintessence with the same value of ω_{JBD} at present, but featuring an exponential and quadratic coupling, while the third one is the QCDM case. For the first two cases, we have set $\omega_{JBD0} = 50$; we stress that we have chosen this small value with respect to the exist-

ing bounds from solar system [16], in order to highlight the differences in the models considered. The value of H_0 is the same, but $H(z)$ are quite different functions in the three cases, in particular for the exponential case with respect to the Λ CDM cosmology. In Figures 5.7 and 5.8 we plot the

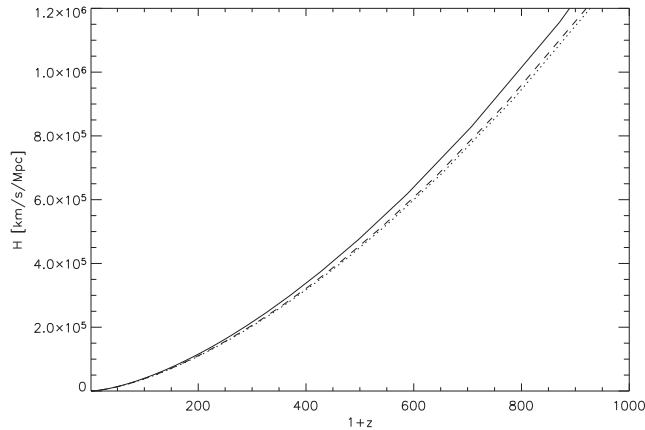


Figure 5.6: The behavior of H as a function of the redshift in three cosmological models, extended quintessence with exponential coupling (solid), quadratic coupling (dashed) and Λ CDM (dotted).

total intensity and polarisation power spectra of anisotropies for the models considered in Figure 5.6. Two features are immediately evident. First the different amplitude in the tail at low multipoles, and second a projection difference in the location of the acoustic peaks. The spectra have been normalized to the amplitude of the first peak, which roughly corresponds to fixing the amplitude of the signal at last scattering. Both the effects come from the different behavior of the coupling F with redshift. The projection feature simply follows from the difference in the curves in Figure 5.6. Indeed, smaller (higher) values of H^{-1} project the CMB power spectrum onto smaller (larger) angular scales in the sky. The power at low multipoles is modified through the Integrated Sachs-Wolfe (ISW) effect, which is sensitive to the change of the cosmic equation of state at low redshift (see [81] and references therein). The larger is that change, the larger is the ISW power.

Summarizing, the different form of the coupling function F determines a relevant difference of amplitude in the effects induced by extended quintessence models on the cosmological perturbations. Larger departures from general relativity in the dynamics of the field in the early universe correspond to larger effects on the perturbations. The latter aspect has to be taken into account when constraining different theories on the basis of the present

observations.

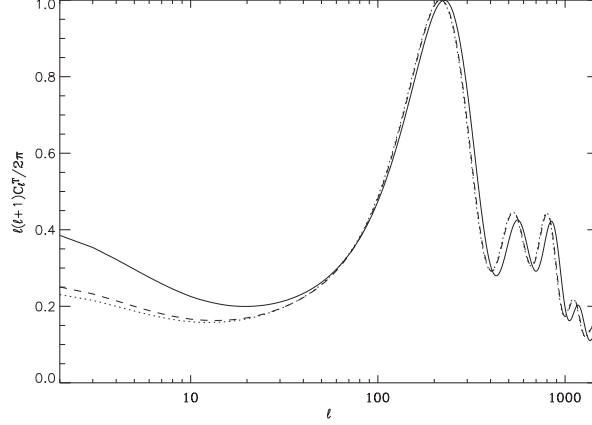


Figure 5.7: CMB angular total intensity power spectra for a QCDM cosmology (dotted), quadratic (dashed) and exponential coupling extended quintessence (solid) with $\omega_{JBD} = 50$. The spectra are in arbitrary units, normalized to 1 at the first acoustic peak in total intensity.

5.7.1 Observational constraints from BBN

We will now derive the up to date bounds set from BBN to extended quintessence with an exponential coupling, specifying to this case the discussion illustrated in section (4.2.4). Using the coupling defined in (5.43), we can solve (5.48) with respect to \mathcal{H} , getting

$$\mathcal{H} = \sqrt{\frac{8\pi G}{3}} \left[\sqrt{a^2 (\rho_{fluid} + \rho_\phi) \exp\left(-\sqrt{\frac{8\pi}{\omega_{JBD0}}} \frac{\phi - \phi_0}{m_P}\right) + \frac{3\dot{\phi}^2}{4\omega_{JBD0}}} + \sqrt{\frac{3}{4\omega_{JBD0}}} \dot{\phi} \right] \quad (5.92)$$

In the following we shall assume that the Universe is indeed radiation dominated during the BBN epoch, so that ρ_ϕ can be neglected with respect to ρ_{fluid} which receives contributions from photons, neutrinos and e^\pm . Moreover the last two terms in Equation (5.92) are suppressed by $1/\sqrt{\omega_{JBD0}}$. In this case the squared Hubble parameter takes the simple form

$$H^2 = \frac{\mathcal{H}^2}{a^2} = \frac{8\pi G}{3} \exp\left[-\frac{\xi(\phi - \phi_0)}{m_P}\right] \rho_{fluid} . \quad (5.93)$$

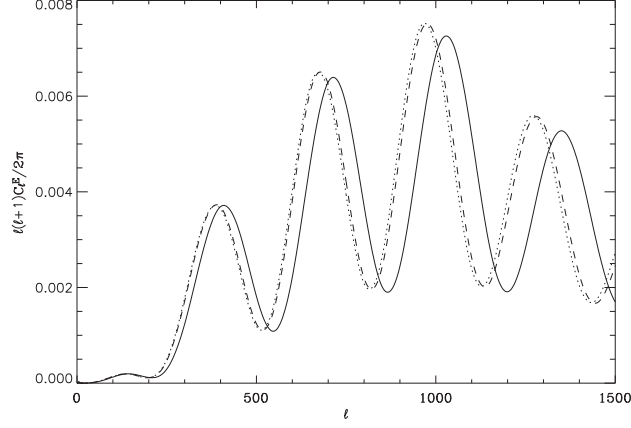


Figure 5.8: CMB angular polarisation power spectra for a QCDM cosmology (dotted), quadratic (dashed) and exponential coupling extended quintessence (solid) with $\omega_{JBD} = 50$. The spectra are in arbitrary units, normalized to 1 at the first acoustic peak.

In this limit we see that by comparing the theoretical values for the light nuclei abundances with the corresponding experimental determinations we can constrain the value of the effective gravitational constant during the BBN epoch, *i.e.* the quantity $\xi(\phi - \phi_0)/m_P$.

To bound the value of the quintessence field we construct the likelihood function

$$\mathcal{L}(\xi\phi) \propto e^{-\chi^2[\xi(\phi - \phi_0)/m_P]/2} , \quad (5.94)$$

with

$$\chi^2[\xi(\phi - \phi_0)/m_P] = \sum_{i,j=D,{}^4He} \left[X_i^{th}[\xi(\phi - \phi_0)/m_P] - X_i^{exp} \right] W_{ij} \left[X_j^{th}[\xi(\phi - \phi_0)/m_P] - X_j^{exp} \right] \quad (5.95)$$

The proportionality constant can be obtained by requiring normalization to unity of the integral of \mathcal{L} , and with W_{ij} we denote the inverse covariance matrix

$$W_{ij} = [\sigma_{ij,th}^2 + \sigma_{i,exp}^2 \delta_{ij}]^{-1} , \quad (5.96)$$

where $\sigma_{i,exp}$ is the uncertainty in the experimental determination of nuclide abundance X_i and $\sigma_{ij,th}^2$ the theoretical error matrix. We also consider the two likelihood functions for each of the two nuclei to show how at present

the Deuterium and ${}^4\text{He}$ can separately constrain the value of the effective gravitational constant at the BBN epoch.

It is important to stress that we consider the simplest case of a constant value of ϕ during the whole BBN phase. This is justified a posteriori by the fact that although the dynamics of the field in the radiation dominated era is cosmologically relevant, it is too small to provide any change of ϕ during BBN which is significant compared with the bounds we derive here. It is also worth mentioning that in view of the possible systematics affecting mainly the experimental determination of ${}^4\text{He}$ it is unfortunately impossible at present to use BBN to get detailed constraints on the time evolution of the quintessence field during this phase, while it can only provide a conservative bound on the largest (or smaller) values attainable by $\xi(\phi - \phi_0)/m_P$ during the nuclei formation era.

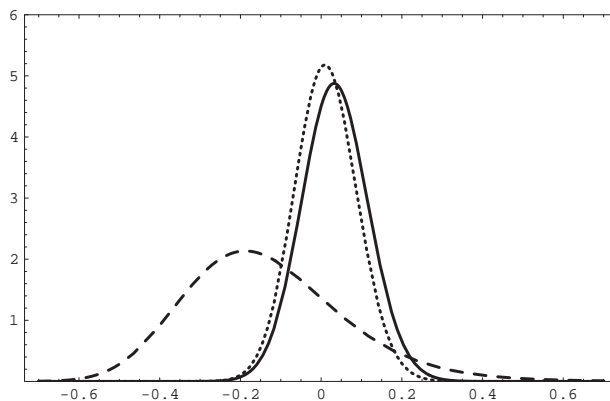


Figure 5.9: The behavior of the likelihood functions versus the parameter $\xi(\phi - \phi_0)/m_P$ for $\omega_b = 0.023$. The three curves refer to the D (dashed curve), ${}^4\text{He}$ (solid) and the combined D+ ${}^4\text{He}$ (dotted) analysis discussed in the text.

Results are summarized in Figure 5.9, where the likelihood contours obtained using Deuterium are shown [112], ${}^4\text{He}$ and finally, combining the two nuclei. As expected the ${}^4\text{He}$ mass fraction gives the most stringent constraint since it is much more sensitive to the value of the Hubble parameter with respect to Deuterium. In particular using ${}^4\text{He}$ only we get

$$-0.13 \leq \xi(\phi - \phi_0)/m_P \leq 0.20 \quad , \quad 95\% \text{ C.L.} \quad (5.97)$$

while adding the information on D abundance does not change this result significantly:

$$-0.14 \leq \xi(\phi - \phi_0)/m_P \leq 0.17 \quad , \quad 95\% \text{ C.L.} \quad (5.98)$$

We see how a clear understanding of the role of systematics in the Y_p measurements would have a large impact on further constraints on the value of the effective gravitational constant, at least in the minimal BBN scenario we are here considering, with no other extra parameters, such as extra relativistic degrees of freedom.

We close this Section by recalling that for a constant value of ϕ during the BBN epoch, the effect of the field on the gravitational constant can be also conveniently recasted in terms of the effective number of relativistic species contributing to the total energy density, as it was noticed in earlier works [118, 108, 42] and as it has been illustrated in the previous chapter, in section (4.2.4). Specifying eq.(4.96) to our case, it is straightforward to get the simple relation

$$\xi \frac{\phi - \phi_0}{M} = -\log \left(\frac{\delta g_*}{g_*} - 1 \right) . \quad (5.99)$$

This relation can be used to recast the bounds on the effective number of neutrinos, which are routinely used in the literature, in terms of a constraint on $\xi(\phi - \phi_0)/m_P$ for the exponential coupling considered in this paper. Note that interesting values of the field at Nucleosynthesis largely satisfy the bounds represented in Figure 5.9.

Conclusion

The possibility that a modification of gravity could ‘solve the dark’ is very appealing. In this sense, the interpretation of Dark Energy as a purely gravitational effect has always been very tempting, due to the desire of attributing the presence of the dark part of the Universe to a general lack of understanding of a fundamental theory. Furthermore, the difficulties encountered by quintessence models in finding a clear solution to the fine tuning and coincidence problems which affect the cosmological constant, encourage the search for alternatives which might go beyond General Relativity.

With this aim in mind we have worked in the context of scalar-tensor theories, one of the most natural alternatives to General Relativity, defined as generalized theories of gravity in which the metric tensor interacts with a scalar field via an explicit coupling to the Ricci scalar. We have followed the path of Extended Quintessence, traced out recently by several works, in which the scalar field of the Brans-Dicke-like theory acts as Dark Energy and provides the cosmological accelerated expansion required by experimental data. At this regard, several appealing features which characterize these models had already been object of many analysis concerning both the background and cosmological perturbations as well as constraints imposed by experiments [2, 8, 13, 34, 43, 68, 84, 96, 108, 110, 111, 118, 136, 140]. In particular, a major achievement of Extended Quintessence concerns the early universe dynamics of the quintessence field, whose motion at early times is dominated by an effective gravitational potential which appears in the Klein-Gordon equation, via a term which is entirely due to the non-minimal interaction with gravity. During radiation dominated era, the presence of non-relativistic species, although sub-dominant with respect to radiation, makes the behavior of the Ricci scalar playing a dominant role in determining the dynamics of the field. The resulting motion of the field is the R -boost, an effect first shown in [8]. In particular, it was pointed out in [96] that the R -boost trajectory might preserve the most appealing property of minimally coupled tracker models, i.e. that of having attractor solutions which try to solve the problem of fine tuning of the initial conditions. Minimally coupled quintessence models, however, are severely constrained by recent data coming from different cosmological probes such as Cosmic Microwave Background, Large Scale Structures and Type Ia Supernovae which all concord to

indicate that the Dark Energy closely mimics a Cosmological Constant, and that the crossing of the “phantom line”, with an equation of state smaller than -1 , is currently allowed. Within minimal coupling quintessence it is, in particular, hard to reconcile the presence of attractor solutions with a value of ω_ϕ very near to -1 : as ω_ϕ approaches the latter value, potentials need to be flattened, squeezing on a cosmological constant like behavior; as a consequence the range of initial condition allowed to go into the attractor shrinks, threatening the basis of the whole quintessence picture [18]. Interestingly, it was recently argued that in these conditions coupling Dark Energy to other entities may be very relevant, especially at early times, possibly saving the existence of attractors for the initial field dynamics [96]; moreover several authors [19] [65] [99] [107] [136] have shown that Extended Quintessence scenarios can even cross the cosmological constant value and reach $\omega_\phi < -1$.

Our work has consisted in further investigating the issue of a coupling between Dark Energy and Gravity. Although there is not a priori a particularly motivated form of the coupling and the possibilities among which it can be selected cover a wide range, most of the works on Extended Quintessence focused on non minimal coupling or induced gravity, in which the coupling has a quadratic dependence on the scalar field. A general treatment of Extended Quintessence theories was therefore still missing.

As a first step, we provided a complete and general theoretical classification of all those scalar-tensor theories which guarantee the existence of attractor solutions to the Klein Gordon equation [113]. In other words, we identified all the possible choices of the coupling which give rise to R-boost trajectories behaving as attractors in the early Universe in the form of scaling solutions. Our analysis resulted in selecting three classes of couplings, namely functions of the exponential form (5.19), polynomial functions (5.23), and the exponential of polynomial (5.24), depending on the coefficient m characterizing the scaling (5.8) and on its relation to the background scaling through the value of the B function in (5.22).

Our analysis recovers all the possibilities to have a scaling behavior. Most importantly, it has been found that these solutions actually possess stable attractor properties, which represent an extremely appealing feature able to encompass the fine-tuning problem of the initial conditions, which still affects minimally-coupled Quintessence models. In particular, we have shown that all the solutions of the form (5.9) which scale shallower than the background represent attractors, generated only by a modification of gravity and not by a particular choice of the true potential $V(\phi)$. This enforces the case for extending the theory of gravity beyond General Relativity, and opens the way to the solution of the initial fine tuning problem, in view of which new cosmological models, characterized by the non-minimal couplings we have selected out in this papers, will deserve a further investigation.

A second effort we have made in order to generalize past works on Extended Quintessence, consisted in investigating in details the particular case

of a coupling which depends exponentially on the scalar field, hence different from the usual quadratic choice; the exponential case may be relevant for string cosmology, where the dilaton appears as an exponential which multiplies the fundamental lagrangian [76]. At this regard we have recovered the attractor features of the solution to the Klein Gordon equation, remarking the enhanced dynamics that this model provides with respect to both minimal and non minimal coupling models previously investigated. In particular, with respect to the case of a non-minimal quadratic coupling, we find relevant new results concerning both background expansion and perturbations. Interestingly, in the exponential scenario the R -boost loses any sensitivity on the initial conditions of the field, while in the case of a quadratic coupling the latter enters into the expression for the energy density along the trajectory. The R -boost solution is equivalent to a tracking one with equation of state $-1/3$ so that the exponential coupling is able to restore the existence of attractors for the initial dynamics of the scalar field.

Furthermore, we have Weyl scaled the exponential extended quintessence theory, in view of the fact that coupling a scalar field to gravity is equivalent to coupling the scalar field universally to all matter scalar fields. We have numerically solved the model in both the Jordan and the Einstein reference frames, making use of two independent codes and of two different sets of equations, eventually obtaining the same dynamical pattern for the background. The successful comparison has represented a valuable test for the implementation of the DEfast code we had accomplished, in which we can now be confident, in the sense that we have excluded the possibility that the dynamics of the model was in some way related to numerical instabilities of the code more than to the physics of the model. Weyl scaling can be used to compare with ease our exponential scalar-tensor model with scalar-scalar coupled quintessence models [4, 93, 95]; also, it opens the way to an eventual future perturbation analysis of the model which might be done in the Einstein frame, using numerical codes like CMBeasy [45] and its implementation to coupled quintessence models [73, 100] in order to constrain the theory with cosmology [5, 6] and compare predictions of the Boltzmann code to observations.

We studied the predicted impact of extended quintessence cosmology on the observations, considering the case of our exponential model as a reference scenario. In particular, we considered the Cosmic Microwave Background (CMB) perturbation spectra, comparing the effects in the cases of exponential, quadratic and minimal couplings. The main effects derive from the fact that the cosmological expansion rate changes, due to the time variation of the effective gravitational constant. Consequently, angular scales and distances are modified, shifting the angular location of the acoustic peaks in the CMB power spectrum, and enhancing its tail at low multipoles, by means of the modified dynamics of the gravitational potentials on large scales (Integrated Sachs-Wolfe). For a fixed ω_{JBD} at present, the imprint on the amplitude of

the cosmological perturbation spectra markedly depends on the actual form of the non-minimal interaction: indeed, the exponential form enhances the departure from General Relativity as the field moves, with respect to the case of a quadratic coupling, the reason being just the shape of the coupling, for which the motion of the field gets exponentially amplified. This leads to the consequence that the effect on cosmological perturbations has to be investigated properly case by case: this aspect is particularly relevant having in view the possibility to constrain the theory of gravity on cosmological scales and from cosmological observations, in a complementary way with respect to what is done via observations in the solar system. As far as the exponential model is concerned, we also derived the limits from the Big Bang Nucleosynthesis; the constraints affect both the strength of the non-minimal coupling as well as the field value during the nuclide formation epoch. For interesting trajectories, those bounds are largely satisfied.

We conclude remarking that, as we have already pointed out, generalized theories of gravity can provide attractors for the early universe dynamics of the Dark Energy scalar field ϕ , independently of the shape of the potential $V(\phi)$ chosen for ϕ . The relevance of this issue goes beyond the mere capability of avoiding the fine tuning of the initial conditions: indeed, it enforces the need of a deeper understanding of Dark Energy interaction with other entities, both with regard to gravity and with regard to matter, especially in view of the Weyl scaling test that has been performed. On one side, in extended quintessence models, the gravitational coupling is responsible for the R-boost effect, enhancing the dynamics of the field during RDE: at that epoch the energy density of the field is mainly kinetic and doesn't depend on the choice of the potential neither on the initial conditions, the R-boost being an attractor solution. On the other side, the same effect can be provided by coupling Dark Energy to matter fields. The latter result suggests to look more in detail at the effects of such couplings on the dark components dynamics. In particular, as noted in [9], coupling Dark Energy to gravity might lead the field ϕ to show non linear features and clumps through gravitational dragging. It would then be important to understand whether this effect can be enhanced in the case of an exponential coupling. Furthermore, it would be very interesting to further investigate the effects of the mutual interaction of Dark Matter and Dark Energy perturbations within Coupled Quintessence models: the existence in the latter of a 'Dark Matter dragging' mechanism, analogue to the gravitational dragging one, would be very appealing; at this regard it would be worth verifying whether Dark Matter perturbation injection manage to drag the quintessence field perturbations to non-linearity inside the horizon, leading Dark Energy to form structures. Eventually, if Dark Energy density perturbations managed to be present also on sub-horizon scales, there would be the need of a modification of the N-body codes involved in the description of structure formation.

It is then clear that the relation between Dark Energy and other entities

can be extremely relevant for the understanding of the dark sector dynamics and deserves a careful study. In this sense, extended quintessence gives a charming insight in the rich physics that can be hidden beyond a constant-like behavior of Dark Energy.

Bibliography

- [1] Arcminute Cosmology Bolometer Array Receiver (ACBAR), <http://cosmology.berkeley.edu/group/swlh/acbar/index.html>
- [2] Acquaviva V., Baccigalupi C., Perrotta F. 2004, *Phys. Rev. D* **70**, 023515 astro-ph/0403654
- [3] Acquaviva V., Baccigalupi C., Leach S.L., Liddle A.R., Perrotta F. 2005, *Phys. Rev. D* **71**, 104025 astro-ph/0412052
- [4] Amendola L. 2000 *Phys. Rev. D* **62** 043511 astro-ph/9908023
- [5] Amendola L., Gasperini M., Piazza F. 2004 astro-ph/0407573
- [6] Amendola L., Quercellini C. 2003 *Phys. Rev. D* **68** 023514 astro-ph/0303228
- [7] Armendariz-Picon C., Mukhanov V., Steinhardt P.J. 2001 *Phys. Rev. D* **63** 103510 astro-ph/0006373
- [8] Baccigalupi C., Matarrese S., Perrotta F. 2000, *Phys. Rev. D* **62**, 123510 astro-ph/0005543
- [9] Baccigalupi C., Balbi A., Matarrese S., Perrotta F., Vittorio N. 2002, *Phys. Rev. D* **65**, 063520
- [10] Baccigalupi C., Balbi A. et al 2003, *Nucl. Phys. Proc. Suppl. Astrophys. J.* **124**, 68 astro-ph/0205217
- [11] Balbi A., Baccigalupi C., Matarrese S., Perrotta F., Vittorio N. 2001, *Astrophys. J.* **547**, 89 astro-ph/0009432
- [12] Bartelmann M., Perrotta F., Baccigalupi C. 2002, *Astron. & Astrophys.* **396**, 21 astro-ph/0206507
- [13] Bartolo N., Pietroni M. 2000, *Phys. Rev. D* **61**, 023518 hep-ph/9908521

-
- [14] Begeman K.G., Broeils A.H., Sanders R.H. 1991, *Mon. Not. Roy. Astron. Soc.* **249**, 523
- [15] Bennett C.L. et al 2003, *Astrophys. J. Supp.* **148** 1 astro-ph/0302224
- [16] Bertotti B., Iess L., Tortora P. 2003, *Nature* **425**, 374
- [17] Bertschinger E. 2000, astro-ph/0101009
- [18] Bludman S. 2004, *Phys. Rev. D* **69** 122002 astro-ph/0403526
- [19] Boisseau B., Esposito-Farese G., Polarski D., Starobinsky A.A. 2000, *Phys. Rev. Lett.* **85**, 2236 gr-qc/0001066
- [20] BOOMerang, <http://cmb.phys.cwru.edu/boomerang/>
- [21] BOOMerang, De Bernardis P. et al 2000, *Nature* **404** 955 astro-ph/0004404
- [22] BOOMerang, Jones W.C. et al 2005, astro-ph/0507494
- [23] BOOMerang, Piacentini F. et al 2005, astro-ph/0507507
- [24] BOOMerang, Montroy T.E. et al 2005, astro-ph/0507514
- [25] Boughn S., Crittenden R. 2004, *Nature* **427** 45 astro-ph/0305001
- [26] Brax P., Martin J. 1999, *Phys. Lett. B* **468** 40 astro-ph/9905040
- [27] Brax P., Martin J. 2000, *Phys. Rev. D* **61** 103502 astro-ph/9912046
- [28] Caldwell R. et al 1998, *Phys. Rev. Lett.* **80**, 1582 astro-ph/9708069
- [29] Caldwell R. 2002, *Phys. Lett. B* **545**, 23 astro-ph/9908168
- [30] Caldwell R. 2004, *Modern Physics Letters A* **19**, 1063
- [31] Caldwell R., Doran M. 2004, *Phys. Rev. D* **69**, 103517 astro-ph/0305334
- [32] Caldwell R., Doran M., Mueller C.M., Schaefer G., Wetterich C. 2003, *Astrophys. J.* **591**, L75 astro-ph/0302505
- [33] Caldwell R., Linder E. 2005, *Phys. Rev. Lett.* **95** 141301 astro-ph/0505494
- [34] Caresia P., Matarrese S., Moscardini L. 2004, *Astrophys. J.* **605**, 21 astro-ph/0308147
- [35] Carlstrom J.E. 2003, Kovac J., Leitch E.M., Pryke C. astro-ph/0308478

- [36] Carroll S.M. 1997, Lecture notes on General Relativity
- [37] Carroll S.M. 2001, Living Rev. relativity **4**, 1 (cited on 15-11-2005)
<http://www.livingreviews.org/lrr-2001-1>
- [38] Catena R., Fornengo N., Masiero A., Pietroni M., Rosati F. 2004 *Phys. Rev. D* **70** 063519 [astro-ph/0403614](http://arxiv.org/abs/astro-ph/0403614)
- [39] Cosmic Background Imager (CBI) <http://www.astro.caltech.edu/~tjp/CBI/>
- [40] CBI, Readhead A.C.S. et al 2004, *Science* **306**, 836 [astro-ph/0409569](http://arxiv.org/abs/astro-ph/0409569)
- [41] CBI, Readhead A.C.S. et al 2004, *Astrophys. J.* **609**, 498
[astro-ph/0402359](http://arxiv.org/abs/astro-ph/0402359)
- [42] Chen X., Scherrer R.J., Steigman G. 2001, *Phys. Rev. D* **63**, 123504
[astro-ph/0011531](http://arxiv.org/abs/astro-ph/0011531)
- [43] Chiba T. 1999, *Phys. Rev. D* **60**, 083508 [gr-qc/9903094](http://arxiv.org/abs/gr-qc/9903094)
- [44] Clifton T., Mota D.F., Barrow J.D. 2004, *Mon. Not. Roy. Astron. Soc.* **358** 601, [gr-qc/0406001](http://arxiv.org/abs/gr-qc/0406001)
- [45] <http://www.cmbeasy.org/>
- [46] <http://cmbfast.org/>
- [47] COBE, Smoot G.F. et al 1992, *Astrophys. J.* **396** L1
- [48] Coble K., Dodelson S., Frieman J.A., 1997, *Phys. Rev. D* **55** 1851
[astro-ph/9608122](http://arxiv.org/abs/astro-ph/9608122)
- [49] Cuoco A., Iocco F., Mangano G., Miele G., Pisanti O., Serpico P.D. 2004, *International J. Mod. Phys. A* **19**, 4431 [astro-ph/0307213](http://arxiv.org/abs/astro-ph/0307213)
- [50] Cyburt R.H. 2004, *Phys. Rev. D* **70**, 023505 [astro-ph/0401091](http://arxiv.org/abs/astro-ph/0401091)
- [51] DAMA, Barnabei et al 2003, *Riv. Nuovo Cim.* **26** N1 1,
[astro-ph/0307403](http://arxiv.org/abs/astro-ph/0307403)
- [52] DASI, <http://astro.uchicago.edu/dasi/>
- [53] DASI, Kovac J., Leitch E.M., Pryke C., Carlstrom J.E., Halverson N.W., Holzzapfel W.L. 2002, *Nature* **420** 772 [astro-ph/0209478](http://arxiv.org/abs/astro-ph/0209478)
- [54] Dolag K. et al 2004 *Astron. & Astrophys.* **416**, 853 [astro-ph/0309771](http://arxiv.org/abs/astro-ph/0309771)
- [55] Dolgov A.D. 1983 *The Very Early Universe*, ed. G.W. Gibbons, S.W. Hawking, S.T.C. Siklos, Cambridge University Press, Cambridge, p.449
- [56] Doran M. 2002, <http://www.ub.uni-heidelberg.de/archiv/2483>

- [57] Doran M. 2005 *J. Cosm. Astroparticle Phys.* **0510** 011
astro-ph/0302138
- [58] Doran M., Jaeckel J. 2002, *Phys. Rev. D* **66** 043519 astro-ph/0203018
- [59] Doran M., Mueller C. 2004, *J. Cosm. Astroparticle Phys.* **0409** 003
astro-ph/0311311
- [60] Durrer R. 2001, *J. Phys. Stud.* **5** 177 astro-ph/0109522
- [61] Durrer R. 2004, *Lect. Notes. Phys.* **653** 31 astro-ph/0402129
- [62] Eddington A.S. 1923, *The mathematical theory of relativity*, Cambridge Univ. Press, Cambridge, England
- [63] Eisenstein D.J. et al 2005, astro-ph/0501171
- [64] Elizalde E. 2004, gr-qc/0409076
- [65] Elizalde E., Nojiri S., Odintsov S.D. 2004, *Phys. Rev. D* **70** 043539
hep-th/0405034
- [66] Esposito-Farèse G. 2004, *AIP & Conf. Proc.* **736**, 35, gr-qc/0409081
- [67] Esposito-Farèse G. Polarski D. 2001, *Phys. Rev. D* **63**, 063504,
gr-qc/0009034
- [68] Faraoni V. 2000, *Phys. Rev. D* **62**, 023504 gr-qc/0002091
- [69] Ferreira P., Joyce M. 1997, *Phys. Rev. Lett.* **79** 4740
astro-ph/9707286
- [70] Fields B.D., Olive K.A. 1998, *Astrophys. J.* **506**, 177
astro-ph/9803297
- [71] Fiziev P., 2000, *Modern Physics Letters A* **15** 1977
- [72] Freedman W.L. et al 2001, *Astrophys. J.* **553**, 47 astro-ph/0012376
- [73] Frommert M., 2005 Graduation Thesis in progress
- [74] Fujii Y., Maeda K. 2003, *The Scalar-Tensor Theory of Gravitation*, Cambridge University Press
- [75] García-Bellido J. 2004, hep-ph/0407111
- [76] Gasperini M., Veneziano G. 2003, *Phys. Rep.* **373**, 1 hep-th/0207130
- [77] Hebecker A., Wetterich C. 2001, *Phys. Lett. B* **497** 281
hep-ph/0008205

- [78] Hi-Z Supernova Search, cfa-www.harvard.edu/cfa/oir/Research/supernova/HighZ.html
- [79] Hi-Z Supernova Search, Riess A.G. 1998, *Astron. J.* **116**, 1009
astro-ph/9805201
- [80] Hi-Z Supernova Search, Riess A.G. et al 2004, astro-ph/0402512
- [81] W. Hu 1998, *Astrophys. J.* **506**, 485 astro-ph/9801234
- [82] Hu W., Dodelson S. 2002, *Ann. Rev. Astron. Astrophys.* **40** 171,
astro-ph/0110414
- [83] Hu W., White M. 1997, *Phys. Rev. D* **56**, 596 astro-ph/9702170
- [84] Hwang J. 1991, *Astrophys. J.* **375**, 443
- [85] Izotov Y.I., Thuan T.X. 2004, *Astrophys. J.* **602**, 200
astro-ph/0310421
- [86] Kirkman D., Tytler D., Suzuki N., O'Meara J. M., Lubin D. 2003,
Astrophys. J. **149**, 1 astro-ph/0302006
- [87] Kodama H., Sasaki M. 1984, *Prog. Theor. Phys. Suppl.* **78**, 1
- [88] Lahav O., Liddle A.R. 2004, *Phys. Lett. B* **592** 1 astro-ph/0406681
- [89] Liddle A.R. 2001, *New Astron. Rev.* **45**, 235, astro-ph/0009491
- [90] Liddle A.R. Scherrer R.J. 1999, *Phys. Rev. D* **59**, 023509,
astro-ph/9809272
- [91] Linder E. 2004, *Phys. Rev. D* **70**, 023511 astro-ph/0402503
- [92] Ma C.P., Bertschinger E. 1995, *Astrophys. J.* **455** 7,
astro-ph/9506072
- [93] Maccio A.V., Quercellini C., Mainini R., Amendola L., Bonometto S.A.
2004, *Phys. Rev. D* **69** 123516, astro-ph/0309671
- [94] Ma C.P. et al 1999, *Astrophys. J.* **521** L1, astro-ph/9906174
- [95] Mangano G., Miele G., Pettorino V. 2003, *Modern Physics Letters A*
18 831, astro-ph/0212518
- [96] Matarrese S., Baccigalupi C., Perrotta F. 2004, *Phys. Rev. D* **70**,
061301 astro-ph/0403480
- [97] MAXIMA, <http://cosmology.berkeley.edu/group/cmb/>
- [98] Maxima, Balbi A. et al 2000, *Astrophys. J.* **545** L1 [Erratum-ibid. **558**
(2001) L145] astro-ph/0005124

- [99] Ming-Xing L., Qi-Ping S. , 2005 *Phys. Lett. B* **626** 7 astro-ph/0506093
- [100] Müller C.M., Ph-D thesis
- [101] NVSS <http://www.cv.nrao.edu/nvss/>
- [102] Olive K.A. 2005, astro-ph/0503065
- [103] Olive K.A., Peacock J.A. 2002, *Phys. Rev. D* **66** 010001
- [104] Olive K.A., Skillman E.D. 2004, *Astrophys. J.* **617** 29
astro-ph/0405588
- [105] Padmanabhan T., 2003 *Phys. Rep.* **380**, 235 hep-th/0212290
- [106] Peebles P.J.E., Ratra B. 2003, *Rev. Mod. Phys.* **75**, 559
astro-ph/0207347
- [107] Perivolaropoulos L., 2005 *J. Cosm. Astroparticle Phys.* **0510** 001
astro-ph/0504582
- [108] Perrotta F., Baccigalupi C., Matarrese S. 2000, *Phys. Rev. D* **61**,
023507 astro-ph/9906066
- [109] Perrotta F., Baccigalupi C. 1999, *Phys. Rev. D* **59**, 123508
astro-ph/9811156
- [110] Perrotta F., Baccigalupi C. 2002, *Phys. Rev. D* **65**, 123505
astro-ph/0201335
- [111] Perrotta F., Matarrese S., Pietroni M., Schimd C. 2004, *Phys. Rev. D*
69, 084004 astro-ph/0310359
- [112] Pettorino V., Baccigalupi C., Mangano G. 2005, *J. Cosm. Astroparticle
Phys.* **0501**, 014 astro-ph/0412334
- [113] Pettorino V., Baccigalupi C., Perrotta F. 2005, accepted by *J. Cosm.
Astroparticle Phys.* astro-ph/0508586
- [114] PLANCK, <http://www.rssd.esa.int/index.php?project=PLANCK>
- [115] Raffelt G.G. 1997, Menstrup High-energy physics, 235
hep-ph/9712538
- [116] Ratra B., Peebles P.J.E. 1988, *Astrophys. J.* **325**, L17
- [117] Ratra B., Peebles P.J.E. 1988, *Phys. Rev. D* **37**, 3406
- [118] Riazuelo A., Uzan J.P. 2002, *Phys. Rev. D* **66**, 023525
astro-ph/0107386

- [119] Rubakov V.A. 2002, *Beatenberg 2001 High Energy Physics* , 249.
- [120] Sahni V., Starobinsky A.A. 2000, *International J. Mod. Phys. D* **9**, 373 astro-ph/9904398
- [121] Sahni V., Shtanov Y.V. 2003, *J. Cosm. Astroparticle Phys.* **0311**, 014 astro-ph/0202346
- [122] Sanchez A.G. et al 2005, astro-ph/0507583
- [123] SDSS, Prada F. et al 2003, *Astrophys. J.* **598**, 260 astro-ph/0301360
- [124] SDSS, Scranton R. et al 2003, astro-ph/0307335
- [125] SDSS, Tegmark M. et al 2004, *Phys. Rev. D* **69** 103501 astro-ph/0310723
- [126] SDSS, Tegmark M. et al 2004 *Astrophys. J.* **606**, 702 astro-ph/0310725
- [127] SDSS, Eisenstein D.J. et al 2005, astro-ph/0501171
- [128] Sen S., Sen A.A. 2001, *Phys. Rev. D* **63**, 124006 gr-qc/0010092
- [129] Serpico P.D., Esposito S., Iocco F., Mangano G., Miele, G., Pisanti O. 2004, *J. Cosm. Astroparticle Phys.* **0412** 010 astro-ph/0408076
- [130] SNAP, <http://snap.lbl.gov/>
- [131] SnCP, Perlmutter S. et al 1999, *Astrophys. J.* **517**, 565 astro-ph/9812133
- [132] SnCP, Knop R.A. et al 2003, *Astrophys. J.* **598**, 102 astro-ph/0309368
- [133] Stairs I.H. 2003, *Liv. Rev. Rel.* **6** (cited on 15-11-2005): <http://www.livingreviews.org/lrr-2003-5>
- [134] Steinhardt P.J., Wang L., Zlatev I. 1999, *Phys. Rev. D* **59**, 123504 astro-ph/9812313
- [135] Tegmark M. 2004, Proceedings of the Texas Symposium on Relativistic Astrophysics at Stanford University.
- [136] Torres D.F. 2002, *Phys. Rev. D* **66**, 043522 astro-ph/0204504
- [137] 2dF, Colless M. et al 2004, astro-ph/0306581
- [138] 2dF, Cole S. et al 2005, *Mon. Not. Roy. Astron. Soc.* **362** 505 astro-ph/0501174

- [139] 2dF, Percival W.J. et al 2002, *Mon. Not. Roy. Astron. Soc.* **337** 1068
astro-ph/0206256
- [140] Uzan J.P. 1999, *Phys. Rev. D* **59**, 123510 gr-qc/9903004
- [141] Vielva P., Martinez-Gonzalez E., Tucci M. astro-ph/0408252
- [142] Visser M. 2004, *Class. Quant. Grav.* **21**, 2603 gr-qc/0309109
- [143] Very Small Array (VSA), <http://www.iac.es/project/cmb/vsa/>
- [144] Wands D. 1994, *Class. Quant. Grav.* **11**, 269 gr-qc/9307034
- [145] Weinberg S. 1972, *Gravitation and cosmology: principles and applications of the general theory of relativity* New York: Wiley, c1972.
- [146] Weller J., Lewis A.M. 2003, *Mon. Not. Roy. Astron. Soc.* **346**, 987
astro-ph/0307104
- [147] Wetterich C. 1988, *Nucl. Phys. B* **302**, 645
- [148] Wetterich C. 1995, *Astron. & Astrophys.* **301**, 321 hep-th/9408025
- [149] Will C. 2001, *Liv. Rev. Rel.* **4** (cited on 15-11-2005):
<http://www.livingreviews.org/lrr-2001-4>
- [150] WMAP, <http://map.gsfc.nasa.gov/>
- [151] WMAP, Hinshaw G. et al. 2003, *Astrophys. J. Supp.* **148**, 135
astro-ph/0302225
- [152] WMAP, Nolta M.R. et al 2004, *Astrophys. J.* **608** 10
astro-ph/0305097
- [153] WMAP, Spergel D.N. et al. 2003, *Astrophys. J. Supp.* **148**, 175
astro-ph/0302209
- [154] Zaldarriaga M. 1998, PhD Thesis astro-ph/9806122
- [155] Zaldarriaga M., Seljak U. 2000, *Astrophys. J. Supp.* **129**, 431
- [156] Zlatev I., Wang L., Steinhardt P.J. 1999, *Phys. Rev. Lett.* **82**, 896
astro-ph/9807002